ICLIAD 66 (2), 128-230, 2025

p-ISSN 0535-5133
e-ISSN 2477-9393

Volumen 66
No. 2
Junio
2025

Investigación Clínica

65 Aniversario

Universidad del Zulia
Facultad de Medicina
Instituto de Investigaciones Clínicas
"Dr. Américo Negrette"
Maracaibo, Venezuela

Investigación Clínica

https://sites.google.com/site/revistainvestigacionesclinicas

Revista arbitrada dedicada a estudios humanos, animales y de laboratorio relacionados con la investigación clínica y asuntos conexos.

La Revista es de Acceso Abierto, publicada trimestralmente por el Instituto de Investigaciones Clínicas "Dr. Américo Negrette", de la Facultad de Medicina, de la Universidad del Zulia, Maracaibo, Venezuela.

Investigación Clínica está indizada en Science Citation Index Expanded (USA), Excerpta Medica/EMBASE y Scopus (Holanda), Tropical Diseases Bulletin y Global Health (UK), Biblioteca Regional de Medicina/BIREME (Brasil), Ulrich's Periodicals, Journal Citation Reports (USA), Index Copernicus (Polonia), SIIEC Data Bases, Sección Iberoamérica (Argentina) e Infobase Index (India), Redalyc y las bases de datos: SciELO (www.Scielo.org.ve), Revencyt, LILACS, LIVECS, PERIODICA y web de LUZ: http://www.produccioncientificaluz.org/revistas

Para cualquier otra información dirigir su correspondencia a:

Dra. Elena Ryder, Editora
Instituto de Investigaciones Clínicas
"Dr. Américo Negrette"
Facultad de Medicina, Universidad del Zulia
Maracaibo, Venezuela.

Teléfono:
+58-0414-6305451

Correos electrónicos:
elenaryder@gmail.com
riclinicas@gmail.com

Páginas web:
https://sites.google.com/site/revistainvestigacionesclinicas

http://www.produccioncientificaluz.org/revistas

For any information please address correspondence to:

Dr. Elena Ryder, Editor
Instituto de Investigaciones Clínicas
"Dr. Américo Negrette"
Facultad de Medicina, Universidad del Zulia
Maracaibo, Venezuela.

Phone:
+58-0414-6305451

E-mails:
elenaryder@gmail.com
riclinicas@gmail.com

Web pages:
https://sites.google.com/site/revistainvestigacionesclinicas

http://www.produccioncientificaluz.org/revistas

Universidad del Zulia
Publicación auspiciada por el
Vicerrectorado Académico
Serbiluz-CONDES

CODEN: ICLIAD
Versión impresa ISSN: 0535-5133
Depósito legal pp 196002ZU37
Versión electrónica ISSN: 2477-9393
Depósito legal ppi 201502ZU4667

Artes finales:
Lisbeny Valencia
lisbenyvalencia@gmail.com

ASESORES CIENTÍFICOS (2025-2027)

Invest Clin 66(2): 128 - 130, 2025 https://doi.org/10.54817/IC.v66n2a00

EDITORIAL
Investigación Clínica en sus 65 años continúa adaptándose a los requerimientos universales de publicaciones científicas.

Aprovechando el Editorial del mes de junio, deseo recordar a nuestros lectores que el próximo mes de julio, se cumplen 65 años de la aparición del primer número de Investigación Clínica. Sueño cumplido, gracias al tenaz esfuerzo de quien fuera su primer Editor, el Director-fundador del entonces Centro de Investigación Clínica (hoy Instituto de Investigaciones Clínicas) de la Facultad de Medicina de LUZ, el Dr. Américo Negrette.

En mis 35 años ininterrumpidos como Editora de Investigación Clínica, he dedicado varios Editoriales ofreciendo información sobre la evolución de la Revista. En esta oportunidad, comentaré los eventos sucedidos en los últimos años, cuando hemos tenido en primer lugar, que seguir adaptándonos al cambio del formato de la Revista, de impreso a digital, hecho ocurrido en el 2018. Esto no fue difícil, puesto que contábamos con una página web, diseñada de tal forma, que se ajustó perfectamente al cambio, ello gracias a nuestro administrador Dr. Enrique Torres, lo cual sirvió de plantilla para la versión electrónica. Así la revista Investigación Clínica, puede ser consultada libremente en toda su extensión, tanto en la página web https://sites.google.com/site/revistainvestigacionesclinicas/, como en el repositorio de la Universidad del Zulia https://www.produccioncientificaluz.org, además de Scielo. Venezuela https://ve.scielo.org/

En segundo lugar, debimos enfrentar la pandemia del CoVID 19 y sus dos años de permanencia, pero de igual forma seguimos trabajando de manera virtual: comité editorial, autores, árbitros, diseñadora gráfica, índices internacionales, y demás colaboradores. No hubo ningún retraso en la frecuencia de aparición de los números, ni incidentes que lamentar. Cabe mencionar que, durante este período de pandemia, publicamos varias comunicaciones relacionadas con la enfermedad y su trascendencia.

Este nuevo período se caracterizó por varias razones. Hemos tenido un incremento notable de participación foránea en el envío y posterior publicación de trabajos, procedentes tanto de Latinoamérica, como de países asiáticos. De Latinoamérica, además de México y Ecuador que han sido siempre muy activos en el envío de artículos, recibimos contribuciones de Perú, Brasil, Chile y Paraguay. Del Asia, predomina China, luego Turquía, seguido de Irak e Irán. De Venezuela hemos mantenido la participación de colaboradores tradicionales, como las universidades Central de Venezuela, de Carabobo, de Oriente y de Los Andes y del Instituto Venezolano de Investigaciones Científicas (IVIC).

La cantidad de trabajos publicados por número ha sido de 7 a 10, los cuales ocupan entre 400 y 500 páginas por año. Aunque los trabajos originales siguen siendo mayoría, hemos notado un aumento de las revisiones sistemáticas y meta análisis. Los trabajos en idioma ingles superaron en forma importante a los escritos en español. El porcentaje de rechazo estuvo en el orden del 34%.

Hemos incluido en nuestros requerimientos de publicación, las nuevas exigencias de las publicaciones científicas, como son la colocación del DOI a cada trabajo, nú-

mero ORCID de todos los autores y la definición de la participación de cada uno de ellos en la publicación; además de mencionar la fuente de financiamiento, el conocimiento de la Comisión de Ética de la institución donde se realizó el trabajo, y la existencia o no de conflicto de intereses. Debido a la falta de financiamiento por parte de la institución universitaria responsable, por desaparición de las partidas que ofrecía el Gobierno Nacional, debemos solicitar colaboración económica para el Manejo Editorial de los trabajos, colaboración cuyo monto depende de varios factores geopolíticos, razón por la cual muchos no nos consideran "Ciencia Abierta"; sin embargo, como mencioné anteriormente, todos los trabajos publicados en los 65 años de existencia de Investigación Clínica, pueden ser leídos y copiados sin costo alguno.

Hemos dado cabida en nuestras páginas, en forma de Suplementos, a múltiples eventos científicos locales, nacionales e internacionales, habiendo decidido, en los dos últimos años, hacer uso para la publicación de estos eventos, de un nuevo formato de difusión estilo "Libro de frecuencia anual, que hemos denominado Investigación Clínica-Memoria de Eventos", con caracterización propia: ISBN, Depósito Legal y doi. Este libro, que ya posee dos números, se puede localizar en nuestra página web, donde verificamos la frecuencia de visitas, al igual que hacemos con los números regulares.

Hemos mantenido nuestra indización, con una clasificación similar en la Web of Science y Scopus. Reactivamos nuestra indización en Scielo. No hemos podido solicitar nuestra re-inclusión en PubMed, por carecer aun de la plataforma tecnológica necesaria para sus requerimientos; sin embargo, nuestra permanencia en dicho índice desde 1989 al 2017, permite que 879 trabajos publicados en Investigación Clínica en ese periodo, puedan ser ubicados allí. Nos encontramos ahora en Google Académico y a través de Crossref estamos al tanto de la búsqueda de los trabajos publicados a través de los dois. Por otro lado, nuestra página web es continuamente visitada por individuos procedentes de países de todo el mundo.

Agradezco a los autores que nos han preferido para publicar sus trabajos, a los árbitros que generosamente colaboran con la revisión de los artículos, a los miembros del Comité Editorial, que semana a semana están pendientes de los asuntos a tratar, especialmente al administrador de la página web, a las Comisiones de Estilo, Idioma, Estadística, y de revisión del material de expresión gráfica y a nuestra eficiente diseñadora gráfica, por todo el apoyo que permite a Investigación Clínica, estar vigente y mantenerse en un sitial honroso nacional e internacional. Una palabra de agradecimiento también a muchos otros colaboradores que nos ayudan en la difusión del material publicado.

Elena Ryder
ORCID: 0000-0003-4613-6424

Feliz 65 Aniversario Investigación Clinica

Investigación Clínica continue to adapt to all the requirements for scientific publications

In celebrating our 65th anniversary, we continue to adapt to all the requirements for scientific publications. We have shifted from print to digital and continued publishing quarterly on time, despite adverse circumstances like the COVID-19 pandemic. We have published systematic reviews and meta-analyses. We have used the ORCID number for authors, referees, and the editorial board, as well as the DOI number for all published works. We have also provided disclosure of authors' participation in the publication, funding sources, approval by the ethics committee of the institution responsible for the work, disclosure of conflicts of interest, and the use of artificial intelligence in writing the manuscript. We remain indexed in Web of Science and Scopus and have reactivated our indexing in Scielo. All works published over the past 65 years are freely available on our website and/or in the repositories of the University of Zulia and Scielo-Venezuela. The 879 papers published between 1989 and 2017 remain in PubMed, an index we had to abandon due to our country's technological limitations. We are listed on Google Scholar; and CrossRef reports the papers' readership by their respective DOIs. This information about the journal's search is also monitored through our website, which reflects its widespread worldwide dissemination. I want to thank the authors who have chosen to publish their work, the referees who generously collaborated with the review of articles, the members of the Editorial Committee, especially the website administrator, the Style, Language, and Statistics Committees, and our efficient graphic designer, for all the support that allows "Investigación Clínica" to remain current and maintain a place of national and international honor. A word of thanks also goes to the many other collaborators who help us disseminate our published material.

Happy 65th Anniversary, "Investigación Clínica" !

Invest Clin 66(2): 131 - 146, 2025 https://doi.org/10.54817/IC.v66n2a01

Correlation between human papillomavirus infection and vaginal microecological environment, and the effect of *Lactobacillus* vaginal capsules combined with recombinant human interferon α-2b gel on human papillomavirus infection.

Yanling Sun, Li Li, Wenxin Xu and Cen Ma

Department of Obstetrics and Gynecology Laboratory, The First Affiliated Hospital of Soochow University, Soochow 215006, Jiangsu, China.

Keywords: human papillomavirus infection; vaginal microecology; bacterial vaginosis; *Lactobacillus* vaginal capsule; recombinant human interferon α-2b gel.

Abstract. This study mainly analyzed the correlation between human papillomavirus infection (HPV) and vaginal microecological environment and explored the effect of *Lactobacillus* vaginal capsule combined with recombinant human interferon α-2b gel on HPV infection. Five hundred patients who underwent a gynecological examination in our hospital from June 2021 to June 2023 were selected and divided into HPV-positive and HPV-negative groups. Relative to the HPV-negative group, the HPV-positive group presented a higher abnormal rate of *Lactobacillus*, catalase, cleanliness, neuraminidase and proline aminopeptidase ($p<0.05$) and a higher positive rate of bacterial vaginosis (BV) ($p<0.05$). Multivariate logistic regression analysis showed that catalase, proline aminopeptidase and BV were risk factors for HPV infection ($p<0.05$). In addition, 180 HPV-positive patients were randomly divided into a control group (CG) and an observation group (OG). The CG was given recombinant human interferon α-2b gel, and the OG was treated with recombinant human interferon α-2b gel plus a *Lactobacillus* vaginal capsule. Relative to the CG, the OG presented a higher total effective rate ($p<0.05$), lower inflammation ($p<0.01$), better immune function ($p<0.01$), and a higher proportion of grade II-III vaginal flora density and grade II-III vaginal flora diversity ($p<0.001$). Collectively, HPV is significantly correlated with the vaginal microecological environment, and catalase, proline aminopeptidase and BV were closely related to HPV infection. In addition, *Lactobacillus* vaginal capsule plus recombinant human interferon α-2b gel has practical clinical efficacy, which can reduce inflammation, promote immune function, improve vaginal microecological environment, and is safe in the treatment of patients with HPV infection.

Corresponding author: Cen Ma. Department of Obstetrics and Gynecology Laboratory, The First Affiliated Hospital of Soochow University, 188 Shizi Street, Soochow 215006, Jiangsu, China. E-mail: ydm1368@163.com

Correlación entre la infección por el virus del papiloma humano y el entorno microecológico vaginal, y el efecto de cápsulas vaginales de *Lactobacillus* combinada con gel de interferón α-2b humano recombinante sobre la infección por el virus del papiloma humano.

Invest Clin 2025; 66 (2): 131 – 146

Palabras clave: infección por virus del papiloma humano; microecología vaginal; vaginosis bacteriana; cápsula vaginal de *Lactobacillus;* gel recombinante humano de interferón α-2b.

Resumen. Este estudio analizó principalmente la correlación entre la infección por el virus del papiloma humano (VPH) y el entorno microecológico vaginal, y exploró el efecto de cápsulas vaginales de *Lactobacillus* combinadas con gel de interferón humano recombinante α-2b sobre la infección por VPH. Se seleccionaron 500 pacientes que se sometieron a examen ginecológico en nuestro hospital de junio de 2021 a junio de 2023 y se las dividió en un grupo positivo para VPH y un grupo negativo para VPH. En relación con el grupo VPH negativo, el grupo VPH positivo presentó mayor tasa anormal de *Lactobacillus*, catalasa, neuraminidasa, prolina aminopeptidasa y limpieza ($p<0,05$) y mayor tasa positiva de vaginosis bacteriana (BV) ($p<0,05$). El análisis multivariado de regresión logística mostró que la catalasa, la prolina aminopeptidasa y la BV fueron factores de riesgo para la infección por VPH ($p<0,05$). Además, 180 pacientes VPH positivos se dividieron aleatoriamente en un grupo control (GC) y un grupo de observación (OG). Al CG se le administró gel recombinante humano de interferón − -2b, y al OG se le administró gel recombinante humano de interferón − -2b más cápsulas vaginales de *Lactobacillus*. En relación con el GC, el OG presentó mayor tasa efectiva total ($p<0,05$), menor inflamación ($p<0,01$), mejor función inmune ($p<0,01$) y mayor proporción de densidad de flora vaginal de grado II-III y diversidad de flora vaginal de grado II-III ($p< 0,001$). Colectivamente, el VPH se correlaciona significativamente con el entorno microecológico vaginal, y la catalasa, la prolina aminopeptidasa y el BV se relación estrechamente con la infección por VPH. Además, las cápsulas vaginales de *Lactobacillus* más el gel de interferón α-2b recombinante humano tienen eficacia clínica efectiva, lo que puede reducir la inflamación, promover la función inmune, mejorar el entorno microecológico vaginal, y es seguro en el tratamiento de pacientes con infección por VPH.

Received: 29-12-2024 Accepted: 12-04-2025

INTRODUCTION

Cervical cancer is a serious threat to the majority of women's health. In developing countries, its incidence is second only to breast cancer, ranking second in female malignant tumors, and is the most common female reproductive system tumor [1]. According to the cancer report released by the International Agency for Research on Cancer under the World Health Organization, in 2020, about 604,000 women around the

world were diagnosed with cervical cancer, and about 342,000 women died from the disease, among which the number of cervical cancer cases in China was about 110,000, and the number of deaths was 60,000 [2]. Etiological studies have found that persistent infection by human papillomavirus (HPV) is a significant factor in cervical cancer [3]. HPV is a kind of virus which can be classified into low-risk human papillomavirus (LR-HPV) and high-risk human papillomavirus (HR-HPV) according to the strength of the pathogenicity or carcinogenic risk of HPV [4]. HPV is highly host-specific and easily infects human epidermal and mucous squamous epithelium, mainly through sexual transmission[5]. HPV infection is the leading cause of most cervical cancer, anal and oropharyngeal invasive cancers and preinvasive lesions, and is also the cause of genital warts (*condyloma acuminatum*) and recurrent respiratory papillomatosis [6]. Therefore, the prevention of HPV infection and intervention in the disease process after HPV infection are the key to reducing the incidence and mortality of cervical cancer.

There is evidence that maintaining the balance of vaginal microecology plays an important role in preventing female reproductive system infection, and when the vaginal microecology is destroyed, it may lead to cervical lesions [7]. Under normal circumstances, the vaginal microecology is in a state of dynamic balance. When the loss of this dynamic balance, the immune system of the vaginal mucosa, is damaged, and foreign microorganisms are more likely to invade the reproductive tract and cause inflammation [8]. Studies have shown that changes in the vaginal microenvironment, such as vaginal douching, bacterial vaginosis (BV), as well as sexually transmitted infections, are thought to be cofactors in the persistence of HPV infection [9]. Studies have also found that reconstructing vaginal microecological homeostasis can reduce the risk of HPV infection [10].

Antiviral drugs are commonly used in clinical treatment for patients with HPV infection, such as recombinant human interferon α-2b gel, which can inhibit the replication of the virus and increase the immune regulation of lymphocytes to specific cytotoxicity after medication, thus playing a particular therapeutic effect [11]. However, with the single use of antiviral drugs, the drug interacts with the vaginal environment and affects the overall effect. *Lactobacillus* vaginal capsules is a kind of microecological preparation whose main ingredient is living intestinal streptococcus; it is a common drug to treat bacterial disorder vaginosis and can play a role in the decomposition of lactic acid produced by sugar and regulate the pH of the vagina [12].

In our study, we intended to explore the correlation between HPV infection and the vaginal microecological environment and the effect of *Lactobacillus* vaginal capsules combined with recombinant human interferon α-2b gel on HPV infection.

PATIENTS AND METHODS

Patients

Five hundred patients who underwent gynecological examination in the gynecological outpatient department of our hospital from June 2021 to June 2023 were selected as the study participants. Inclusion criteria: (1) Non-pregnant and lactation period; (2) Regular menstrual cycle; (3) No vaginal bleeding; (4) No serious diseases of other systems; (5) No history of vaginal douching treatment and other vaginal operations within three days; (6) No sexual intercourse within three days; (7) No drugs taken within one month, no abnormalities in cervical cytology within one year. Exclusion criteria: (1) Patients had other systemic diseases; (2) Patients had no sexual history. The hospital Medical Ethics Committee approved this study, and all patients signed an informed consent. According to the HPV test results, 180 cases were divided into the HPV-positive group and 320 cases were the HPV-negative group. The HPV-positive group was 22-65

years, with a median age of (37.36±3.75) years. The HPV-negative group was 23-68 years, with a median age of (37.28±3.67) years. The two groups exhibited no significant difference in age ($p>0.05$). In addition, 180 HPV-positive patients were randomly divided into a control group (CG) and an observation group (OG); each group had 90 cases. The control group was 22-68 years old, with a median age of (38.36±3.78) years. The observation group was aged 23-65, with a median age of (37.45±3.69) years. The two groups exhibited no significant difference in age ($p>0.05$).

HPV detection

All 500 enrolled patients underwent HPV testing during the gynecological examination phase of the study, including the 180 patients later identified as HPV-positive. HPV detection was carried out using the second-generation Hybrid Capture 2 (HC2) DNA assay (Qiagen Digene, USA), a gold-standard, FDA-approved diagnostic method for detecting high-risk and low-risk human papillomavirus DNA in cervical samples. This method employs RNA probes complementary to 13 high-risk (e.g., HPV16, 18, 31, 33) and five low-risk HPV genotypes. Sample collection involved using a cervical sampler brush (Digene), which was rotated clockwise three times at the cervical ostium to obtain epithelial cells. The brush was then placed into the HPV DNA collection medium and stored at 4°C. Samples were processed according to the manufacturer's protocol. In the HC2 system, RNA:DNA hybrids formed during hybridization were captured and detected via chemiluminescence, and results were interpreted quantitatively based on a Relative Light Unit (RLU) ratio ≥1.0, with values above this threshold considered HPV-positive. This method was used consistently across all participants to ensure homogeneity of diagnostic criteria, including initial diagnosis in the 180 HPV-positive patients and post-treatment evaluation of viral clearance. All HPV-positive patients (n=180) were subjected to this post-treatment re-evaluation 4–6 weeks after completion of therapy to minimize false negatives due to transient viral suppression. This re-evaluation enabled an accurate assessment of HPV viral persistence or clearance.

HPV Detection Pre- and Post-Treatment
Vaginal microecological examination

The patient was instructed to take the bladder lithotomy position, and the disposable vaginal speculum was slowly inserted into the vagina along the lateral posterior wall of the vagina. As the speculum went deeper, the speculum was turned straight and slowly opened to expose the vaginal wall, fornix, and cervix fully. The vaginal mucus and cells were gently scraped from the upper 1/3 side of the vagina's wall with a disposable sterile cotton swab and then placed in a disposable sterile test tube for sealing. The samples were immediately sent to our hospital's laboratory.

Diagnostic criteria of vaginal microecology

The results were determined by the vaginitis five-test kit (Autobio, Zhengzhou, China). Light yellow or no color of catalase was positive (+), indicating the presence of a small amount of *Lactobacillus*; light red was weakly positive (±), indicating the presence of moderate *Lactobacillus*, and red or purple-red was negative (-); indicating the presence of a large number of *Lactobacillus*. Leucocyte esterase displayed blue for positive (+, ++, +++), light blue for weak positive (±), and no color or light color for negative (-).

Neuraminidase displayed red, purple, blue, brown or black for positive (+), light red for weak positive (±), and no color or orange for negative (-). Proline aminopeptidase showed positive (+) in yellow, weakly positive (±) in light yellow, and negative (-) in no color or light color. Acetylglucosaminidase showed yellow as positive (+), light yellow as weakly positive (±), and no color

or light color as negative (-). Proline aminopeptidase showed positive, and acetylglucosaminidase showed negative, indicating positive BV. Proline aminopeptidase showed positive with a pH ≥4.8, indicating positive trichomonas vaginitis (TV), and proline aminopeptidase showed positive with a PH ≤4.5, indicating positive vulvovaginal candidiasis (VVC). The PH color from yellow-cyan-green-blue indicated a change from 3.8 to 5.4, and the PH value was obtained against the colorimetric card. Vaginal PH of 3.8 to 4.5 was normal. Cleanliness I and II were normal. A large or medium amount of *Lactobacillus* was normal. The negative and weak positive of catalase and leucocyte esterase were normal. Negative neuraminidase, proline aminopeptidase, and acetylglucosaminidase were normal. Negative BV, candida, trichomonas was normal. If there was any abnormality, the vaginal microecology was in an unbalanced state.

Treatment methods

The control group was given recombinant human interferon α-2b gel (Zhaoke Pharmaceutical (Hefei) Co., LTD.; specification: 100,000 IU/g, 5 g/ branch). After the menstrual period was clear, the vulva was cleaned every night, and 1 g of gel was applied to the vaginal dome using a disposable thruster. Seven to ten times was used in a menstrual cycle as a course of treatment, for a total of three courses of treatment.

The observation group was treated with recombinant human interferon α-2b gel combined with *Lactobacillus* vaginal capsules. The treatment method of recombinant human interferon α-2b gel was the same as that of the control group. A *Lactobacillus* vaginal capsule (Xi'an Zhenghao Bio-pharmaceutical Co., LTD., specification: 0.25 g: 6 million live lactic acid bacteria) was added in the recombinant human interferon α-2b gel administration daily, transvaginal medication, two capsules/time, one time/day, with the same treatment course as the control group. During the treatment period, both groups suspended sexual activity and prohibited from vaginal irrigation.

Observation indicators

1. **Clinical efficacy**: a. Obvious effect: After treatment, the characteristics of vaginal secretions returned to normal, all symptoms disappeared, HPV was negative; b. Effective: After treatment, the characteristics and symptoms of the vaginal secretions were significantly improved, and HPV was negative; c. Ineffective: After treatment, HPV was still positive, and symptoms and vaginal secretion traits did not improve or even worsen. Total effective rate = (Obvious effect + Effective) Number of cases/Total cases ×100%.
2. **Inflammation**: 3 mL fasting venous blood samples were taken from the patient and centrifuged for 10 min at a rotational speed of 3000 r/min and a radius of 15 cm. After that, an automatic biochemical analyzer measured the levels of tumor necrosis factor-α (TNF-α) and interleukin-6 (IL-6).
3. **Immune function**: Fasting venous blood was collected and centrifuged in parallel according to (2). The levels of $CD4^+$ and $CD8^+$ were measured by flow cytometry, and the ratio of $CD4^+/CD8^+$ was calculated.
4. **Vaginal microecology**: A sterile cotton swab was used to collect secretions on 1/3 of the vaginal wall and detect them under a microscope. The *density of vaginal flora* was divided into grade I (average bacterial count of field ≤9), grade II (average bacterial count of field 10-99), grade III (average bacterial count of field ≥100), and grade IV (bacteria gathered into clusters or densely covered mucosal epithelial cells). Among them, grade II and III were considered as normal concentrations of vaginal flora. *Vaginal flora diversity* was divided into grade I (identify 1 ~ 3 kinds of bacteria), grade II (identify 4 ~ 6 kinds

of bacteria), grade III (identify 7 ~ 9 kinds of bacteria), grade IV (identify ≥10 kinds of bacteria), of which grade II and grade III were considered as normal vaginal flora diversity.

5. **The occurrence of adverse reactions**, including a burning sensation of the vulva, pruritus and gastrointestinal discomfort in the two groups were recorded.

Statistical analysis

The data were analyzed using SPSS 22.0 statistical software. Measurement data were expressed as ($\bar{x}\pm s$), and the t-test was adopted for comparison. Statistical data were expressed as n (%), and the χ^2 test was used for comparison. A logistic regression model was used to analyze the influencing factors. The difference was statistically significant at $p<0.05$.

RESULTS

Comparison of vaginal microecology between two groups

As Table 1 reveals, relative to the HPV-negative group, the HPV-positive group presented a higher abnormal rate of *Lactobacillus*, catalase, cleanliness, neuraminidase and proline aminopeptidase ($p<0.05$). However, no difference was exhibited in the abnormal rates of pH value, leukocyte esterase and acetylglucosaminidase between the two groups ($p>0.05$).

Comparison of positive rates of Bacterial vaginosis, Trichomonas vaginitis and Vulvovaginal candidiasis between the two groups

As Table 2 indicates, relative to the HPV-negative group, the HPV-positive group presented a higher positive rate of BV ($p<0.05$). However, no differences were exhibited in the positive rates of TV and VVC between the two groups ($p>0.05$).

Correlation between HPV infection and vaginal microecology

According to the results of univariate analysis between the two groups, *Lactobacillus*, catalase, cleanliness, neuraminidase, proline aminopeptidase and BV were taken as covariables, and HPV infection as dependent variables, and a multivariate logistic regression analysis was performed. The multivariate logistic regression analysis results showed that catalase, proline aminopeptidase and BV were closely related to HPV infection ($p<0.05$), and were risk factors for HPV infection, as shown in Table 3.

Clinical efficacy between two groups

Relative to the CG, the OG presented a higher total effective rate ($p<0.05$, Table 4).

Inflammation between the two groups

Before therapy, there were no differences in levels of inflammatory markers between the two groups ($p>0.05$). After therapy, TNF-α and IL-6 levels were declined in the two groups ($p<0.01$). Importantly, relative to the CG, the OG presented lower levels of the above inflammatory markers after therapy ($p<0.01$, Fig. 1).

Immune function between two groups

Prior to therapy, there were no differences in levels of immune function indexes between the two groups ($p>0.05$). After therapy, $CD4^+$ and $CD4^+/CD8^+$ levels were elevated, while $CD8^+$ levels declined in the two groups ($p<0.01$). Importantly, relative to the CG, the OG presented better improvements in the above immune function indexes after therapy ($p<0.01$, Fig. 2).

Vaginal microecology between two groups

The proportion of grade II-III vaginal flora density and grade II-III vaginal flora diversity in group 2 were higher than those before treatment ($p<0.001$ and $p=0.002$). Importantly, relative to the CG, the OG presented a higher proportion of grade II-III

Table 1. Comparison of vaginal microecology between two groups.

Index	HPV-negative group (n=320)	HPV-positive group (n=180)	χ^2	p
Lactobacillus			8.638	0.003
Normal	131 (40.94)*	50 (27.78)		
Abnormal	189 (59.06)	130 (72.22)		
Catalase			8.316	0.004
Normal	134 (41.88)	52 (28.89)		
Abnormal	186 (58.12)	128 (71.11)		
pH			0.278	0.598
≤4.5	304 (95.00)	169 (93.89)		
>4.5	16 (5.00)	11 (6.11)		
Cleanliness			5.532	0.019
Normal	163 (50.94)	72 (40.00)		
Abnormal	157 (49.06)	108 (60.00)		
Leukocyte esterase			1.468	0.226
Normal	80 (25.00)	54 (30.00)		
Abnormal	240 (75.00)	126 (70.00)		
Neuraminidase			12.90	<0.001
Normal	272 (85.00)	129 (71.67)		
Abnormal	48 (15.00)	51 (28.33)		
Proline aminopeptidase			40.47	<0.001
Normal	265 (98.75)	147 (81.67)		
Abnormal	4 (1.25)	33 (18.33)		
Acetylglucosaminidase			0.015	0.904
Normal	268 (83.75)	150 (83.33)		
Abnormal	52 (16.25)	30 (16.67)		

*Data is express as n (%)

vaginal flora density and grade II-III vaginal flora diversity ($p<0.001$, Tables 5 and 6).

Occurrence of adverse reactions between two groups

As Table 7 shows, no difference was seen in adverse reactions between the two groups ($p>0.05$).

HPV clearance between two groups

Following the three-month treatment period, HPV testing was repeated. The clearance rate of HPV in the observation group (OG) (interferon α-2b + *Lactobacillus*) was significantly higher compared to the control group (CG) (interferon α-2b alone) (Table 8). Specifically, HPV clearance was observed in:

- OG: 68 of 90 cases (75.56%)
- CG: 51 of 90 cases (56.67%)
- $\chi^2 = 7.156$, $P = 0.0076$

This finding strongly suggests that the addition of *Lactobacillus* vaginal capsules

Table 2. Comparison of positive rate of Bacterial vaginosis, Trichomonas vaginitis y Vulvovaginal candidiasis between the two groups.

Index	HPV-negative group (n=320)	HPV-positive group (n=180)	χ^2	*p*
Bacterial vaginosis			5.023	0.025
Positive	30 (9.38)*	29 (16.11)		
Negative	290 (90.62)	151 (83.89)		
Trichomonas vaginitis			0.183	0.669
Positive	15 (4.69)	10 (5.56)		
Negative	305 (95.31)	170 (94.44)		
Vulvovaginal candidiasis			0.020	0.142
Positive	29 (9.06)	17 (9.44)		
Negative	291 (90.94)	163 (90.56)		

*Data is expressed as n (%)

Table 3. Correlation between HPV infection and vaginal microecology.

Influencing factors	β	SE	Wald	OR	95% CI	p
Catalase	1.0	0.1	66.5	2.8	2.2-3.6	<0.05
Proline aminopeptidase	1.7	0.4	15.0	5.6	2.3-13.5	<0.05
Bacterial vaginosis	1.1	0.5	4.5	3.1	1.1-8.9	<0.05

Table 4. Clinical efficacy between the two groups.

Groups	Cases (n)	Obvious Effect n (%)	Effective n (%)	Ineffective n (%)	Total Effective Rate n (%)	χ^2	*p*
Control Group	90	38 (42.23%)*	32 (35.55%)	20 (22.22%)	70 (77.78%)	10.22	0.001
Observation Group	90	57 (63.33%)	28 (31.11%)	5 (5.56%)	85 (94.44%)		

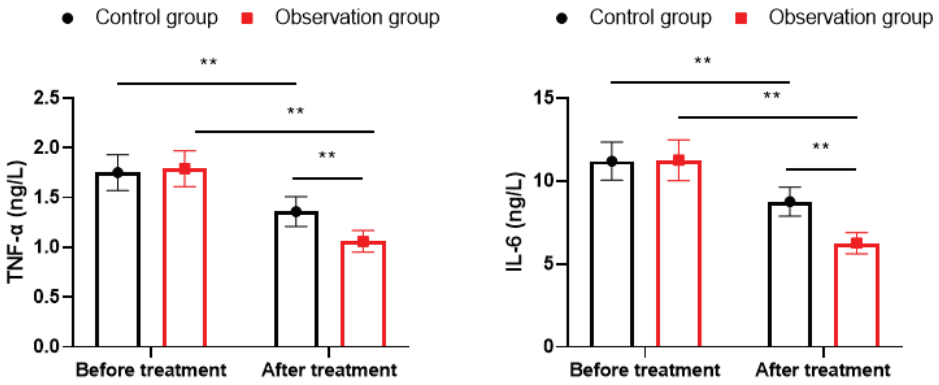

Fig. 1. Comparison of inflammation between the two groups. **p<0.01.

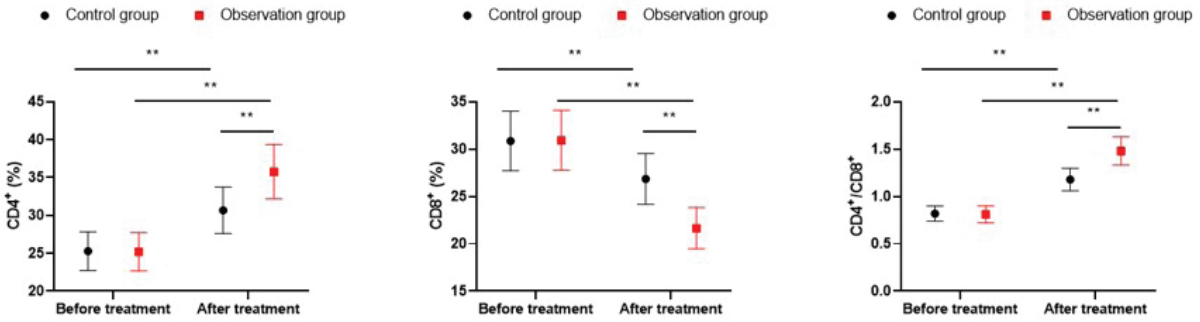

Fig. 2. Immune function between the two groups. **p<0.01.

Table 5. Vaginal flora density (grade II-III).

Groups	Cases	Vaginal flora density				χ^2	p
		Before treatment		After treatment			
		Cases	%	Cases	%		
Control group	90	36	40.00	61	67.78	13.97	<0.001
Observation group	90	34	37.78	81	90.00	53.19	<0.001
χ^2		0.093		13.34			
p		0.759		<0.001			

Table 6. Vaginal flora diversity (grade II-III).

Groups	Cases	Vaginal flora density				χ^2	p
		Before treatment		After treatment			
		Cases	%	Cases	%		
Control group	90	39	43.33	60	66.67	9.899	0.002
Observation group	90	41	45.56	83	92.23	45.73	<0.001
χ^2		0.090		18.00			
p		0.764		<0.001			

Table 7. Occurrence of adverse reactions between two groups.

Groups	Cases	Burning sensation of vulva	Pruritus	Gastrointestinal discomfort	Total incidence rate
Control group	90	2 (2.22)*	0 (0.00)	2 (2.22)	4 (4.44)
Observation group	90	2 (2.22)	1 (1.11)	2 (2.22)	5 (5.55)
χ^2					0.117
p					0.732

*Data is express as n (%).

Table 8. Comparison of HPV clearance between the two groups after treatment.

Group	Total Cases (n)	HPV Negative (Cleared)	HPV Positive (Persistent)	Clearance Rate (%)	χ^2	p
Control Group	90	51	39	56.67%		
Observation Group	90	68	22	75.56%	7.156	0.0076

improves the antiviral effect of interferon α-2b and contributes to a more favorable microecological environment for viral clearance.

DISCUSSION

About 10% to 30% of adults are infected with HPV, and sexually active people are even higher, reaching 50% to 80%, and the most susceptible age is 20 to 29 years old [13]. After HPV infection, some patients continue to be infected with high-risk HPV, cervical intraepithelial tumour-like lesions, after 10 to 15 years, the development of early cervical cancer, and then advanced cervical cancer [14]. HR-HPV is the leading cause of cervical cancer, with 99% of cervical cancer HPV positive, of which HPV16 and HPV18 accounted for about 70%. HPV infection is necessary to cause cervical cancer, but the number of copies of HPV-DNA is not directly related to disease progression, and only persistent high-risk HPV infection increases the risk of cervical cancer [15]. At present, HPV monitoring is the primary screening method for cervical cancer, the tracking method of cervical lesions after treatment and the indicator of the risk of cervical intraepithelial neoplasia [16].

The vaginal microecosystem is a relatively complex system among the four major human ecosystems, which plays an important role in preventing microbial invasion [17]. In our study, the results showed that compared to the HPV-negative group, the HPV-positive group presented a higher abnormal rate of *Lactobacillus*, catalase, cleanliness, neuraminidase, and proline aminopeptidase, consistent with previous reports [18,19]. The typical vaginal microecological environment of women is *Lactobacillus* as the dominant bacteria [20]. *Lactobacillus* can maintain a stable pH value (pH ≤4.5) in the vagina by producing lactic acid, lactobacillin, H_2O_2, and bioactive substances so that the vaginal flora can maintain a balanced state, and through its adsorption on the vaginal mucosa, the formation of a biological barrier against pathogenic microorganisms [21]. Hydrogen peroxide can inhibit or kill bacteria, and the function of catalase is to promote the decomposition of hydrogen peroxide, and reduce the effect of hydrogen peroxide on killing pathogens, resulting in the survival and proliferation of pathogens in the vagina, increasing HPV susceptibility [22]. Reproductive system infections can also lead to changes in cleanliness, abnormal levels of neuraminidase and proline aminopeptidase, aggravate vaginal microecological environment disorders, form a vicious cycle, and increase the risk of HPV infection [23]. In addition, HPV infection may also cause oxidative stress, damage the antioxidant oxidase system in the patient, reduce the level of antioxidants, and damage cellular DNA. In the process of cellular DNA replication, HPV DNA can be transferred to the DNA of host cells, aggravating the degree of mucosal damage, further aggravating the abnormality of the vaginal microecological environment, and forming a vicious cycle [24]. Therefore, the vaginal flora is the first line of defense against pathogenic microorganisms.

Our study also revealed that relative to the HPV-negative group, the HPV-positive group presented a higher positive rate of BV. The reason is as follows: (1) The decrease or disappearance of vaginal *Lactobacillus* in BV patients provides opportunities for the growth and reproduction of other bacteria

such as Gardner-bacteria and anaerobic bacteria, causing the imbalance of vaginal microecological environment, the reduction of the protective function of *Lactobacillus* on the vagina, and the decreased ability of vaginal virus clearance, thus susceptible to HPV infection [25]; (2) BV can affect the expression of vaginal local immune factors, thereby destroying the immune response and making it more susceptible to HPV infection [26]; (3) BV can cause the destruction of cytoskeleton protein of vaginal mucosal epithelium, accelerate the damage of vaginal mucosal epithelial cells, and increase susceptibility to HPV[27]; (4) The sialoglycoidase produced by BV leads to the degradation of vaginal mucosal epithelial protective factors, which enables bacteria to adhere and form biofilms, further leading to the difficulty of HPV removal and the formation of persistent infection [28]. For these reasons, BV not only increases the susceptibility to HPV but also delays the body's clearance of HPV.

Antiviral therapy is the preferred treatment for HPV infection, with commonly used drugs such as recombinant human interferon α-2b gel, an important glycoprotein produced by white blood cells that play a key role in fighting viral infection and has antibacterial activity against a variety of pathogens [29]. Interferon α-2b can inhibit cell proliferation, inhibit angiogenesis, and have cytotoxic effects on tumor cells in various ways [30]. On the one hand, it can bind to specific receptors on the cell surface, thereby inhibiting the growth of virus-infected cells and prolonging the cell cycle of malignant cells [31]. On the other hand, biosynthase plays an important role in promoting cell proliferation in viral cells, and the inhibition of interferon α-2b can play a good role in inhibiting viral replication [32]. In treating HPV infection, transvaginal medication can directly act on cervical epithelial cells and has a specific effect. However, the vagina has a complex microenvironment, which can produce metabolites that compete with drug receptors under the action of the microbiome, resulting in limited effects of single drugs [33].

In this study, the observation group was given *Lactobacillus* vaginal capsules based on interferon α-2b, and the results manifested that relative to the CG, the OG presented a higher total effective rate. The reason may be that *Lactobacillus* vaginal capsule is a kind of microbial preparation, with living intestinal streptococcus as the main component [34], which can increase the production of acidic substances through the decomposition of internal glycogen, thus reducing the pH value of the vaginal environment, effectively promoting the proliferation of *Lactobacillus* in the host body, adjusting the microecological environment, strengthening the self-purification function of the mucosal immune system, and thus enabling the mucosal immune system to rebuild more effectively [35]. In addition, *Lactobacillus* vaginal capsules play a particular role in regulating the immune system, stimulating the release of antibodies in the body and inhibiting the reproduction of bacteria [36]. By rebuilding a good vaginal environment and establishing a protective barrier, the effect of interferon α-2b can be reduced, and the clinical efficacy can be improved.

IL-6 and TNF-α are inflammatory factors that correlate specifically with HPV infection[37]. When the body is infected with HPV, the levels of IL-6 and TNF-α as pro-inflammatory factors will increase abnormally [38]. Therefore, the body's inflammation can be judged by observing the changes of IL-6 and TNF-α levels in the body. The results of our study manifested that relative to the CG, the OG presented lower levels of the above inflammatory markers after therapy, suggesting that *Lactobacillus* vaginal capsules combined with recombinant human interferon α-2b gel could suppress inflammation of the body. Similarly, Dobrohotova et al. suggested that the additional use of *Lactobacillus* vaginal capsules in the complex therapy of lower urinary tract infections reduced inflammation [39].

Under normal circumstances, the body's own immune system can resist the invasion of pathogenic microorganisms, but the immune system has obstacles; the resistance to viruses will decline, easy to cause viral infections, such as HPV infection [40]. The immune function of the body mainly depends on T lymphocytes. $CD4^+$ can coordinate B cells, promote their differentiation and produce antibodies; $CD8^+$ are viral T lymphocytes. When the body's $CD4^+$, $CD8^+$, and $CD4^+/CD8^+$ decline, the body's immune function is disturbed and vulnerable to HPV invasion [41]. Our study demonstrated that relative to the CG, the OG presented better improvements of $CD4^+$, $CD8^+$ and $CD4^+/CD8^+$ levels after therapy, suggesting that *Lactobacillus* vaginal capsule combined with recombinant human interferon α-2b gel could enhance the immune function of the body, which was following a study proposed by Ang et al. [42].

In addition, our study pointed out that relative to the CG, the OG presented a higher proportion of grade II-III vaginal flora density and grade II-III vaginal flora diversity. The reason is that recombinant human interferon α-2b can regulate immune responses by activating intracellular signalling pathways [43]. The drug acts on immune cells, such as macrophages and dendritic cells, thereby enhancing their phagocytosis [44]. Recombinant human interferon α-2b induces a series of cell signalling events by binding to specific receptors, ultimately activating and enhancing immune cells [45]. Besides, HPV infection is directly related to the dysregulation of the vaginal microenvironment and the lack of *Lactobacillus*, which leads to a vicious cycle of the disease [46]. After the application of recombinant human interferon α-2b, the proliferation of antiviral protein in the body was promoted, and the antiviral ability was improved [47]. At the same time, the *lactobacillus* vaginal capsule is vaginally administered, which takes live lactic acid bacteria as the main component and has a certain antibacterial effect, and inhibits the reproduction of harmful bacteria by producing organic acids and other antibacterial substances [48]. In addition, *Lactobacillus* vaginal capsules contain a large number of active lactic acid bacteria cells. After vaginal medication, it can increase the number of beneficial bacteria, inhibit the excessive reproduction of harmful bacteria, promote the balance of vaginal flora and maintain a healthy microecological environment [49].

Moreover, the results of this study showed that there was no statistical difference in the total incidence of adverse reactions between the two groups, which reflected that the adverse reactions produced by *Lactobacillus* vaginal capsule combined with recombinant human interferon α-2b gel were within the acceptable range and the safety was reasonable.

In conclusion, our study indicates that HPV is significantly correlated with vaginal microecological environment, and catalase, proline aminopeptidase and BV were closely related to HPV infection. In addition, the *Lactobacillus* vaginal capsule combined with recombinant human interferon α-2b gel has practical clinical efficacy, which can reduce inflammation, promote immune function, improve vaginal microecological environment, and is safe in the treatment of patients with HPV infection.

ACKNOWLEDGMENTS

None.

Funding

There was no funding for the study.

Conflict of interest

There is no conflict of interest with this manuscript.

Numbers ORCID of authors

- Yanling Sun (YS): 0009-0003-1834-8742
- Li Li (LL): 0009-0007-9455-7027

- Wenxin Xu (WX): 0009-0009-8991-6560
- Cen Ma (CM): 0009-0003-1178-199X

Participation of the authors

YS and LL: conceived and designed the study, as well as collected and analysed the data. WX and CM: drafted and reviewed the manuscript, and finally approved the manuscript.

REFERENCES

1. **Abu-Rustum NR, Yashar CM, Arend R, Barber E, Bradley K, Brooks R, et al.**. NCCN Guidelines® Insights: Cervical Cancer, Version 1.2024. J Natl Compr Canc Netw 2023; 21(12): 1224-1233. *https://doi.org10.6004/jnccn.2023.0062.*
2. **Singh D, Vignat J, Lorenzoni V, Eslahi M, Ginsburg O, Lauby-Secretan B,** et al. Global estimates of incidence and mortality of cervical cancer in 2020: a baseline analysis of the WHO Global Cervical Cancer Elimination Initiative. Lancet Glob Health 2023; 11(2): e197-e206. *https://doi.org10.1016/s2214-109x(22)00501-0.*
3. **Rahangdale L, Mungo C, O'Connor S, Chibwesha CJ, Brewer NT**. Human papillomavirus vaccination and cervical cancer risk. Bmj 2022; 379: e070115. *https://doi.org10.1136/bmj-2022-070115.*
4. **Sucato A, Buttà M, Bosco L, Di Gregorio L, Perino A, Capra G**. Human Papillomavirus and male infertility: What do we know? Int J Mol Sci 2023; 24(24). *https://doi.org10.3390/ijms242417562.*
5. **Nelson CW, Mirabello L**. Human papillomavirus genomics: Understanding carcinogenicity. Tumour virus research 2023; 15: 200258. *https://doi.org10.1016/j.tvr.2023.200258.*
6. **Oyouni AAA**. Human papillomavirus in cancer: Infection, disease transmission, and progress in vaccines. J Infect Public Health 2023; 16(4): 626-631. *https://doi.org10.1016/j.jiph.2023.02.014.*
7. **Zhang Z, Ma Q, Zhang L, Ma L, Wang D, Yang Y, et al**. Human papillomavirus and cervical cancer in the microbial world: exploring the vaginal microecology. Front Cell Infect Microbiol 2024; 14: 1325500. *https://doi.org10.3389/fcimb.2024.1325500.*
8. **Zang L, Feng R, Huang Y, Huang J, Hu Y**. Relationship between vaginal microecology and human papillomavirus infection as well as cervical intraepithelial neoplasia in 2,147 women from Wenzhou, the southeast of China. Front Oncol 2023; 13: 1306376. *https://doi.org10.3389/fonc.2023.1306376.*
9. **Ye J, Qi X**. Vaginal microecology and its role in human papillomavirus infection and human papillomavirus associated cervical lesions. Apmis 2023. *https://doi.org10.1111/apm.13356.*
10. **Fan Z, Han D, Fan X, Zeng Y, Zhao L**. Analysis of the correlation between cervical HPV infection, cervical lesions and vaginal microecology. Front Cell Infect Microbiol 2024; 14: 1405789. *https://doi.org10.3389/fcimb.2024.1405789.*
11. **Zhao HD, Feng XL, Zhao Y, Li N**. Randomized controlled study: Sophora flavescens gel in treatment of cervical HPV infection]. Zhongguo Zhong Yao Za Zhi 2016; 41(21): 4072-4075. *https://doi.org10.4268/cjcmm20162129.*
12. **Mändar R, Sõerunurk G, Štšepetova J, Smidt I, Rööp T, Kõljalg S, et al.** Impact of *Lactobacillus crispatus*-containing oral and vaginal probiotics on vaginal health: a randomised double-blind placebo controlled clinical trial. Benef Microbes 2023; 14(2): 143-152. *https://doi.org10.3920/bm2022.0091.*
13. **Li M, Zhao C, Zhao Y, Li J and Wei L**. Immunogenicity, efficacy, and safety of human papillomavirus vaccine: Data from China. Front Immunol 2023; 14: 1112750. *https://doi.org10.3389/fimmu.2023.1112750.*
14. **Piña-Sánchez P**. Human papillomavirus: challenges and opportunities for the control of cervical cancer. Archi Med Res 2022; 53(8): 753-769. *https://doi.org10.1016/j.arcmed.2022.11.009.*

15. **Le D, Coriolan Ciceron A, Jeon MJ, Gonzalez LI, Jordan JA, Bordon J, Long B**. Cervical cancer prevention and high-risk HPV self-sampling awareness and acceptability among women living with HIV: A qualitative investigation from the patients' and providers' perspectives. Curr Oncol 2022; 29(2): 516-533. *https://doi.org10.3390/curroncol29020047.*
16. **Ye J, Zheng L, He Y, Qi X**. Human papillomavirus associated cervical lesion: pathogenesis and therapeutic interventions. MedComm (2020) 2023; 4(5): e368. *https://doi.org10.1002/mco2.368.*
17. **Chen X, Lu Y, Chen T, Li R**. The female vaginal microbiome in health and bacterial vaginosis. Front Cell Infect Microbiol 2021; 11: 631972. *https://doi.org10.3389/fcimb.2021.631972.*
18. **Li X, Wu J, Wu Y, Duan Z, Luo M, Li L, Li S, Jia Y**. Imbalance of vaginal microbiota and immunity: two main accomplices of cervical Cancer in Chinese women. Int J Womens Health 2023; 15: 987-1002. *https://doi.org10.2147/ijwh.S406596.*
19. **Zheng JJ, Miao JR, Wu Q, Yu CX, Mu L, Song JH**. Correlation between HPV-negative cervical lesions and cervical microenvironment. Taiwan J Obstet Gynecol 2020; 59(6): 855-861. *https://doi.org10.1016/j.tjog.2020.08.002.*
20. **Deka N, Hassan S, Seghal Kiran G, Selvin J**. Insights into the role of vaginal microbiome in women's health. J Basic Microbiol 2021; 61(12): 1071-1084. *https://doi.org10.1002/jobm.202100421.*
21. **Scillato M, Spitale A, Mongelli G, Privitera GF, Mangano K, Cianci A, et al.**. Antimicrobial properties of *Lactobacillus* cell-free supernatants against multidrug-resistant urogenital pathogens. MicrobiologyOpen 2021; 10(2): e1173. *https://doi.org10.1002/mbo3.1173.*
22. **Preci DP, Almeida A, Weiler AL, Mukai Franciosi ML, Cardoso AM**. Oxidative damage and antioxidants in cervical cancer. Int J Gynecol Cancer 2021; 31(2): 265-271. *https://doi.org10.1136/ijgc-2020-001587.*
23. **Li J, Jiang L, Wang C, Meng J, Wang H, Jin H**. Investigation of the relationship between the changes in vaginal microecological enzymes and human papillomavirus (HPV) infection. Medicine (Baltimore) 2024; 103(6): e37068. *https://doi.org10.1097/md.0000000000037068.*
24. **Cruz-Gregorio A, Aranda-Rivera AK, Ortega-Lozano AJ, Pedraza-Chaverri J, Mendoza-Hoffmann F**. Lipid metabolism and oxidative stress in HPV-related cancers. Free Radic Biol Med 2021; 172: 226-236. *https://doi.org10.1016/j.freeradbiomed.2021.06.009.*
25. **Ntuli L, Mtshali A, Mzobe G, Liebenberg LJ, Ngcapu S**. Role of immunity and vaginal microbiome in clearance and persistence of human papillomavirus infection. Front Cell Infect Microbiol 2022; 12: 927131. *https://doi.org10.3389/fcimb.2022.927131.*
26. **Martins BCT, Guimarães RA, Alves RRF, Saddi VA**. Bacterial vaginosis and cervical human papillomavirus infection in young and adult women: a systematic review and meta-analysis. Revista de saude publica 2023; 56: 113. *https://doi.org10.11606/s1518-8787.2022056004412.*
27. **Guo YL, You K, Qiao J, Zhao YM, Geng L**. Bacterial vaginosis is conducive to the persistence of HPV infection. Int J STD AIDS 2012; 23(8): 581-584. *https://doi.org10.1258/ijsa.2012.011342.*
28. **Xu X, Zhang Y, Yu L, Shi X, Min M, Xiong L, et al.** . A cross-sectional analysis about bacterial vaginosis, high-risk human papillomavirus infection, and cervical intraepithelial neoplasia in Chinese women. Sci Rep 2022; 12(1): 6609. *https://doi.org10.1038/s41598-022-10532-1.*
29. **Kaur K, Kush P, Pandey RS, Madan J, Jain UK, Katare OP**. Stealth lipid coated aquasomes bearing recombinant human interferon-α-2b offered prolonged release and enhanced cytotoxicity in ovarian cancer cells. Biomed Pharmacother 2015; 69: 267-276. *https://doi.org10.1016/j.biopha.2014.12.007.*
30. **Yu J, Lu X, Tong L, Shi X, Ma J, Lv F, et al.** Interferon-α-2b aerosol inhalation is associated with improved clinical outcomes in patients with coronavirus disease-2019.

Br J Clin Pharmacol 2021; 87(12): 4737-4746. *https://doi.org10.1111/bcp.14898.*

31. **Khan WA**. Recombinant interferon Alpha-2b is ahigh-affinity antigen for Type 1d diabetes autoantibodies. Can J Diabetes 2017; 41(2): 217-223. *https://doi.org10.1016/j.jcjd.2016.10.001.*
32. **Yang A, Yang C, Yang B**. Use of hydroxychloroquine and interferon alpha-2b for the prophylaxis of COVID-19. Med Hypotheses 2020; 144: 109802. *https://doi.org10.1016/j.mehy.2020.109802.*
33. **Mahajan G, Doherty E, To T, Sutherland A, Grant J, Junaid A, et al.** Vaginal microbiome-host interactions modeled in a human vagina-on-a-chip. Microbiome 2022; 10(1): 201. *https://doi.org10.1186/s40168-022-01400-1.*
34. **Ang XY, Mageswaran UM, Chung YLF, Lee BK, Azhar SNA, Roslan NS, et al.** Probiotics reduce vaginal candidiasis in pregnant women via modulating abundance of Candida and *Lactobacillus* in vaginal and cervicovaginal regions. Microorganisms 2022; 10(2). *https://doi.org10.3390/microorganisms10020285.*
35. **Koirala R, Gargari G, Arioli S, Taverniti V, Fiore W, Grossi E, et al.** Effect of oral consumption of capsules containing *Lactobacillus* paracasei LPC-S01 on the vaginal microbiota of healthy adult women: a randomized, placebo-controlled, double-blind crossover study. FEMS microbiology ecology 2020; 96(6). *https://doi.org10.1093/femsec/fiaa084.*
36. **Marrazzo JM, Cook RL, Wiesenfeld HC, Murray PJ, Busse B, Krohn M, Hillier SL**. Women's satisfaction with an intravaginal *Lactobacillus* capsule for the treatment of bacterial vaginosis. J Women's Health (2002) 2006; 15(9): 1053-1060. *https://doi.org10.1089/jwh.2006.15.1053.*
37. **Yamaguchi M, Mtali YS, Sonokawa H, Takashima K, Fukushima Y, Kouwaki T, Oshiumi H**. HPV vaccines induce trained immunity and modulate pro-inflammatory cytokine expression in response to secondary Toll-like receptor stimulations. Microbiol Immmunol, 2024; 68(2): 65-74. *https://doi.org10.1111/1348-0421.13108.*
38. **Wu DW, Tsai LH, Chen PM, Lee MC, Wang L, Chen CY, Cheng YW, Lee H**. Loss of TIMP-3 promotes tumor invasion via elevated IL-6 production and predicts poor survival and relapse in HPV-infected non-small cell lung cancer. Am J Pathol 2012; 181(5): 1796-1806. *https://doi.org10.1016/j.ajpath.2012.07.032.*
39. **Dobrohotova YE, Korotkikh IN, Kuzmenko AV, VKV Gyaurgiev TA**. [The efficiency of probiotics in the prevention of recurrent lower urinary tract infections and bacterial vaginosis]. Urologiia (Moscow, Russia : 1999) 2021(4): 30-34.
40. **Joshi S, Anantharaman D, Muwonge R, Bhatla N, Panicker G, Butt J, et al.** Evaluation of immune response to single dose of quadrivalent HPV vaccine at 10-year post-vaccination. Vaccine 2023; 41(1): 236-245. *https://doi.org10.1016/j.vaccine.2022.11.044.*
41. **Dolina JS, Lee J, Brightman SE, McArdle S, Hall SM, Thota RR, et al.** Linked CD4+/CD8+ T cell neoantigen vaccination overcomes immune checkpoint blockade resistance and enables tumor regression. J Clin Invest 2023; 133(17). *https://doi.org10.1172/jci164258.*
42. **Ang XY, Roslan NS, Ahmad N, Yusof SM, Abdullah N, Nik Ab Rahman NN, et al**. *Lactobacillus* probiotics restore vaginal and gut microbiota of pregnant women with vaginal candidiasis. Benef Microbes 2023; 14(5): 421-431. *https://doi.org10.1163/18762891-20220103.*
43. **Shahid S, Nawaz Chaudhry M, Mahmood N and Sheikh S**. Mutations of the human interferon alpha-2b gene in brain tumor patients exposed to different environmental conditions. Cancer Gene Ther 2015; 22(5): 246-261. *https://doi.org10.1038/cgt.2015.12.*
44. **Ding GQ, Yu YL, Shen ZJ, Zhou XL, Chen SW, Liao GD, Zhang Y**. Antitumor effects of human interferon-alpha 2b secreted by recombinant bacillus Calmette-Guérin vaccine on bladder cancer cells. J Zhejiang Univ Sci B 2012; 13(5): 335-341. *https://doi.org10.1631/jzus.B1100366.*
45. **Kanca H, Tez G, Bal K, Ozen D, Alcigir E, Atalay Vural S**. Intratumoral recombinant

human interferon alpha-2a and vincristine combination therapy in canine transmissible venereal tumour. Vet Med Sci 2018; 4(4): 364-372. *https://doi.org10.1002/vms3.119.*

46. **Ilhan ZE, Łaniewski P, Thomas N, Roe DJ, Chase DM ,Herbst-Kralovetz MM**. Deciphering the complex interplay between microbiota, HPV, inflammation and cancer through cervicovaginal metabolic profiling. EBioMedicine 2019; 44: 675-690. *https://doi.org10.1016/j.ebiom.2019.04.028.*
47. **Hermeling S, Aranha L, Damen JM, Slijper M, Schellekens H, Crommelin DJ, Jiskoot W**. Structural characterization and immunogenicity in wild-type and immune tolerant mice of degraded recombinant human interferon alpha2b. Pharm Res 2005; 22(12): 1997-2006. *https://doi.org10.1007/s11095-005-8177-9.*
48. **Bi Z, Wang Q, Yang T, Liu Y, Yuan J, Li L, Guo Y**. Effect of *Lactobacillus delbrueckii* subsp. lactis on vaginal radiotherapy for gynecological cancer. Sci Rep 2023; 13(1): 10105. *https://doi.org10.1038/s41598-023-37241-7.*
49. **Lan J, Chen C**. The role of lactic acid bacteria in maintaining vaginal internal environment homeostasis in patients with infertility. Microb Pathog 2023; 176: 106004. *https://doi.org10.1016/j.micpath.2023.106004.*

Invest Clin 66(2): 147 - 156, 2025 https://doi.org/10.54817/IC.v66n2a02

Value of ultrasound shear wave elastography and gray-scale ultrasonography for assessing the bladder neck status of women with stress urinary incontinence.

Huaying Shan, Jingying Fei, Hua Chu, Mingsong Liu, Yan Lu and Xuekui Pan

Department of Ultrasound, Huzhou Maternal and Child Health Hospital, Huzhou, Zhejiang Province, China.

Keywords: bladder neck; elastography; stress urinary incontinence; ultrasonography.

Abstract. We aimed to investigate the value of ultrasound shear wave elastography (US-SWE) and gray-scale ultrasonography for assessing the bladder neck status of patients with stress urinary incontinence (SUI). Seventy-two puerperal women with SUI treated from February 2022 to September 2023 were selected as a research group, while another 50 healthy pregnant women receiving physical examination in the same period were selected as a control group. US-SWE and gray-scale ultrasonography were performed for all subjects. The height, length, circumference and area of the perineal body at rest and the maximum, as well as the thicknesses and elastic moduli of anterior and posterior lips of the bladder neck, were compared. At the maximum Valsalva maneuver (VM), the research group had higher height, smaller length and area, and shorter circumference of the perineal body than those of the control group ($p<0.05$). Maternal SUI was positively correlated with the height of the perineal body ($r>0$, $p<0.05$) but negatively correlated with the length, circumference and area of the perineal body and the elastic moduli of anterior and posterior lips of the bladder neck ($r<0$, $p<0.05$). The elastic moduli of the anterior and posterior lips of the bladder neck and the height, length, circumference, and area of the perineal body at the maximum VM were valuable for assessing maternal SUI. US-SWE and gray-scale ultrasonography parameters are closely related to maternal SUI, and the risk of maternal SUI can be assessed early by the bladder neck status.

Corresponding author: Xuekui Pan. Department of Ultrasound, Huzhou Maternal and Child Health Hospital, Huzhou 313000, Zhejiang Province, China. E-mail: panxkhmchh@csc-edu.cn

Valor de la elastografía ultrasónica de onda cortante y de la ecografía en escala de grises para evaluar el estado del cuello vesical de mujeres con incontinencia urinaria de esfuerzo.

Invest Clin 2025; 66 (2): 147 – 156

Palabras clave: cuello vesical; elastografia; incontinencia urinaria de esfuerzo; ultrasonografía.

Resumen. Nuestro objetivo fue investigar el valor de la elastografía ultrasónica de onda cortante (US-SWE) y la ecografía en escala de grises para evaluar el estado del cuello vesical de pacientes con incontinencia urinaria de esfuerzo (IUE). Setenta y dos mujeres puerperales con IUE tratadas entre febrero de 2022 y septiembre de 2023 fueron seleccionadas como grupo de investigación, mientras que otras 50 mujeres embarazadas sanas que recibieron examen físico en el mismo período fueron seleccionadas como grupo control. A todos los sujetos se les realizó eco de US-SWE y escala de grises. Se compararon la altura, longitud, circunferencia y área del cuerpo perineal en reposo y el máximo, así como los espesores y los módulos elásticos de los labios anterior y posterior del cuello vesical. En el momento de la maniobra de Valsalva máxima (VM), el grupo de investigación tuvo mayor altura, menores longitud y área y menor circunferencia del cuerpo perineal que el grupo control ($p<0,05$). La IUE materna se correlacionó positivamente con la altura del cuerpo perineal ($r>0$, $p<0,05$), pero negativamente con la longitud, circunferencia y área del cuerpo perineal y los módulos elásticos de los labios anterior y posterior del cuello vesical ($r<0$, $p<0,05$). Los módulos elásticos de los labios anterior y posterior del cuello vesical y la altura, longitud, circunferencia y área del cuerpo perineal en el VM máximo fueron valiosos para evaluar la IUE materna. Los parámetros de ecografía de US-SWE y escala de grises están estrechamente relacionados con la IUE materna, y el riesgo de IUE materna se puede evaluar tempranamente por el estado del cuello vesical.

Received: 20-08-2024 Accepted: 15-04-2025

INTRODUCTION

Maternal stress urinary incontinence (SUI) is a common pelvic floor dysfunction in postpartum women, mainly because the postpartum pelvic floor fascia is too weak to support the bladder and maintain the urethral closure pressure. SUI does not threaten the life safety of puerperae. However, patients are highly prone to leakage of urine when the intra-abdominal pressure increases due to sneezing, laughing, coughing and exercise, which, if not treated promptly, may lead to eczema, local skin ulceration, vaginitis and urinary system diseases. Moreover, negative emotions, such as inferiority and anxiety, may be produced from all kinds of embarrassment, affecting the patient's mental health [1,2]. Female pelvic floor dysfunction is related to perineal injury and abnormal bladder neck status. Therefore, it is crucial to detect perineal injury and bladder neck elasticity to diagnose and treat maternal SUI[3,4]. Characterized by non-invasiveness, simple operation and repeatability, ultrasonography is commonly used in clinical prac-

tice. In particular, gray-scale ultrasonography can record the internal echo of tissue and process the echo into gray-scale images to accurately display the structure and shape of the examination site. Besides, ultrasound shear wave elastography (US-SWE) can objectively quantify tissue hardness and accurately monitor tissue elasticity [5,6]. Based on this, US-SWE and gray-scale ultrasonography were performed in this study to analyze their values for assessing the bladder neck status of patients with SUI.

PATIENTS AND METHODS

Subjects

A power analysis was conducted using G*Power software for the two-tailed independent-samples t-test, assuming a moderate effect size (Cohen's d = 0.5), a significance level of $\alpha = 0.05$, and 80% power. Using the equation $n = 2 \times [(Z_{1-\alpha/2} + Z_{1-\beta})/d]^2$ (with $Z_{1-0.05/2} \approx 1.96$ and $Z_{1-0.20} \approx 0.84$), $n \approx 63$ participants per group was obtained. With 72 puerperae with SUI and 50 healthy controls enrolled, the post hoc analysis confirmed an overall power of approximately 0.78-0.80, supporting the adequacy of our sample sizes to detect clinically significant differences. Seventy-two puerperae with SUI treated in our hospital from February 2022 to September 2023 were selected as the research group, while another 50 healthy pregnant women receiving the physical examination in the same period were selected as the control group.

Inclusion and exclusion criteria

Inclusion criteria were as follows: (1) puerperae who met the diagnostic criteria for maternal SUI in the research group [7], (2) those with a single pregnancy, (3) those aged 22-35 years old, and (4) those who and whose families signed the informed consent form.

Exclusion criteria involved: (1) subjects with a history of constipation or chronic cough, (2) those with a history of pelvic surgery, (3) those with a history of urinary incontinence before pregnancy, (4) those complicated with urinary system diseases, (5) those complicated with pelvic organ prolapse, pelvic tumor or other diseases that can lead to pelvic function impairment, (6) those with infection or neurogenic urinary incontinence, (7) those with a history of bladder or urethral diseases, (8) those who took hormone drugs within the past six months, or (9) those unable to cooperate in the study due to mental illness or communication disorders.

Examination apparatus

Mindray Resona 8S Diagnostic Ultrasound System (China) equipped with an abdominal probe SC5-1U (frequency: 1-5 MHz) and a superficial probe L14-5WU (frequency: 5-14 MHz) or Mindray Neuwa R9 Diagnostic Ultrasound System (China) equipped with an abdominal probe SC6-1U (frequency: 1-6 MHz) and superficial probes L15-3WU (frequency: 3-15 MHz) and DE10-3WU (frequency: 3-10 MHz) was used.

Examination methods and processes

Before examination, the subject was instructed to empty the bladder. First, gray-scale ultrasonography was performed on the subject in the lithotomy position, and the ultrasonic probe was placed in the perineal body at a depth of 3-4 cm on the anorectal median sagittal plane to display the perineal body (a high-echo wedge-shaped muscular tissue) with the bottom facing upward and the tip facing downward. Then, the morphology, peripheral conditions and internal echo of the perineal body were observed, and its height, length, and circumference area at rest and at the maximum Valsalva maneuver (VM) were measured. Afterwards, the ultrasonic probe was adjusted to make the beam perpendicular to the anorectum, and the image was continuously enlarged by gain regulation. When the long axis of the bladder neck became deformed, the image was frozen, and the thicknesses of the anterior and posterior lips of the bladder neck were measured. In addition, in the STE mode, the sam-

pling frame was placed at an appropriate depth, and its size was adjusted so the sampling frame could completely cover the bladder neck, with a measurement range of 100 kPa. The stable images with no mosaics and color loss were frozen and saved. Then, a circle with a diameter of 3 cm and uniform color was selected as the region of interest. The elastic moduli of the anterior and posterior lips of the bladder neck were measured three times by Q-BOX, and the average value was taken. All examinations were performed by the same sonographer with more than three years of experience.

Outcome evaluation

The height, length, circumference and area of the perineal body at rest and the maximum VM were compared between the two groups. Comparisons were also made on the thicknesses and elastic moduli of the anterior and posterior lips of the bladder neck.

Statistical analysis

SPSS 23.0 software was used for statistical analysis. Measurement data (the height, length, circumference and area of the perineal body, and the thicknesses and elastic moduli of anterior and posterior lips of the bladder neck) were described by (mean ± standard deviation) and subjected to the *t*-test. Count data were described by percentage and subjected to the chi-square test. The point-biserial correlation test analyzed the correlations of maternal SUI with US-SWE and gray-scale ultrasonography parameters. The assessment values of US-SWE and gray-scale ultrasonography parameters were analyzed using receiver operating characteristic (ROC) curves, $p<0.05$ was considered statistically significant.

RESULTS

Baseline clinical data

Age, pre-pregnancy body mass index, gestational age, fetal birth weight, parity and delivery mode were comparable between the two groups ($p>0.05$) (Table 1).

Height, length, circumference and area of the perineal body at rest

There were no significant differences in the height, length, circumference and area of the perineal body at rest between the two groups ($p>0.05$) (Table 2).

Height, length, circumference and area of the perineal body at the maximum Valsalva maneuver

At the maximum VM, the research group had higher height, smaller length and area, and shorter circumference of the perineal body than those of the control group ($p<0.05$) (Table 3).

Table 1. Clinical Data Baseline.

Variable		Research group (n=72)	Control group (n=50)	Statistical	p
Age ($\bar{X}$ ± SD, year)		29.04±3.92	28.69±4.12	t=0.475	0.636
Pre-pregnancy BMI ($\bar{X}$ ± SD, kg/m^2)		22.54±1.18	22.37±1.32	t=0.745	0.458
Gestation age ($\bar{X}$ ± SD, weeks)		39.52±0.96	39.46±0.91	t=0.347	0.729
Fetal birth weight ($\bar{X}$ ± SD, g)		3156.28±493.14	3112.09±502.36	t=0.483	0.630
Parity ($\bar{X}$ ± SD, times)		1.42±0.49	1.35±0.43	t=0.815	0.417
Delivery mode [n (%)]	Natural delivery	46 (63.89)	32 (64.00)	χ^2=0.048	0.977
	Cesarean section	21 (29.17)	15 (30.00)		
	Conversion to cesarean section	5 (6.94)	3 (6.00.)		

Table 2. Height, length, circumference and area of the perineal body at rest.

Group	Height (mm)	Length (mm)	Circumference (mm)	Area (cm^2)
Research (n=72)	8.42±1.12	16.06±2.16	10.26±1.14	2.41±0.79
Control (n=50)	8.29±1.29	16.49±2.03	10.34±0.93	2.53±0.65
t	0.592	1.108	0.410	0.886
p	0.555	0.270	0.682	0.378

Data are expressed as $\bar{x}$ ± SD.

Table 3. Height, length, circumference and area of the perineal body at the maximum Valsalva maneuver.

Group	Height (mm)	Length (mm)	Circumference (mm)	Area (cm^2)
Research (n=72)	8.09±1.23	16.58±2.12	12.86±1.11	2.66±0.81
Control (n=50)	6.87±1.34	18.21±2.64	14.15±0.96	3.52±0.60
t	5.194	3.774	6.665	6.386
p	0.000	0.000	0.000	0.000

Data are expressed as $\bar{x}$ ± SD.

Thickness and elastic moduli of anterior and posterior lips of the bladder neck

The elastic moduli of the anterior and posterior lips of the bladder neck were smaller in the research group than those in the control group ($p<0.05$), while the thicknesses of the anterior and posterior lips of the bladder neck had no significant difference between the two groups ($p>0.05$) (Table 4).

Correlations of maternal SUI with US-SWE and gray-scale ultrasonography parameters

Maternal SUI was positively correlated with the height of the perineal body ($r>0$, $p<0.05$) but negatively correlated with the length, circumference and area of the perineal body and the elastic moduli of anterior and posterior lips of the bladder neck ($r<0$, $p<0.05$) (Table 5).

Assessment values of US-SWE and gray-scale ultrasonography parameters for maternal SUI

ROC curves were plotted by using US-SWE parameters (elastic moduli of the anterior and posterior lips of the bladder neck) and gray-scale ultrasonography parameters (height, length, circumference and area of the perineal body at the maximum VM) that differed between research group and control group as test variables, and the incidence of maternal SUI as a state variable (1=Yes, 0=No). The results revealed that the elastic moduli of anterior and posterior lips of the bladder neck and the height, length, circumference and area of the perineal body at the maximum VM were valuable for assessing maternal SUI (areas under the ROC curves: 0.765, 0.667, 0.809, 0.800, 0.828 and 0.833). The predictive value was optimal when their cut-off values were 7.630 mm, 16.850 mm, 13.305 mm, 3.070 cm, 26.205 kPa and 22.010 kPa, respectively (Table 6 and Fig. 1).

DISCUSSION

The dynamic balance and muscle function of pelvic floor support structures are the main factors controlling normal urination. Once such balance is destroyed and

Table 4. Thickness and elastic moduli of the anterior and posterior lips of the bladder neck.

Group	Thickness of anterior lip (mm)	Elastic modulus of anterior lip (kPa)	Thickness of posterior lip (mm)	Elastic modulus of posterior lip (kPa)
Research (n=72)	4.42±0.59	24.68±4.16	5.13±0.76	19.37±3.78
Control (n=50)	4.38±0.61	30.72±4.97	5.09±0.84	25.22±5.49
t	0.363	7.278	0.274	6.974
p	0.717	0.000	0.785	0.000

Data are expressed as $\bar{x} \pm SD$.

muscle function is impaired, it is difficult to maintain the urethral closure pressure, resulting in SUI [8,9]. Transvaginal ultrasonography is commonly used for the clinical diagnosis of SUI, and observation of the perineal body and bladder neck status at rest and the maximum VM by gray-scale ultrasonography play an important auxiliary role in diagnosing SUI [10]. US-SWE can detect soft tissue hardness, quantitatively assess muscle elasticity and reflect muscle strength [11]. Zhao *et al*. found that the state of urethral striated muscle can be quantitatively assessed by US-SWE, which had important significance in diagnosing and treating SUI in females [12].

In the case of muscle damage of the perineal body, the support capacity declines, resulting in pelvic floor dysfunction [13]. The urethral sphincter of females is mainly composed of circular smooth muscle fibers surrounding the bladder neck. Pregnancy and childbirth may alter the bladder neck status and thus impair its function, so the patients cannot consciously store urine [14]. Therefore, imaging is necessary to measure relevant parameters of the perineal body and bladder neck. The gray-scale ultrasonic probe placed in the vagina emits ultrasonic waves to surrounding tissues, and gray-scale images are obtained, by which doctors can observe the height, length, circumference and area of the perineal body. US-SWE reflects the changes in morphology and hardness of the bladder neck in real-time, thereby indirectly reflecting the degree of damage to the neck[15,16]. In this study, at the maximum VM, the research group had higher height, smaller length and area, and shorter circumference of the perineal body than those of the control group, suggesting that the parameters of the perineal body at the maximum VM of SUI patients were inferior to those of healthy pregnant women.

Moreover, the elastic moduli of anterior and posterior lips of the bladder neck were smaller in the research group than those in the control group, indicating that the bladder neck of SUI patients was less elastic than that of healthy pregnant women. During childbirth, the perineal body is passively expanded, and the mobility of the posterior wall of the bladder and trigonum vesicae accordingly increases with rising abdominal pressure, which may lead to the shortening of the perineal body and loose closure of the bladder neck [17,18]. In the third trimester of pregnancy, the pelvic floor muscles are directly pulled and compressed, resulting in pelvic floor muscle dysfunction. During childbirth, the perineal body is exceptionally pulled (up to 200%) as the fetus passes through the birth canal, so SUI and other pelvic floor dysfunction diseases occur easily [19,20].

We herein found that maternal SUI was positively correlated with the height of the perineal body but negatively correlated with the length, circumference and area of the perineal body and the elastic moduli of the anterior and posterior lips of the blad-

Table 5. Correlations of maternal SUI with US-SWE and gray-scale ultrasonography parameters.

	Group	Height	Length	Circumference	Area	Elastic modulus of the anterior lip	Elastic modulus of the posterior lip
Group	-	0.430/0.000	-0.326/0.000	-0.518/0.00	-0.501/0.000	-0.553/0.00	-0.538/0.000
Height	0.430/0.000	-	-0.210/0.020	-0.297/0.001	-0.256/0.004	-0.309/0.001	-0.268/0.003
Length	-0.326/0.000	-0.210/0.020	-	0.257/0.004	0.180/0.048	0.332/0.000	0.213/0.018
Circumference	-0.518/0.00	-0.297/0.001	0.257/0.004	-	0.172/0.058	0.356/0.000	0.294/0.001
Area	-0.501/0.000	-0.256/0.004	0.180/0.048	0.172/0.058	-	0.298/0.001	0.304/0.001
Elastic modulus of anterior lip	-0.553/0.00	-0.309/0.001	0.332/0.000	0.356/0.000	0.298/0.001	-	0.323/0.000
Elastic modulus of posterior lip	-0.538/0.000	-0.268/0.003	0.213/0.018	0.294/0.001	0.304/0.001	0.323/0.000	-

The values are represented as r/p; the point-biserial correlation test was used.

Table 6. Assessment value of US-SWE and gray-scale ultrasonography parameters for maternal SUI.

Variable	AUC	Standard error	p	95%CI		Cut-off value	Sensitivity	Specificity	Youden index
				Lower limit	Upper limit				
Height	0.765	0.045	0.000	0.678	0.852	7.630 mm	0.780	0.653	0.433
Length	0.667	0.051	0.002	0.566	0.768	16.850 mm	0.660	0.528	0.188
Circumference	0.809	0.040	0.000	0.732	0.887	13.305 mm	0.800	0.681	0.481
Area	0.800	0.039	0.000	0.724	0.877	3.070 cm	0.780	0.681	0.461
Elastic modulus of the anterior lip	0.828	0.038	0.000	0.753	0.903	26.205 kPa	0.860	0.667	0.527
Elastic modulus of the posterior lip	0.833	0.040	0.000	0.755	0.911	22.010 kPa	0.800	0.764	0.564

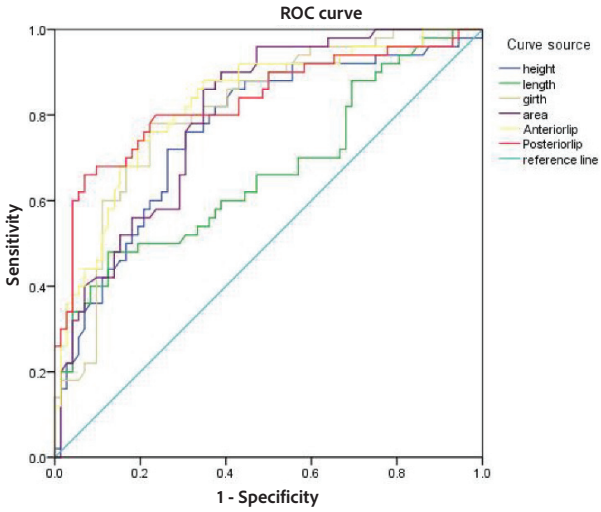

Fig. 1. ROC curves of US-SWE and gray-scale ultrasonography parameters for assessing maternal SUI.

der neck. As indicated by the ROC curve analysis, the elastic moduli of the anterior and posterior lips of the bladder neck and the height, length, circumference and area of the perineal body at the maximum VM were valuable for assessing maternal SUI. The perineal body is the ultimate line of defense against pelvic floor dysfunction and plays an important role in supporting the urethra. Morphological changes of the perineal body affect its support to the vagina and urethra, resulting in cystocele and rectocele, and ultimately SUI [21]. When the bladder neck is less elastic, and the muscle is weak in contraction, it is difficult to control urine, thereby effectively increasing the risk of SUI22. Therefore, patients with postpartum SUI are recommended to receive hot compress and massage to relieve local muscle dysfunction, take anus-lifting exercises to improve muscle relaxation, and undergo medication and surgery to restore the anatomical structure of local tissues if necessary, aiming to ameliorate the prognosis.

Nevertheless, this study is limited. First, the ultrasound technique may have variabilities. Second, this is a single-center study with a small sample size. Third, a subgroup analysis of patients whose ultrasound varies considerably was not conducted. Hence, further multicenter studies with larger sample sizes must confirm our findings.

In conclusion, US-SWE and gray-scale ultrasonography parameters are closely related to maternal SUI, and the risk of maternal SUI can be assessed early by the bladder neck status. US-SWE may be recommended in cases with higher-risk factors, such as a history of multiple pregnancies or advanced maternal age, where monitoring the elasticity and perineal body status of the bladder neck can provide valuable insights into SUI development.

ACKNOWLEDGEMENTS

None.

Funding

This study was financially supported by Grant No. 2022GYB31.

Conflicts of interest

The authors declare they have no conflicts of interest.

ORCID numbers of authors

- Xuekui Pan (XP): 0009-0008-0275-4099
- Huaying Shan (HS): 0009-0006-4354-0893
- Jingying Fei (JF): 0009-0003-9619-6887
- Hua Chu (HC): 0009-0004-7455-6703
- Mingsong Liu (ML): 0009-0002-6541-0732
- Yan Lu (YL): 0009-0006-8693-3750

Participation of each author

HS, XP designed this study and prepared this manuscript; JF, HC, ML, YL performed this study and analyzed the data. All authors have approved the submission and publication of this paper.

REFERENCES

1. **Moore IS, James ML, Brockwell E, Perkins J, Jones AL, Donnelly GM.** Multidisciplinary, biopsychosocial factors contributing to return to running and running related stress urinary incontinence in postpartum women. Br J Sports Med 2021; 55(22): 1286-1292. *https://doi.org/10.1136/bjsports-2021-104168*
2. **Gonzalez G, Vaculik K, Khalil C, Zektser Y, Arnold C, Almario CV, Spiegel BMR, Anger JT.** Women's Experience with Stress Urinary Incontinence: Insights from Social Media Analytics. J Urol 2020; 203(5): 962-968. *https://doi.org/10.1097/JU.0000000000000706*
3. **Pannek J, Wöllner J.** Management of stress urinary incontinence in female patients with spinal cord injury by autologous fascial sling: time for a revival? Spinal Cord Ser Cases 2022; 8(1): 57. *https://doi.org/10.1038/s41394-022-00524-8*
4. **Bracchitta D, Costa P, Borojeni S, Ménard J, Bryckaert PE, Mandron É.** Laparoscopic artificial urinary sphincter implantation in women with stress urinary incontinence: update on 13 years' experience in a single centre. BJU Int 2019; 123(5A): E14-E19. *https://doi.org/10.1111/bju.14653*
5. **Kadekawa K, Kawamorita N, Shimizu T, Kurobe M, Turnbull PS, Chandra S, Kambara T, Barton JC, Russell AJ, Yoshimura N.** Effects of a selective androgen receptor modulator (SARM), GSK2849466A, on stress urinary incontinence and bladder activity in rats with ovariectomy-induced oestrogen deficiency. BJU Int 2020; 125(6): 911-919. *https://doi.org/10.1111/bju.15022*
6. **Ličen U, Kozinc Ž.** Using Shear-Wave Elastography to assess exercise-induced muscle damage: a review. Sensors 2022; 22(19): 7574. *https://doi.org/10.3390/s22197574*
7. **Sussman RD, Syan R, Brucker BM.** Guideline of guidelines: urinary incontinence in women. BJU Int 2020; 125(5): 638-655. *https://doi.org/10.1111/bju.14927*
8. **Wang K, Xu X, Jia G, Jiang H.** Risk factors for postpartum stress urinary incontinence: a systematic review and meta-analysis. Reprod Sci 2020; 27(12): 2129-2145. *https://doi.org/10.1007/s43032-020-00254-y*
9. **Moossdorff-Steinhauser HFA, Berghmans BCM, Spaanderman MEA, Bols EMJ.** Prevalence, incidence and bothersomeness of urinary incontinence between 6 weeks and 1-year postpartum: a systematic review and meta-analysis. Int Urogynecol J 2021; 32(7): 1675-1693. *https://doi.org/10.1007/s00192-021-04877-w*
10. **Griebling TL.** Re: Ultrasound-assisted prompted voiding care for managing urinary incontinence in Nursing Homes: a randomized clinical trial. J Urol 2019; 202(4): 640. *https://doi.org/10.1097/01.JU.0000577292.92810.d8*
11. **Hofstetter LW, Odéen H, Bolster BD Jr, Mueller A, Christensen DA, Payne A, Parker DL.** Efficient shear wave elastography using transient acoustic radiation force excitations and MR displacement encoding. Magn Reson Med 2019; 81(5): 3153-3167. *https://doi.org/10.1002/mrm.27647*
12. **Zhao B, Wen L, Chen W, Qing Z, Liu D, Liu M.** A preliminary study on quantitative quality measurements of the urethral rhabdosphincter muscle by supersonic shear wave imaging in women with stress urinary incontinence. J Ultrasound Med 2020; 39(8): 1615-1621. *https://doi.org/10.1002/jum.15255*
13. **Kochová P, Hympánová L, Rynkevic R, Cimrman R, Tonar Z, Deprest J, Kalis V.** The histological microstructure and in vitro mechanical properties of pregnant and postmenopausal ewe perineal body. Menopause 2019; 26(11): 1289-1301. *https://doi.org/10.1097/GME.0000000000001395*
14. **Burton CS, González G, Vaculik K, Khalil C, Zektser Y, Arnold C, et al.** Female

lower urinary tract symptom prevention and treatment strategies on social media: mixed correlation with evidence. Urology 2021; 49(150): 139-145. *https://doi.org/10.1016/j.urology.2020.06.056*

15. **Bai X, Ma J, Xu W, Wang J, Liu S.** Off-epicentral measurement of laser-ultrasonic shear-wave velocity and its application to elastic-moduli evaluation. Ultrasonics 2023; 61(127): 106850. *https://doi.org/10.1016/j.ultras.2022.106850*
16. **Aghaei H, Penkov GM, Solomoichenko DA, Toorajipour A, Petrakov DG, Jafarpour H, Ghosh S**. Density-dependent relationship between changes in ultrasonic wave velocities, effective stress, and petrophysical-elastic properties of sandstone. Ultrasonics 2023; 61(132): 106985. *https://doi.org/10.1016/j.ultras.2023.106985*
17. **Cashman S, Biers S, Greenwell T, Harding C, Morley R, Cooper D, Fowler S, Thiruchelvam N; BAUS Section of Female Neurological and Urodynamic Urology.** Results of the British Association of Urological Surgeons female stress urinary incontinence procedures outcomes audit 2014-2017. BJU Int 2019; 123(1): 149-159. *https://doi.org/10.1111/bju.14541*
18. **Du C, Lee W, Lucioni A, Kobashi K, Lee U.** Do patient education materials on female pelvic floor disorders meet readability standards? Putting them to the test. Urol Pract 2020; 7(4): 288-293. *https://doi.org/10.1097/UPJ.0000000000000100*
19. **Ling C, Shek KL, Gillor M, Caudwell-Hall J, Dietz HP.** Is location of urethral kinking a confounder of association between urethral closure pressure and stress urinary incontinence? Ultrasound Obstet Gynecol 2021; 57(3): 488-492. *https://doi.org/10.1002/uog.22153*
20. **Yang E, Yang SH, Huang WC, Yeh SC, Yang JM.** Association of baseline pelvic floor muscle activities with sexual and urinary functions in female stress urinary incontinence. J Sex Med, 2021; 18(10): 1698-1704. *https://doi.org/10.1016/j.jsxm.2021.07.013*
21. **Kuprasertkul A, Christie AL, Lemack GE, Zimmern P.** Long-term results of Burch and autologous sling procedures for stress urinary incontinence in E-SISTEr participants at 1 Site. J Urol 2019; 202(6): 1224-1229. *https://doi.org/10.1097/JU.0000000000000421*
22. **Illiano E, Costantini E.** Re: Long-term results of Burch and autologous sling procedures for stress urinary incontinence in E-SISTEr Participants at 1 Site. Eur Urol 2020; 77(6): 756. *https://doi.org/10.1016/j.eururo.2020.02.022.*

Invest Clin 66(2): 157 - 165, 2025 https://doi.org/10.54817/IC.v66n2a03

Correlation between thyroid hormone values and anemia in elderly patients with diabetic nephropathy.

Jingjing Yu[1#], Keke Tang[2#] and Yan Song[3]

[1]Department of Endocrinology, The Second People's Hospital of Beilun District, Ningbo Zhejiang Province, China.
[2]Department of Endocrinology, The First Affiliated Hospital of Ningbo University, Ningbo Zhejiang Province, China.
[3]Department of Surgery, The Second People's Hospital of Beilun District, Ningbo, Zhejiang Province, China.
[#]The two authors contributed equally to this study.

Keywords: correlation; diabetic nephropathy; elderly; anemia severity; thyroid hormone.

Abstract. We aimed to explore the correlation between thyroid hormone levels and anemia severity in elderly diabetic nephropathy (DN) patients. Elderly DN patients (140 in total) diagnosed and treated during November 2019 and December 2023 were retrospectively recruited as a DN group, 140 patients with uncomplicated diabetes mellitus as a simple diabetes group, and 140 healthy subjects as a healthy group. A non-anemia group (n=63) and an anemia group (n=77) were set up as sets of the DN group according to the hemoglobin (Hb) level, and the anemia group was further divided into a severe group (n=48) (Hb<60 g/L), a moderate group (n=16) (60 g/L≤Hb<90 g/L) and a mild group (n=13) (Hb≥90 g/L). Compared to the simple diabetes group, significantly increased levels of serum TSH and significantly decreased levels of FT4 and FT3 were found in the DN group ($p<0.05$). A significant increase in TSH levels and significant decreases in FT4 and FT3 levels were detected in the serum from the moderate group compared with those from the mild group ($p<0.05$). The same trends in these levels were observed from the severe group compared to the moderate group ($p<0.05$). Hb had a negative correlation with TSH and positive correlations with FT4 and FT3 ($p<0.05$). High TSH and low FT4 and FT3 may be related to anemia in elderly patients with DN, and they have correlations with the severity of anemia.

Corresponding author: Yan Song, Department of Surgery, The Second People's Hospital of Beilun District, Ningbo 315809, Zhejiang Province, China. E-mail: songyansphbd@hosp-edu.cn

Correlación entre los valores de hormonas tiroideas y anemia en pacientes ancianos con nefropatía diabética.

Invest Clin 2025; 66 (2): 157 – 165

Palabras clave: correlación; nefropatía diabética; ancianos; gravedad de la anemia; hormona tiroidea.

Resumen. Nuestro objetivo fue explorar la correlación entre el nivel de hormona tiroidea y la severidad de la anemia en pacientes ancianos con nefropatía diabética (ND). Se reclutaron retrospectivamente 140 pacientes ancianos con ND diagnosticados y tratados entre noviembre de 2019 y diciembre de 2023, 140 pacientes con diabetes mellitus sin nefropatía y 140 sujetos sanos como grupo control sano. El grupo de ND se dividió en un grupo sin anemia (n=63) y un grupo con anemia (n=77) de acuerdo con el nivel de hemoglobina (Hb). El grupo con anemia fue subdividido en grave (n=48) (Hb<60 g/L), moderada (n=16) (60 g/L-Hb<90 g/L) y leve (n=13) (Hb-90 g/L). En comparación con el grupo de diabetes simple, se encontró un aumento significativo de los niveles séricos de TSH y una disminución significativa de los niveles de FT4 y FT3 en el grupo de DN (p<0,05). Se encontró un aumento significativo del nivel de TSH junto con disminuciones significativas de los niveles de FT4 y FT3 en el suero del grupo moderado en comparación con los del grupo leve (p<0,05). Las mismas tendencias en estos niveles se observaron en el grupo grave cuando se compararon con el grupo moderado (p<0,05). La Hb tuvo una correlación negativa con TSH y correlación positiva con FT4 y FT3 (p<0,05). Niveles altos de TSH y bajos de FT4 y FT3 podrían estar relacionados con anemia y su gravedad en pacientes ancianos con ND.

Received: 24-01-2025 Accepted: 27-04-2025

INTRODUCTION

With the development of population aging, the incidence of diabetes mellitus and other chronic diseases has been increasing year by year. It is estimated that diabetes mellitus may affect 642 million people globally by 2040, with an incidence rate of 8.8-10.4% [1]. Being a microvascular complication of diabetes mellitus characterized by the highest prevalence and severity, diabetic nephropathy (DN) has become the leading contributor to end-stage renal disease [2]. As the disease progresses, the patient's renal function gradually declines, decreasing erythropoietin (EPO) produced by the kidney, iron absorption, and red blood cell survival time, thus significantly increasing the incidence of anemia [3]. Anemia suggests that DN has progressed to a severe stage, and renal failure occurs, resulting in ineffective excretion of metabolites and toxins in the body and further worsening the condition of the disease. In addition, anemia can lead to insufficient oxygen supply to organs, aggravating complications of diabetes mellitus, such as cardiovascular diseases and retinopathy. Diabetic patients with chronic anemia are at higher risk of developing cardio-cerebrovascular diseases, retinopathy, nephropathy and neuropathy.

In addition, due to a significant decrease in urine protein and gradual impact

on the hypothalamic-pituitary-thyroid axis function with the progression of the disease, the synthesis of thyroid hormones declines in DN patients, and thyroid dysfunction occurs. Thyroid hormones may be implicated in glomerular filtration rate (GFR) regulation and blood circulation in the kidneys [4]. The rate of thyroid function abnormality in patients with kidney disease at stage G5 is significantly higher than that at stage G1 (39.1% *vs.* 8.3%), and it is considered that the severity of kidney disease may be closely related to thyroid function [5]. Moreover, the severity of type 2 diabetes mellitus (T2DM) in elderly patients also correlates with blood glucose-related indicators and thyroid hormone levels. Free triiodothyronine (FT3), free thyroxine (FT4) and other thyroid hormones in mild and severe T2DM in elderly patients are at significantly lower levels than in healthy controls [6], suggesting that the changes in thyroid hormone levels may be related to the severity of T2DM in elderly patients. However, no reports are available yet on whether thyroid hormone level is related to the severity of anemia in elderly DN patients.

Because of this, the level changes of thyroid hormones in patients with different severities of anemia were analyzed in this study to explore the correlations of thyroid hormones with anemia severity in elderly DN subjects, aiming to provide a reference for diagnosis and treatment in clinical practice.

PATIENTS AND METHODS

Subjects

One hundred and forty older adults diagnosed with DN and hospitalized for treatment herein during November 2019 and December 2023 were retrospectively recruited into the DN group. The following inclusion criteria were utilized: 1) patients satisfying the diagnosis and classification criteria for diabetes mellitus in the *Guideline for Prevention and Treatment of Type 2 Diabetes Mellitus in China* (2020 Edition) [7], 2) those who met the diagnostic and treatment criteria for DN [8], 3) those with urinary albumin excretion rate (AER) ≥30 mg/24 h, GFR≤60 mL/min·1.73 m^2 or urinary microalbumin/creatinine ratio (ACR) ≥3 mg/g, and 4) those without renal transplantation or dialysis history. The adopted exclusion criteria included: 1) patients who had taken drugs that may affect urinary protein excretion before participating in the study, 2) those with no obvious hepatic and renal dysfunction previously and no severe complications of diabetes mellitus recently, 3) those complicated with other kidney diseases, or 4) those complicated with mental illness or cognitive dysfunction. Another 140 patients with uncomplicated diabetes mellitus entered the simple diabetes group, in addition to 140 healthy subjects as the healthy group. Their gender, age, and body mass index were not significantly different from those in the DN group.

Grouping criteria

According to the GFR, patients with chronic DN were divided into stage 5 group (n=11, GFR<15 mL/min·1.73 m^2), stage 4 group (n=20, 15 mL/min·1.73 m^2≤GFR<30 mL/min·1.73 m^2), stage 3 group (n=43, 30 mL/min·1.73 m^2≤GFR<60 mL/min·1.73 m^2), stage 2 group (n=39, 60 mL/min·1.73 m^2≤GFR<90 mL/min·1.73 m^2), and stage 1 group (n=27, GFR≥90 mL/min·1.73 m^2).

An anemia group (n=77) plus a non-anemia group (n=63) were established as subsets of the DN group according to the hemoglobin (Hb) level. Hb ≤120 g/L in females and ≤130 g/L in males indicated anemia.

The anemia group was further divided into a severe group (n=48) (Hb<60 g/L), a moderate group (n=16) (60 g/L≤Hb<90 g/L) and a mild group (n=13) (Hb≥90 g/L).

Detection of thyroid hormones

All patients were enrolled to collect fasting venous blood (5 mL) in the morning for centrifugation. Then, the supernatant was

harvested to measure thyroid-stimulating hormone (TSH), FT4 and FT3 using an MPI-A electrochemiluminescence analyzer (Xi'an Remex Analysis Instruments Co., Ltd.) in strict accordance with the kit instructions. TSH (Item No.: ZY-TSH-Hu), FT4 (Item No.: ZY-fT4-Ge) and FT3 test kits (Item No.: ZY-fT3-Ge) were purchased from Shanghai Zeye Biotechnology Co., Ltd.

Statistical analysis

The SPSS 24.0 software for statistical analysis was employed. The description format of ($\bar{X} \pm SD$) was utilized for the measurement data distributed normally, which were compared by the independent-sample *t*-test between two groups and by the univariate multi-sample mean test among multiple groups. The count data were described by [n (%)] and subjected to the chi-square test for comparisons. The correlations of thyroid hormone level with anemia severity were explored by the Pearson analysis. A difference with statistical significance was marked with $p<0.05$.

RESULTS

Baseline data

Table 1 exhibits the three groups of baseline data.

Thyroid hormone levels in DN patients

Compared to the healthy group, a significant increase in TSH levels and significant decreases in FT4 and FT3 levels were detected in the serum from the simple diabetes group ($t=19.307$, -6.34, -16.16; $p<0.05$). In comparison with the simple diabetes group, significantly increased levels of serum TSH and significantly decreased levels of FT4 and FT3 were observed in the DN group ($t=17.989$, -6.702, -14.076; $p<0.05$) (Table 2).

Association between DN and anemia

In the DN group, anemia occurred in 77 cases, including 7, 11, 32, 16 and 11 cases in stages 1-5, respectively. The incidence and severity of anemia were found to rise gradually as the stage of DN increased ($p<0.05$) (Table 3).

Changes in thyroid hormone levels in patients with different severities of anemia

The serum levels of TSH, FT4 and FT3 in the severe, moderate, mild, and non-anemia groups were detected with significant differences ($p<0.05$). Compared to the mild group, the moderate group exhibited evident elevations in serum TSH levels and marked decreases in FT4 and FT3 levels ($t=2.613$,

Table 1. Baseline data.

Group	n	Sex n (%)		Age (years) $\bar{X} \pm SD$	Body mass index (kg/m^2) $\bar{X} \pm SD$	Smoking history n (%)	Drinking history n (%)
		Female	Male				
DN	140	77 (55)	63 (45)	52.84±8.15	23.69±2.26	81 (57.86)	87 (62.14)
Simple diabetes	140	71 (50.71)	69 (49.29)	53.15±7.26	24.12±2.24	76 (54.29)	80 (57.14)
Healthy	140	74 (52.86)	66 (47.14)	52.77±7.49	24.08±2.32	75 (53.57)	82 (58.57)
F/χ^2		0.516		0.10	1.53	0.597	0.769
p		0.773		0.907	0.218	0.742	0.681

DN: Diabetic nephropathy. The measurement data were compared by univariate multi-sample mean test among multiple groups. The count data were subjected to the chi-square test for comparisons.

Table 2. Thyroid hormone levels in diabetic nephropathy patients.

Group	n	TSH (μIU/mL) $\bar{x} \pm SD$	FT4 (pmol/L) $\bar{x} \pm SD$	FT3 (pmol/L) $\bar{x} \pm SD$
DN	140	5.83±1.72 [ab]	13.75±4.01 [ab]	3.55±0.93 [ab]
Simple diabetes	140	2.85±0.94 [a]	17.31±4.84 [a]	5.51±1.36 [a]
Healthy	140	1.17±0.42	20.79±4.33	9.70±2.75
F		582.14	89.34	403.37
p		<0.001	<0.001	<0.001

The measurement data were compared by univariate multi-sample mean test among multiple groups. [a]p<0.05 *vs.* healthy group, [b]p<0.05 *vs.* simple diabetes group.

Table 3. Association between diabetic nephropathy and incidence and severity of anemia.

Group	n	Severe n (%)	Moderate n (%)	Mild n (%)	None n (%)
Stage 5	11	9 (81.82)	1 (9.09)	1 (9.09)	0 (0)
Stage 4	20	11 (55)	4 (20)	1 (5)	4 (20)
Stage 3	43	24 (55.81)	5 (11.63)	3 (6.98)	11 (25.58)
Stage 2	39	4 (10.26)	3 (7.69)	4 (10.26)	28 (71.79)
Stage 1	27	0 (0)	3 (11.11)	4 (14.81)	20 (74.07)
χ^2					57.405
p					<0.001

The count data were subjected to the chi-square test for comparisons.

-1.88, -3.439; p<0.05). The TSH levels climbed significantly, whereas the FT4 and FT3 levels dropped significantly in the serum from the severe group when compared with the moderate group (t=3.555, -4.598, 6.366; p<0.05) (Table 4).

Correlation of thyroid hormone levels with anemia severity

As revealed by the Pearson's correlation analysis, Hb had a negative correlation with TSH, but it had a positive correlation with FT4 and FT3 (p<0.05) (Fig. 1).

DISCUSSION

DN has the early pathological characteristics of glomerular basement membrane thickening and mesangial expansion and the late characteristics of glomerulosclerosis and renal tubule interstitial fibrosis [9]. Early diagnosis and intervention are crucial for managing DN, particularly in elderly patients, who are often more vulnerable to its progression due to poor diabetes management and comorbidities. Therefore, predicting disease progression and achieving timely intervention in elderly DN patients are vital for improving the outcomes.

A growing body of research has highlighted the correlation between thyroid dysfunction and DN. Hypothyroidism, a common thyroid disorder in patients with T2DM, has been identified as a potentially significant contributing factor to DN [10,11]. Thyroid hormones play a critical role in regulating metabolic processes. These hormones contribute to the development of the body, support cardiac output, and promote myocardial contractility. Additionally, they are involved in maintaining renal function stability [12].

Table 4. Changes in thyroid hormone levels in diabetic nephropathy subjects with various severities of anemia and no anemia.

Group	n	TSH (μIIU/mL) $\bar{x} \pm SD$	FT4 (pmol/L) $\bar{x} \pm SD$	FT3 (pmol/L) $\bar{x} \pm SD$
Non-anemia	63	3.30±0.76	15.17±2.30	4.29±1.02
Anemia				
Mild	13	6.28±1.19 [a]	12.42±3.15 [a]	3.07±0.86 [a]
Moderate	16	7.64±1.61 [ab]	10.37±2.61 [ab]	2.14±0.51 [ab]
Severe	48	9.41±2.03 [abc]	7.16±1.72 [abc]	1.26±0.37 [abc]
F		168.00	117.38	141.03
p		<0.001	<0.001	<0.001

The measurement data were compared by univariate multi-sample mean test among multiple groups. [a]p<0.05 *vs.* non-anemia group, [b]p<0.05 *vs.* mild group, [c]<0.05 *vs.* moderate group.

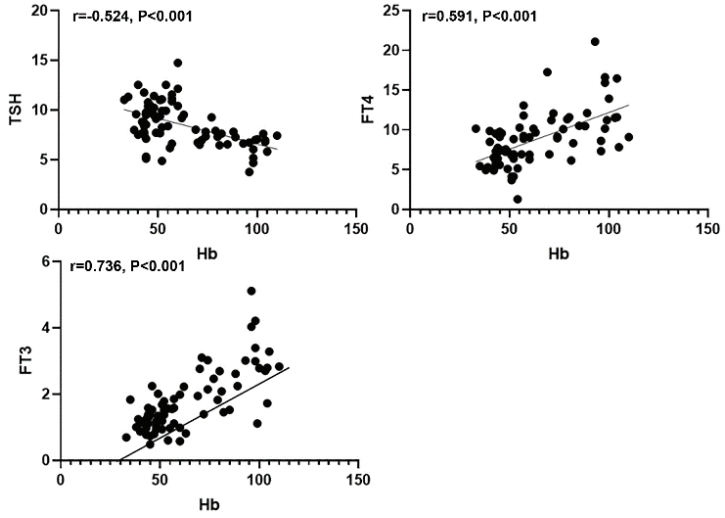

Fig. 1. Correlation between thyroid hormones and anemia severity.

Hypothyroidism may exacerbate DN through several mechanisms. One of the most critical effects is the reduction in insulin sensitivity, which leads to worsened blood glucose control and insulin resistance. This dysfunction is compounded by the inflammatory response triggered by hyperglycemia, which inhibits 5'-deiodinase activity, a key enzyme involved in converting T4 to T3. This reduction in FT3 levels damages the renal tubular function and reduces the renal plasma flow and glomerular capillary hydrostatic pressure, further compromising renal function [13]. In addition, DN-associated hyperglycemia and other metabolic disturbances can directly or indirectly affect the hypothalamic-pituitary-thyroid axis, impairing thyroid hormone production and contributing to worsening renal function.

In this study, DN patients had significantly increased levels of serum TSH and decreased levels of FT3 and FT4, indicating that thyroid hormone dysregulation may be an important factor in the progression of DN. As kidney function declines, the ability of the kidney to convert T4 to T3 through 5'-deiodinase activity is diminished. Additionally, metabolic disturbances in DN, including selenium deficiency (a cofactor for 5'-deiodinase), further exacerbate the dys-

function of thyroid hormone conversion [14]. As the disease progresses, T3 levels continue to decrease, and this reduction is correlated with worsening renal function [15]. Furthermore, serum T3 levels have been shown to serve as an independent risk factor for DN, with lower T3 levels associated with greater disease severity [16,17]

Another important aspect of DN progression is anemia, which frequently occurs as a complication and significantly affects patient outcomes [18]. Anemia in DN is primarily caused by reduced EPO production as kidney function deteriorates. EPO, which is secreted by the kidneys, plays a central role in red blood cell production [19]. As kidney function declines, EPO secretion is impaired, leading to anemia. The incidence of anemia in DN can reach 100% in stage 5 DN, and its severity is correlated with the degree of renal dysfunction [20]. Consistently, we found in this study that the anemia severity was closely related to the progression of DN, with Hb levels as an important marker for disease severity.

In addition to kidney dysfunction, thyroid hormone levels also influence anemia. Disruption of thyroid hormone function may exacerbate anemia in DN patients through various mechanisms. Specifically, thyroid hormone resistance can disrupt the balance between erythropoiesis and the differentiation of erythrocyte progenitor cells. Besides, chronic anemia can lead to altered endocrine function and impaired EPO secretion [21]. In the present study, the serum TSH levels increased significantly, and the levels of FT4 and FT3 decreased with increasing severity of anemia. All of these levels had significant associations with Hb. Hence, the impaired kidney function in DN reduces the kidney's ability to regulate thyroid hormones, contributing to further disturbances in thyroid function [22].

Furthermore, anemia itself may induce a stress state, thus affecting the hypothalamic-pituitary-thyroid axis function. Under stress, more thyrotropin-releasing hormone may be secreted from the hypothalamus to promote the secretion of more TSH by the pituitary gland. However, due to renal dysfunction and the loss of thyroid hormone-binding proteins, the synthesis and secretion of thyroid hormones remain impaired, resulting in decreased levels of FT4 and FT3 [23]. This cycle may aggravate the anemia and accelerate the progression of DN.

Exploring the relationship between thyroid hormone disruption and anemia severity in elderly DN patients provides important insights for clinical management. By monitoring thyroid hormone levels besides kidney function and anemia status, healthcare providers may be able to predict better disease progression and tailor interventions to mitigate adverse outcomes. Our study contributes to this understanding by demonstrating that thyroid hormone imbalances, particularly low FT3 and FT4 levels, are closely associated with the severity of anemia in DN patients.

Nevertheless, this study has limitations. The duration of this study was short, the sample size was small, and no data were collected on the association between the severity of anemia and thyroid hormone levels in patients undergoing kidney transplantation or dialysis. Therefore, further studies are still required.

In conclusion, high TSH and low FT4 and FT3 may be the factors related to anemia in elderly patients with DN, and they have associations with the severity of anemia.

ACKNOWLEDGEMENTS

None.

Funding

None.

Conflict of Interest

The authors declare no conflict of interest.

Number ORCID of authors

- Jingjing Yu (JY): 0009-0003-7126-9306
- Keke Tang (KT): 0009-0000-9354-2543
- Yan Song (YS): 0009-0006-1900-3203

Participation of the authors

All authors had participated in the development and writing of the paper.

REFERENCES

1. **Cao X, Chen P.** The effects of alprostadil combined with α-lipoic acid in the treatment of senile diabetic nephropathy. Am J Transl Res. 2021; 13(9): 10823-10829. *PMID: 34650761*
2. **Samsu N.** Diabetic Nephropathy: Challenges in Pathogenesis, Diagnosis, and Treatment. Biomed Res Int. 2021; 2021(1): 1497449. *https://doi.org/10.1155/2021/1497449*
3. **Natale P, Palmer SC, Jaure A, Hodson EM, Ruospo M, Cooper TE, Hahn D, Saglimbene VM, Craig JC, Strippoli GF.** Hypoxia-inducible factor stabilizers for the anaemia of chronic kidney disease. Cochrane Database Syst Rev. 2022; 8(8): CD013751. *https://doi.org/10.1002/14651858.CD013751.pub2*
4. **Gao J, Liu J.** Correlation of serum thyrotropin and thyroid hormone levels with diabetic kidney disease: a cross-sectional study. BMC Endocr Disord. 2024; 24(1): 170. *https://doi.org/10.1186/s12902-024-01699-x*
5. **Pavan Kumar JTVK, A UM.** Comparison of Thyroid Function Tests Among Type 2 Diabetes Patients With and Without Diabetic Nephropathy and Controls. Cureus. 2024; 16(9): e70462. *https://doi.org/10.7759/cureus.70462*
6. **Feng X, Huang J, Peng Y, Xu Y.** Association between decreased thyroid stimulating hormone and hyperuricemia in type 2 diabetic patients with early-stage diabetic kidney disease. BMC Endocr Disord. 2021; 21(1): 1. *https://doi.org/10.1186/s12902-020-00672-8*
7. **Moran GM, Bakhai C, Song SH, Agwu JC; Guideline Committee.**. Type 2 diabetes: summary of updated NICE guidance. BMJ. 2022; 377: o775. *https://doi.org/10.1136/bmj.o775*
8. **Kalra S.** The KDIGO guidelines on diabetes and chronic kidney disease, 2020: An appraisal. Diabet Med. 2021; 38(7): e14561. *https://doi.org/10.1111/dme.14561*
9. **Thipsawat S.** Early detection of diabetic nephropathy in patient with type 2 diabetes mellitus: A review of the literature. Diab Vasc Dis Res. 2021; 18(6): 14791641211058856. *https://doi.org/10.1177/14791641211058856*
10. **Yang W, Jin C, Wang H, Lai Y, Li J, Shan Z.** Subclinical hypothyroidism increases insulin resistance in normoglycemic people. Front Endocrinol. 2023; 14(1): 1106968. *https://doi.org/10.3389/fendo.2023.1106968*
11. **Kim SW, Jeon JH, Moon JS, Jeon EJ, Kim MK, Lee IK, Seo JB, Park KG.** Low-normal free thyroxine levels in euthyroid male are associated with prediabetes. Diabetes Metab J. 2019; 43(5): 718-726. *https://doi.org/10.4093/dmj.2018.0222*
12. **Reinhardt W, Mülling N, Behrendt S, Benson S, Dolff S, Führer D, Tan S.** Association between albuminuria and thyroid function in patients with chronic kidney disease. Endocrine. 2021; 73(2): 367-373. *https://doi.org/10.1007/s12020-021-02640-1*
13. **Liu MC, Li JL, Wang YF, Meng Y, Cai Z, Shen C, Wang MD, Zhao WJ, Niu WQ.** Association between thyroid hormones and diabetic kidney disease in Chinese adults. BMC Endocr Disord. 2023; 23(1): 56. *https://doi.org/10.1186/s12902-023-01299-1*
14. **Shi C, Liu X, Du Z, Tian L.** Impaired sensitivity to thyroid hormones is associated with the risk of eiabetic nephropathy in euthyroid patients with Type 1

Diabetes mellitus. Diabetes Metab Syndr Obes. 2024; 17: 611-618. *https://doi.org/10.2147/DMSO.S449870*

15. **Liu Z.** Advance in the correlation between diabetic nephropathy and abnormal serum thyroid hormone levels in patients. Emerg Med Int. 2023; 2023: 8947035. *https://doi.org/10.1155/2023/8947035*
16. **Han Q, Zhang J, Wang Y, Li H, Zhang R, Guo R, Li L, Teng G, et al.** Thyroid hormones and diabetic nephropathy: An essential relationship to recognize. Nephrology. 2019; 24(2): 160-169. *https://doi.org/10.1111/nep.13388*
17. **Chen Y, Zhang W, Wang N, Wang Y, Wang C, Wan H, Lu Y.** Thyroid parameters and kidney disorder in Type 2 diabetes: Results from the METAL Study. J Diabetes Res. 2020; 2020: 4798947. *https://doi.org/10.1155/2020/4798947*
18. **Chung EY, Palmer SC, Saglimbene VM, Craig JC, Tonelli M, Strippoli GF.** Erythropoiesis-stimulating agents for anaemia in adults with chronic kidney disease: a network meta-analysis. Cochrane Database Syst Rev. 2023; 2(2): CD010590. *https://doi.org/10.1002/14651858.CD010590.pub3*
19. **Ito K, Yokota S, Watanabe M, Inoue Y, Takahashi K, Himuro N, et al.** Anemia in diabetic patients reflects severe tubulointerstitial injury and Aids in clinically predicting a diagnosis of diabetic nephropathy. Intern Med. 2021; 60(9): 1349-1357. *https://doi.org/10.2169/internalmedicine.5455-20*
20. **Ryu SR, Park SK, Jung JY, Kim YH, Oh YK, Yoo TH, Sung S.** The prevalence and management of anemia in chronic kidney disease patients: Result from the KoreaN Cohort Study for Outcomes in Patients With Chronic Kidney Disease (KNOW-CKD). J Korean Med Sci. 2017; 32(2): 249-256. *https://doi.org/10.3346/jkms.2017.32.2.249*
21. **van Vliet NA, Kamphuis AEP, den Elzen WPJ, Blauw GJ, Gussekloo J, Noordam R, van Heemst D.** Thyroid function and risk of anemia: a multivariable-adjusted and mendelian randomization analysis in the UK Biobank. J Clin Endocrinol Metab. 2022; 107(2): e643-e652. *https://doi.org/10.1210/clinem/dgab674*
22. **Zhao X, Liu F, Yuan S, Wang F, Li C, Guo C, Zhao J.** Thyroid hormone replacement therapy in dialysis/renal insufficiency patients. Front Endocrinol. 2025; 16: 1540802. *https://doi.org/10.3389/fendo.2025.1540802*
23. **Khassawneh AH, Al-Mistarehi AH, Zein Alaabdin AM, Khasawneh L, AlQuran TM, Kheirallah KA, et al.** Prevalence and predictors of thyroid dysfunction among type 2 diabetic patients: A case–control study. Int J Gen Med. 2020; 13: 803-816. *https://doi.org/10.2147/IJGM.S273900.*

Invest Clin 66(2): 166 - 174, 2025 https://doi.org/10.54817/IC.v66n2a04

Optimization of a real-time PCR assay for hepatitis B virus load determination in infected patients.

María Zulay Sulbarán, Yoneira Fabiola Sulbarán, Carmen Luisa Loureiro, Héctor Rafael Rangel, Rossana Celeste Jaspe and Flor Helene Pujol

Laboratorio de Virología Molecular, CMBC, Instituto Venezolano de Investigaciones Científicas (IVIC), Caracas, Venezuela.

Keywords: hepatitis B virus; viral load; optimization; qPCR; genotype.

Abstract. Hepatitis B virus (HBV) infection is a significant health problem in the world, with around 294 million chronic carriers. Determination of viral load is crucial for the monitoring and treatment follow-up of HBV-infected patients. In-house methods are economical alternatives for those settings where HBV viral load determination might not be widely available commercially. Molecular diagnostic techniques need to take into account the variability of this virus. The aim of this study was the evaluation and optimization of a real-time PCR method for the determination of HBV load. After optimization, the in-house assay evaluated in this study showed acceptable sensitivity and specificity, allowing its use for monitoring patients in low-income settings.

Corresponding author: Flor Helene Pujol. Laboratorio de Virología Molecular, CMBC, Instituto Venezolano de Investigaciones Científicas (IVIC), Caracas, Venezuela. E-mail: fhpujol@gmail.com

Optimización de un ensayo de PCR en tiempo real para la determinación de carga viral del virus de hepatitis B en pacientes infectados.

Invest Clin 2025; 66 (2): 166 – 174

Palabras clave: virus de hepatitis B; carga viral; qPCR; optimización; genotipo.

Resumen. La infección por el virus de la hepatitis B (VHB) es un gran problema de salud en el mundo, con alrededor de 294 millones de portadores crónicos. La determinación de la carga viral es de importancia crucial para el monitoreo y el seguimiento del tratamiento de los pacientes infectados por el VHB. Los métodos propios son alternativas económicas para aquellos países donde la determinación de la carga viral del VHB podría no estar ampliamente disponible comercialmente. Las técnicas de diagnóstico molecular deben tener en cuenta la variabilidad de este virus. El objetivo de este estudio fue la evaluación y optimización de un método de PCR en tiempo real para la determinación de la carga del VHB. La prueba propia analizada en este estudio mostró, después de la optimización, una sensibilidad y especificidad satisfactorias, lo que permitió su uso para el seguimiento de pacientes en comunidades de bajos ingresos.

Received: 10-03-2025 Accepted: 09-05-2025

INTRODUCTION

Around 294 million persons are chronically infected with the hepatitis B virus (HBV) in the world [1]. HBV chronic infection frequently leads to cirrhosis and hepatocellular carcinoma (HCC), with at least 800,000 deaths each year [1]. This infection is highly endemic in Sub-Saharan Africa, Asia, and Indigenous populations in the Americas and Oceania [2,3].

HBV belongs to the *Hepadnaviridae* family. It is a partially double-stranded DNA virus of around 3200 bp. In addition to the virus, viral-like particles also circulate, composed exclusively of the HBV surface antigen (HBsAg) within a non-infectious envelope [4]. Up to ten genotypes and several subgenotypes have been described for HBV, with the American genotypes being the most divergent. The tenth HBV genotype J seems to be a recombinant one, and only one sequence is available [5].

A recombinant HBV vaccine has been developed, based on the HBsAg [6]. After more than 30 years of worldwide vaccination, viral infection and HCC incidence reduction have been widely demonstrated [6,7]. These measures have led the World Health Organization (WHO) to propose a plan for hepatitis elimination by 2030 [8]. However, nearly 300 million people remain chronically infected, and no effective treatment is currently available.

The functional cure of chronic hepatitis B is defined as HBsAg loss after therapy, which is rarely achieved with the current therapy. Novel agents in development and preexisting ones will probably bring the tools to approach this goal [9]. In the last WHO guidelines of March 2024, HBV treatment is recommended for all adults and adolescents (over 12 years old) with chronic hepatitis B if:

1. Evidence of significant fibrosis
2. HBV DNA viral loads above 2000 IU/mL and ALT levels exceeding the upper limit of the reference range
3. Or presence of coinfections, such as HIV, hepatitis C, hepatitis D, or other comorbidities [10].

The determination of the viral load is then of crucial importance for confirmation of viral replication and the monitoring of chronically infected hepatitis B patients. Several commercial assays are available to assess this biomarker, based on real-time PCR or transcription-mediated amplification (TMA), in most of the laboratories from high-income countries. However, this might not be the case in some low-income countries [11].

In-house methods are economical alternatives for those settings where HBV viral load determination might not be widely available commercially. Molecular diagnostic techniques need to take into account the variability of this virus. Portilho et al.[12] developed a real-time PCR to determine HBV load. This study aimed to evaluate and optimize this real-time PCR method for determining HBV load.

MATERIALS AND METHODS

Sera from HBV-infected patients

This study was approved by the Bioethical Committee of IVIC ("Biología molecular de virus de hepatitis y el Virus de la Inmunodeficiencia adquirida (VIH) en Venezuela", December 5, 2024). The sera of patients diagnosed with HBV infection, and who gave informed consent, were kept at -70°C until use. DNA was extracted from sera using the QIAamp Viral DNA Mini Kit (Hilden, Germany) and used in all the other analyses.

HBV PCR and sequencing

Nested PCR was carried out using previously reported primers 58P-1100N and S6-S3as [13]. PCR-purified fragments were sent to Macrogen Sequencing Service (Macrogen, Korea) for sequencing. The phylogenetic analysis was performed with MEGA11 software [14].

Viral load determination

According to the manufacturer's instructions, HBV viral load was determined with Bosphore® Ultra HBV Quantitation/ Detection (Anatolia Geneworks®, Istanbul, Turkey). This test has been used previously by several groups [15-17].

In-house real-time PCR determination

Real-time PCR for HBV was performed according to the protocol suggested by Portilho et al. [12]. Additionally, an antisense modified primer was designed for an optimized assay: 5'-GGCCAAAATTCG-CAGTCCCCAACC-3'. Real-time PCR was run in a final volume of 15 μL, containing 6 μL of DNA, 1X PCR buffer, 1 mM $MgCl_2$, 0.4mM dNTP mixture, 0.23 μM of each primer and probe, 1.75 U Platinum® Taq DNA Polymerase (Thermofisher, USA). The final conditions for the optimized assay were: 95°C for 10 minutes, then 40 cycles at 97°C for 30 seconds, 54°C for 90 seconds, and a hold stage of 32°C for 60 seconds.

Statistical analysis

The correlation between the values of HBV viral load determined by the commercial assay and the in-house method was evaluated with the Pearson´s coefficient [18].

RESULTS

Serum samples from HBV-infected patients were analyzed by a commercial kit and the in-house real-time PCR to evaluate the performance of an in-house real-time PCR. A total of nine sera (and dilutions of them for a total of 14 samples tested) were tested, with variable HBV loads: five sera were classified as HBV genotype F3 (one not shown in the tree, since the sequence was shorter, but it could be classified as F3), and one each as genotype A2, C2, F2, and F4 (Fig. 1).

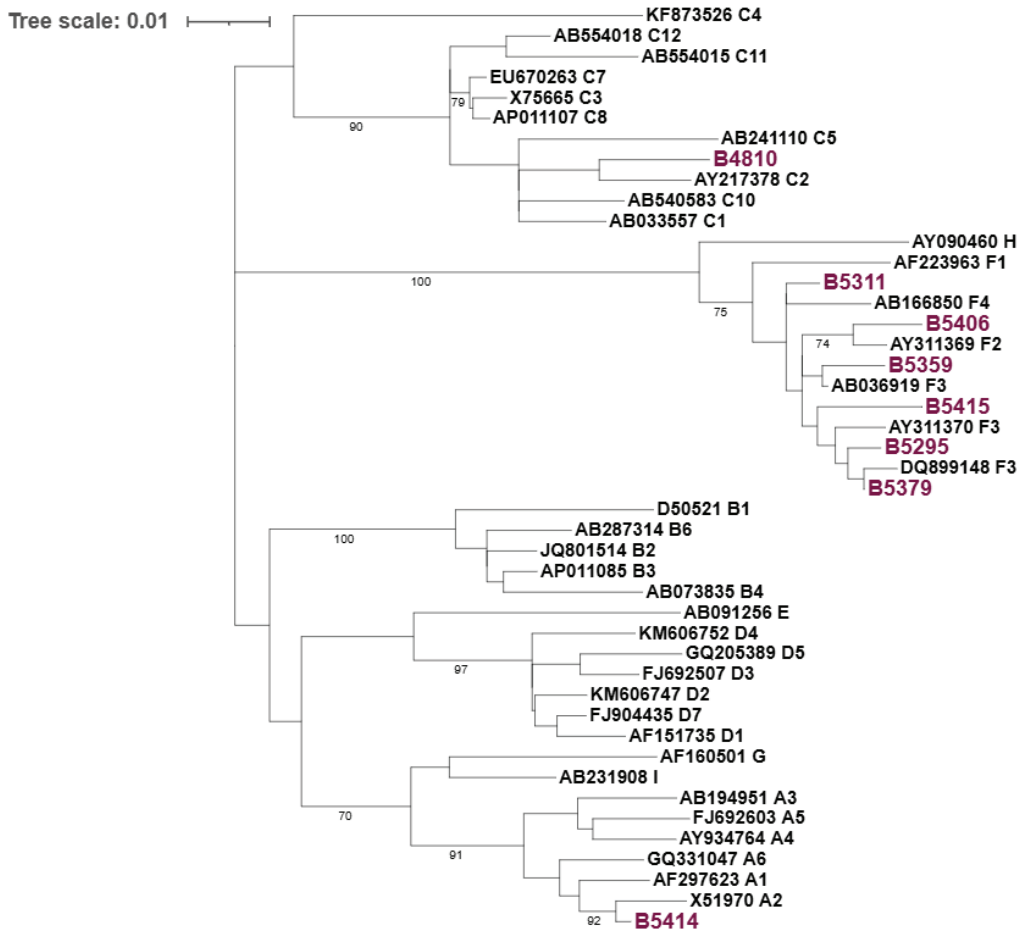

Fig. 1. Phylogenetic tree of the HBV isolates tested in this study. The S gene is analyzed (559 nt). The evolutionary history was inferred using the Maximum Likelihood method and the General Time Reversible model[14]. The tree with the highest log likelihood (-2602.78) is shown. The percentage of trees in which the associated taxa clustered is shown next to the branches. Initial tree(s) for the heuristic search were obtained by applying the Neighbor-Joining method to a matrix of pairwise distances estimated using the Maximum Composite Likelihood (MCL) approach. A discrete Gamma distribution was used to model evolutionary rate differences among sites (4 categories (+G, parameter = 0.6597)). The rate variation model allowed some sites to be evolutionarily invariable ([+I], 62.58% sites). The tree is drawn to scale, with branch lengths measured in the number of substitutions per site. This analysis involved 45 nucleotide sequences. Codon positions included were 1st+2nd+3rd+Noncoding. All positions with less than 80% site coverage were eliminated, i.e., fewer than 20% alignment gaps, missing data, and ambiguous bases were allowed at any position (partial deletion option). Bootstrap values are shown in the branches of the tree. The isolates are named by their genotype and GenBank accession number, except for the ones from this study (n=8), which are shown in purple. An additional HBV isolate (B02023) was not included in the tree since the shorter sequence could also be classified as genotype F3.

A good agreement was found between the commercial assay and the in-house method for 9/14 samples, but with an overall low correlation of R^2=0.47 (Fig. 2A). The samples exhibiting the discrepant results between the two tests were derived from two samples, corresponding to HBV genotype C2 and F3 isolates. When these samples were excluded, the correlation coefficient increased to R^2=0.98 (Fig. 2B).

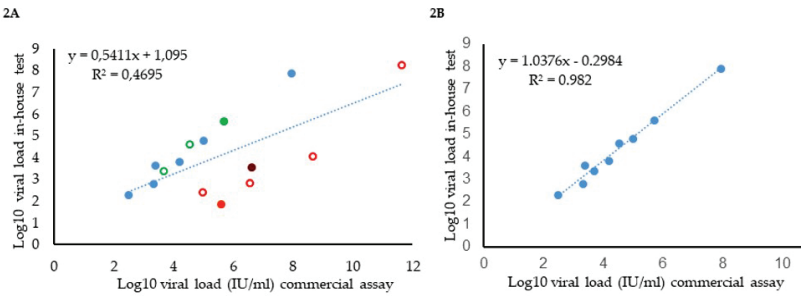

Fig. 2. Correlation between viral load determination with a commercial assay and the in-house method of Portilho et al. [12]. 2A. All the samples were tested. Green and open circles represent the dilution of a sample, as shown in the filled green. Orange open circles represent dilution of a synthetic control (amplicon from sample B4810, which is shown in filled orange). 2B. Correlation for samples without discordant results (orange and purple in Fig. 2A, derived from B4810 and B5415, respectively) were omitted.

An alignment of the sequences of the HBV samples for which discrepant results were observed is shown in Fig. 3. The alignment reveals multiple mismatches between the antisense primer and several HBV isolates, absent in the sequences without discrepant results. The mismatches were present, particularly in genotype C isolates.

A new antisense primer for an optimized real-time PCR was designed (Fig. 3). The complementarity of the three primers (sense, the new antisense and the probe) was evaluated in a total of 16516 sequences from the HBV database [19], as shown in Table 1. The three primers showed high sequence identity with the analyzed HBV sequences from all the genotypes analyzed: for some sequences, one or two internal mismatches were observed, frequently at the 5´end. These few mismatches per sequence (not at the 3´ end of the primer) may not hamper the adequate performance of the real-time PCR. The probe also demonstrated satisfactory performance. In general, the sequence of this probe was well conserved among all the isolates. The only exceptions might be for the recombinant forms of HBV, for which the mismatches were frequent, particularly with the probe, and for some HBV genotype C sequences.

Fig. 4 shows the correlation of the optimized in-house real-time PCR with the commercial assay. A strong correlation was observed across all the tested samples, using the new antisense primer, including discrepant samples and their dilutions (R^2=0.99, Fig. 4).

Fig. 5 shows the performance of the in-house test with HBV-positive and negative samples. Most negative samples did not exhibit any signal during the PCR process (40 cycles), although 1/20 negative samples had a cycle threshold (Ct) value of 39.01. The detection limit was fixed at 50 UI/mL (Ct value around 35), which is acceptable for managing HBV-infected patients.

DISCUSSION

Hepatitis B is still a significant health problem in Venezuela, even if vaccination campaigns may have reduced the burden of this disease, particularly in some indigenous populations, where HBV infection remains highly endemic [20]. The most common HBV genotype in Venezuela is F (F3, followed by F2, and less frequently F1 and F4), followed by HBV genotypes with worldwide distribution (A and D) and infrequently the HBV Asian B and C, particularly these last ones in immigrants [13,20]. The samples from this study included different subgenotypes circulating in the country, and this diversity was important to assess the performance, particularly in terms of sensitivity, of the real-time PCR test analyzed.

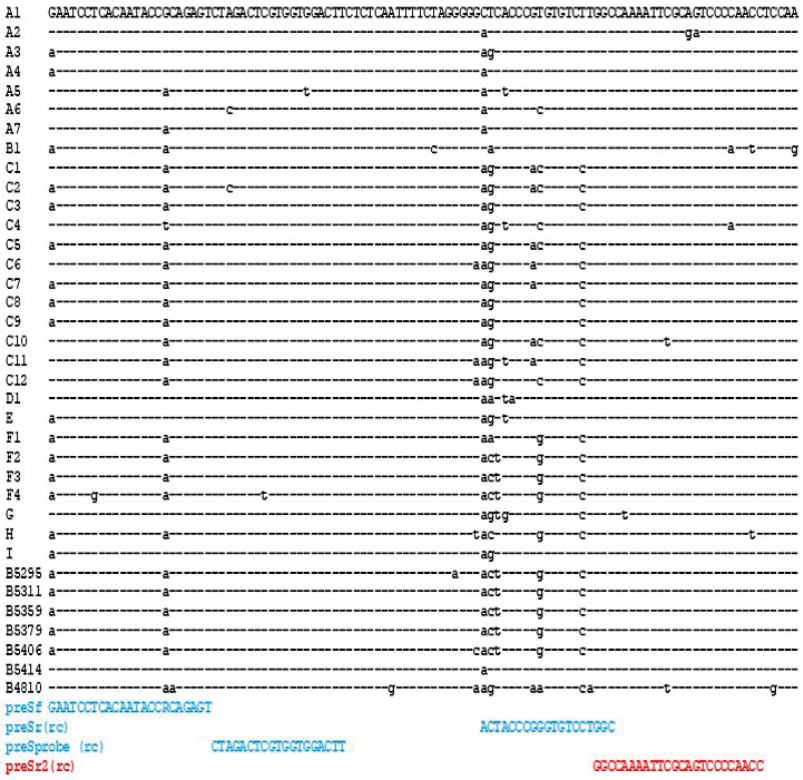

Fig. 3. Sequence alignment of the HBV preS region amplified by the in-house real-time test. Reference sequences are shown with their genotypes. The sequence of the samples used in this study is also included, except for B02023, since the sequence was shorter and does not cover the region. The primers from Portilho et al. [12] for the in-house test are shown in blue. The new modified reverse primer is shown in red. The reverse complement sequences are shown for the reverse primers.

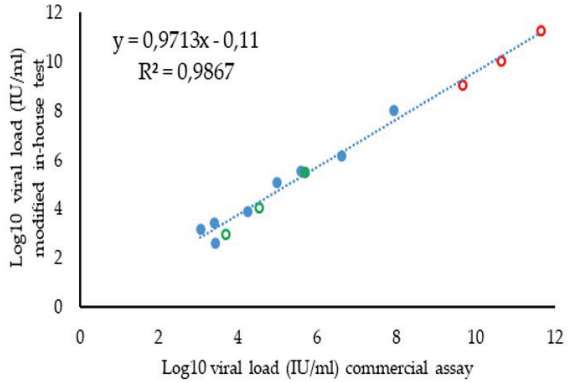

Fig. 4. Correlation between viral load determination with a commercial assay and the optimized in-house method. Dilutions of the sample B4810 (10^{-1}, 10^{-3}, and 10^{-4}) are shown in open orange circles, while sample 5379 and its dilutions (10^{-1} and 10^{-2} open circles) are shown in green.

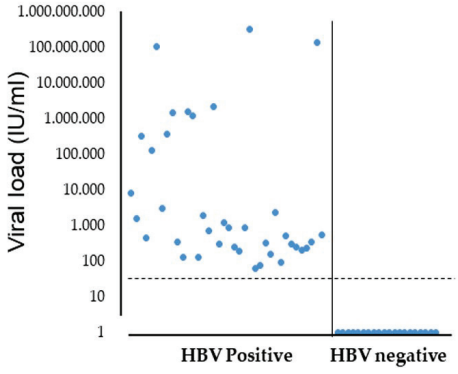

Fig. 5. Performance of the optimized in-house real-time PCR with sera from HBV-infected patients or non-infeected with this virus. Ct values of positive (left, 38 samples) and negative (right, 20 samples) HBV samples. The HBV negative samples were samples from six HCV positive, three dengue virus positive, two HIV-1 positive, 1 HAV positive, 1 HEV positive, and six with any known infecting virus.

Table 1. Complementarity of the primers used in the modified in-house method with HBV sequences available in the HBV database.

HBV genotype	N of sequences	Sequences with divergence[1]		
		preSf	preSr2	preSprobe
A	2359	104	48	64
B[2]	3534	246	64	68
C[3]	5088	386	1639	160
D[4]	3220	399	123	45
E[5]	894	28	124	17
F[5]	357	39	4	5
G[6]	87	2	0	0
H[7]	48	4	3	0
RF[8]	929	237	134	28[7]
Total (%)	16516	8.85%	12.95%	2.34%

[1] The complementarity of the primers tested in the new in-house method were analyzed in the 16516 HBV sequences of the HBV database [19]. Most of the observed divergences in the complementarity with the primers correspond to only one or two internal mismatches. [2] For preSf and PreSr2, most of the sequences exhibited one mismatch at the 5´end, so this first nt of the primer was not considered in the analysis. [3] Some mismatches were found in the 3´end of the primers: 38 sequences exhibited this mismatch for primer preSf, only 3 for preSr2. [4] One sequence with a mismatch at the 3´end. [5] For preSf primer, most of the sequences exhibited one mismatch at the [5,7]´end, so this first nt was not considered in the analysis. [6] All the genotype G isolates have a T instead of an A in the fifth position of the primer preSr2, from 3´to 5´end, so this position was not considered in the analysis. [8] RF: recombinant forms. Many sequences exhibited one or more mismatches, internal or at the 5´end.

A low correlation was observed between the commercial assay and the original in-house primers proposed by Portilho et al. [12]. This finding contrasts with their analysis of 40 serum samples, where a good correlation with the commercial assay was observed [12]. However, the authors did not mention the genotype of their samples.

Although HBV is a DNA virus, it displays a level of variability intermediate between RNA and DNA viruses. The dependence of a reverse transcriptase for its replication, which lacks proof-reading activity, increases the mutation rate of this virus. In contrast, the highly compact genome (one of the smallest animal DNA genomes), with a high degree of overlap in the different open reading frames, reduces the viability of some of these mutations. The result is an intermediate mutation rate, compared to a DNA and an RNA virus [20]. The variability exhibited by different HBV genotypes leads to differential pathogenesis and variable resistance to IFN treatment [21]. In addition, the accuracy of primers in PCR reactions is always limited.

In this study, analyzing more than 16,500 sequences to evaluate the suitability of the new proposed primers suggests that we can be confident in using those modified primers. The only exception might be the recombinant isolates (and some genotype C isolates), although we could not test any recombinant isolates. Recombination is a common phenomenon in HBV [22,23]. Infection with some HBV genotypes has been associated with a more severe disease and more rapid progression to HCC, for example, infection with HBV genotype C: the relationship between HBV recombinant genotypes and pathogenesis is unknown at present [20,21]. The recombinant forms, in any case, may affect the sensitivity of molecular diagnostic techniques.

In conclusion, modifying the HBVpreS reverse primer significantly improved the correlation of the viral load determination by the in-house method, with the commercial assay, increasing then the performance of this test. The new version of the in-house test displayed a satisfactory sensitivity and specificity, allowing its use for monitoring patients in low-income settings. A limitation of this study is the relatively low number of samples evaluated by the commercial assay and the in-house test. The in-house test tested a higher number of samples (n=38 positive samples, and 20 negative, the last ones without any signal). In addition, the *in silico* validation of the assay with more than 16,000 sequences makes us confident in the performance of the optimized test.

ACKNOWLEDGMENTS

To the health personnel who effectively attended to the cases of hepatitis in this study.

Funding

The Ministerio del Poder Popular para Ciencia y Tecnología de Venezuela (MinCyT) financed this project, Proyecto Mujer 2024.

Declaration of conflicts of interest

The authors declare that they have no conflict of interest.

Number ORCID of authors

- María Zulay Sulbarán (MZS): 0009-0008-9798-5593
- Yoneira Sulbaran (YS): 0000-0002-3170-353X
- Rossana C Jaspe (RCJ): 0000-0002-4816-1378
- Carmen L. Loureiro (CLL): 0000-0003-3665-1107
- Héctor R Rangel (HRR): 0000-0001-5937-9690
- Flor H. Pujol (FHP): 0000-0001-6086-6883

Participation of authors

MZS, YS, RJC, CL, FHP: Substantial contribution to the conception and design of the study; data collection or their analysis and interpretation, critical review of the article and approval of the final versión to be published. HRR: critical review of the article and approval of the final versión to be published.

REFERENCES

1. **Jeng WJ, Papatheodoridis GV, Lok ASF**. Hepatitis B. Lancet 2022: S0140-6736(22)01468-4. *https://doi.org/10.1016/S0140-6736(22)01468-4.*
2. **GBD 2019 Hepatitis B Collaborators**. Global, regional, and national burden of hepatitis B, 1990–2019: a systematic analysis for the Global Burden of Disease Study 2019. Lancet Gastroenterol Hepatol 2022; 7: 796-829. *https://doi.org/10.1016/S2468-1253(22)00124-8.*
3. **MacLachlan JH, Cowie BC**. Hepatitis B virus epidemiology. Cold Spring Harb Perspect Med 2015; 5: a021410. *https://doi.org/10.1101/cshperspect.a021410.*
4. **Gerlich WH**. Medical virology of hepatitis B: how it began and where we are now. Virol J 2013; 10: 239. *https://doi.org/10.1186/1743-422X-10-239.*
5. **McNaughton AL, Revill PA, Littlejohn M, Matthews PC, Ansari MA**. Analysis of genomic-length HBV sequences to determine genotype and subgenotype reference sequences. J Gen Virol 2020; 101: 271-283. *https://doi.org/10.1099/jgv.0.001387.*
6. **Pujol FH, Toyé RM, Loureiro CL, Jaspe RC, Chemin I**. Hepatitis B eradication: vaccine as a key player. Am J Transl Res. 2023; 15: 4971-4983.

7. **Huzair F, Sturdy S**. Biotechnology and the transformation of vaccine innovation: The case of the hepatitis B vaccines 1968-2000. Stud Hist Philos Biol Biomed Sci 2017; 64: 11-21. *https://doi.org/10.1016/j.shpsc.2017.05.004.*
8. **World Health Organization**. Combating Hepatitis B and C to Reach Elimination by 2030. Available from: https://apps.who.int/iris/bitstream/handle/10665/206453/WHO_HIV_2016.04_eng.pdf. Accessed on December 22, 2024
9. **Feld JJ, Lok AS, Zoulim F**. New Perspectives on Development of Curative Strategies for Chronic Hepatitis B. Clin Gastroenterol Hepatol. 2023; 21: 2040-2050. *https://doi.org/10.1016/j.cgh.2023.02.032.*
10. **WHO**. Guidelines for the prevention, diagnosis, care and treatment for people with chronic hepatitis B infection. Geneva: World Health Organization; 2024. Licence: CC BY-NC-SA 3.0 IGO.
11. **Pawlotsky JM**. Virological markers for clinical trials in chronic viral hepatitis. Virological markers for clinical trials in chronic viral hepatitis. JHEP Rep. 2024; 6: 101214. *https://doi.org/10.1016/j.jhepr.2024.101214.*
12. **Portilho MM, Mendonça ACDF, Bezerra CS, do Espirito-Santo MP, de Paula VS, Nabuco LC, et al**. Usefulness of in-house real time PCR for HBV DNA quantification in serum and oral fluid samples. J Virol Methods. 2018; 256: 100-106. *https://doi.org/10.1016/j.jviromet.2018.03.001.*
13. **Devesa M, Loureiro CL, Rivas Y, Monsalve F, Cardona N, Duarte MC, et al.**. Subgenotype diversity of hepatitis B virus American genotype F in Amerindians from Venezuela and the general population of Colombia. J Med Virol. 2008; 80: 20-26. *doi: 10.1002/jmv.21024. https://doi.org/*
14. **Tamura K, Stecher G, and Kumar S**. MEGA11: Molecular Evolutionary Genetics Analysis version 11. Mol Biol Evol. 2011; 38: 3022-3027. *https://doi.org/10.1093/molbev/msab120.*
15. **Uzunoğlu E, Şahin AM, Avci E, Kutlu H, Güntepe G**. Can HBsAg Be Used as a Viral Replication Marker in Chronic Hepatitis B Patients? Viral Hepa J. 2017; 23: 55-59.
16. **Aynalia A, Ciftcia E, Aridogana BC, Cetina ES, Kayab S, Carsancaklia SA, Ozturka T**. Evaluation of viral load distribution of HBV DNA positive patients at Suleyman Demirel University Hospital. J Exp Clin Med. 2015; 32: 147-150. *https://doi.org/10.5835/jecm.omu.32.04.002.*
17. **Guney M, Bakir A, Erdal H, Gunal A, Yildiz F, Sig AK, Kurkcu MF, Yavuz MT, Gulsen M**. The Correlation between Histopathological Stages and Viral Markers of Chronic Hepatitis B infection in Ankara, Turkey. Int J Innov Sci Res Technol. 2021; 6: 1066-1070.
18. **Akoglu H**. User's guide to correlation coefficients. Turk J Emerg Med. 2018; 18: 91-93. *https://doi.org/10.1016/j.tjem.2018.08.001.*
19. **HBVdb**. The Hepatitis B Virus database. https://hbvdb.lyon.inserm.fr/HBVdb/HBVdbIndex. Accessed on December 27, 2024.
20. **Pujol F, Jaspe RC, Loureiro CL, Chemin I**. Hepatitis B virus American genotypes: Pathogenic variants? Clin Res Hepatol Gastroenterol. 2020; 44: 825-835. *https://doi.org/10.1016/j.clinre.2020.04.018.*
21. **Chen J, Li L, Yin Q, Shen T**. A review of epidemiology and clinical relevance of Hepatitis B virus genotypes and subgenotypes. Clin Res Hepatol Gastroenterol. 2023; 47: 102180. *https://doi.org/10.1016/j.clinre.2023.102180.*
22. **Araujo NM**. Hepatitis B virus intergenotypic recombinants worldwide: An overview. Infect Genet Evol. 2015; 36: 500-510. *https://doi.org/10.1016/j.meegid.2015.08.024.*
23. **Locarnini SA, Littlejohn M, Yuen LKW**. Origins and Evolution of the Primate Hepatitis B Virus. Front Microbiol. 2021; 12: 653684. *https://doi.org/10.3389/fmicb.2021.653684.*

Invest Clin 66(2): 175 - 190, 2025 https://doi.org/10.54817/IC.v66n2a05

Effects of oral nutritional supplementation in a case-management model on body composition changes in patients after bariatric surgery.

*Juan Cheng*and Yu Guo*

Department of Gastrointestinal Surgery, Jiangsu Province (Suqian Hospital), Suqian, Jiangsu, China.

Keywords: obesity; bariatric surgery; oral nutritional supplementation; case management model; body composition; self-management.

Abstract. This study explores the effects of oral nutritional supplementation in a case-management model on body composition alterations in patients after bariatric surgery. One hundred and twenty obese patients admitted to the Jiangsu Province Suqian Hospital from January 2024 to March 2025 who underwent bariatric surgery were included. Patients were divided into an observation group and a control group. The control group adopted routine nursing measures. Based on routine nursing measures, the observation group adopted an individualized nutritional supplement intervention according to the ideal body weight and the principle of limiting energy intake. One and three months after surgery, compared with the control group, the improvements of body fat percentage, free fat mass (FFM), body mass index (BMI), body weight, skeletal muscle mass, and excess weight loss rate in the observation group were more significant. The albumin, hemoglobin, and total protein levels were higher; emotional eating, external eating, restrained eating, and the Bariatric Surgery Self-management Questionnaire (BSSQ) scores were significantly improved. The scores of physical function, social function, physical pain, emotional function, general health, mental health, physical role, and vitality were higher. The total incidence of postoperative complications was lower, while the total nursing satisfaction rate of patients was higher. To sum up, oral nutritional supplementation in the case-management model can improve body composition, promote nutritional status, reduce the incidence of complications, promote postoperative self-management ability, and enhance the quality of life and nursing satisfaction in patients after bariatric surgery.

Corresponding author: Juan Cheng. Department of Gastrointestinal Surgery, Jiangsu Province (Suqian Hospital), Suqian, 223800 Jiangsu, China. E-mail: syrchengj1984@163.com

Efecto de la suplementación nutricional oral en un modelo de cambios en la composición corporal en pacientes después de cirugía bariátrica.

Invest Clin 2025; 66 (2): 175 – 190

Palabras clave: obesidad; cirugía bar iátrica; suplementación nutricional oral; modelo de manejo de casos; composición corporal; autogestión.

Resumen. Este estudio tiene como objetivo explorar los efectos de la suplementación nutricional oral en un modelo de manejo de casos sobre las alteraciones de la composición corporal en pacientes después de cirugía bariátrica. Se incluyeron 120 pacientes obesos ingresados en el Hospital de la provincia de Jiangsu Suqian desde enero de 2024 hasta marzo de 2025 que se sometieron a cirugía bariátrica. Los pacientes se dividieron en un grupo de observación y un grupo control. Al grupo control se le aplicaron medidas de enfermería de rutina. Con base a las medidas de rutina de enfermería, al grupo de observación se le aplicó una intervención individualizada de suplementos nutricionales de acuerdo con el peso corporal ideal combinado con el principio de limitar la ingesta energética. Uno y tres meses después de la operación, en comparación con el grupo control, las mejorías en porcentaje de grasa corporal, masa libre de grasa, índice de masa corporal , peso corporal, masa muscular esquelética y tasa de pérdida de exceso de peso en el grupo de observación fueron más significativas. Los niveles de albúmina, hemoglobina y proteína total fueron mayores. El dolor físico, la función emocional, el estado general de salud, la salud mental, el papel físico y la vitalidad mejoraron; la incidencia total de complicaciones postoperatorias, los puntajes del Cuestionario de Autogestión de la Cirugía Bariátrica (BSSQ) y la tasa de satisfacción total de enfermería de los pacientes fueron mayores. En resumen, la suplementación nutricional oral en el modelo de manejo de casos puede mejorar la composición corporal, promover el estado nutricional, reducir la incidencia de complicaciones, promover la capacidad de automanejo postoperatoria, junto con una mejoría en la calidad de vida y la satisfacción de la enfermería en pacientes de cirugía bariátrica.

Received: 01-02-2025 Accepted: 08-05-2025

INTRODUCTION

Obesity is recognized as a disease by the World Health Organization, and according to statistics, 38% of the global population was overweight and obese in 2020, and this figure is expected to rise to 51% by 2035 [1]. According to the Dietary Guidelines for Chinese Residents (2022), the number of obese people in China ranks first in the world [2]. At present, the treatment of obesity is mainly based on behavior, diet, exercise, drugs and surgery [3]. Compared with other treatments, bariatric surgery can reduce weight more quickly, effectively and sustainably in patients with morbid obesity or obesity complications by limiting food intake along with reducing nutrient absorption, and has become the most effective treatment for patients with moderate and severe obesity [4]. Studies

have shown that postoperative changes in the digestive tract structure can affect nutrient absorption to varying degrees, thus increasing the risk of malnutrition and associated complications, and eventually leading to malnutrition [5]. Malnutrition is a common clinical problem after bariatric surgery [6]. Therefore, nutrition management is essential for patients after bariatric surgery.

Body composition refers to the content of various components in the body, containing three categories: fat mass, muscle mass and bone mineral salt content [7]. Muscle mass's physiological and metabolic function differs from that of fat mass, and muscle mass is the main metabolically active component of the human body [8]. Muscle mass loss may affect the body mass loss rate after bariatric surgery by reducing resting energy expenditure [9]. Loss of weight includes not only the loss of fat mass, but also the loss of muscle mass [10]. Foreign studies have found that the loss of muscle tissue after bariatric surgery will have a negative impact on the long-term effect of bariatric surgery, human health, and quality of life, and can endanger the life of patients in severe cases [11]. The main components of human muscle tissue include lean body mass (LBM), fat-free mass (FFM), along with skeletal muscle mass (SMM) [12]. The loss of FFM mainly occurs within three months after bariatric surgery, when patients are prone to malnutrition [13]. At present, domestic and foreign studies have shown that in order to avoid the occurrence of postoperative malnutrition and reduce the loss of FFM, patients are usually given at least 60 g/d of protein-rich low-carbohydrate oral nutritional supplement after surgery, and whey protein formula is the preferred formula [14]. However, most patients with bariatric surgery have destructive eating behaviors before surgery, lack of health awareness and poor self-control after surgery, and need different nutritional components and amounts due to individual differences [15]. Therefore, individualized oral nutritional supplementation for patients after bariatric surgery may effectively improve the clinical outcome of patients, decrease the loss of muscle tissue after bariatric surgery, improve the effect of bariatric surgery along with improving patients' dietary behavior compliance, so as to better manage weight loss for patients [16].

Case management belongs to a health care system for a disease that contains assessment, planning, service, coordination, and monitoring to meet the multiple health requirements of individuals and promote cost-effective and high-quality services [17]. The case-management model has been successively applied to burns, acquired immune deficiency syndrome, tuberculosis, cancer, mental illness and other complicated diseases, as well as chronic diseases such as diabetes, hypertension and other long-term care systems [18-20]. In addition, the case management model has achieved specific results in nutritional supplementation, emphasizing the importance of personalized management, and is currently used in all kinds of population interventions with extensive adaptability [21]. However, case management of oral nutritional supplementation in patients with bariatric surgery is rare.

Based on the case-management model, this study constructed an oral nutritional supplement program for patients after bariatric surgery to explore the influence of this program on the related indexes of body composition of patients after bariatric surgery, in order to provide a theoretical basis and practical guidance for nutritional management of patients after bariatric surgery.

PATIENTS AND METHODS

General data

One hundred and twenty obese patients admitted to our hospital from January 2024 to March 2025 who underwent bariatric surgery were selected as study subjects. Inclusion criteria: (1) Age ranged from 18-65 years old; (2) In line with the surgical indications of the "Expert Consensus on nutrition and multidisciplinary management of bariatric

surgery"; (3) Patients undergoing their first bariatric surgery; (4) Normal communication skills, skilled use of mobile APP's. Exclusion criteria: (1) Complicated with serious heart, lung, kidney and other diseases; (2) With mental illness; (3) Patients undergoing corrective surgery; (4) Pregnant or lactating women; (5) Incomplete clinical data collection. Patients were divided into an **observation group** and a **control group** following the time order of operation, with 60 patients in each group. No difference was seen in general data between the two groups ($p>0.05$, Table 1), reflecting comparability. This study was approved by the ethical committee of the Jiangsu Province Suqian Hospital and followed the guidelines of the Declaration of Helsinki of 1975, revised in 2013. Each patient has signed the informed consent.

METHODS

The **control group** adopted routine nursing measures. Before bariatric surgery, the routine preparation plan was conducted. Postoperative education was guided according to the phased diet principle: drinking water (1-3 days after surgery) →blandliquid-diet (1-2 weeks after surgery) → fluid diet (3-4 weeks after surgery) → semi-fluid diet (5-6 weeks after surgery) → soft food (7-12 weeks after surgery) → low-calorie balanced diet (12 weeks after surgery). The daily water intake was at least 1500-2000 mL, and the patients were instructed to take special vitamins for weight loss, orally, after surgery. Patients began taking an oral protein powder for weight loss on day 8 and consumed at least 60 g of protein daily. The weight loss education manual was distributed, and the case manager was responsible for managing the weight loss WeChat group and answering the patients' questions. Patients were urged to eat as required after discharge and informed to go to the hospital for a follow-up visit one and three months after surgery.

Based on routine nursing measures, the **observation group** adopted an individualized nutritional supplement intervention according to the ideal body weight and the principle of limiting energy intake.

(1) Setting up a research team. Nutrition specialist nurse Juan Cheng and nutrition physician Liping Su developed an individualized oral nutrition supplement program for patients after bariatric surgery, and chief physician Guodong Liu made adjustments. Yu Guo taught the patients to use the "Menthol Health" nutritionist app and record their dietary intake for 24 hours. The nutrition specialist nurses analyzed and sorted the collected data every week and dynam-

Table 1. General data of patients in the two groups.

Items		Control group (n=60)	Observation group (n=60)	t/χ^2	p
Gender	Male	20 33.33)	18 (30.00)	0.154	0.694
	Female	40 66.67)	42 (70.00)		
Age (years)		31.26±4.21*	31.31±4.26	0.064	0.948
Marital status	Married	39 65.00)	38 (63.33)	0.036	0.190
	Unmarried	21 35.00)	22 (36.67)		
Degree of education	Junior high school and below	10 (16.67)	11 (18.34)	0.068	0.966
	Senior high school	24 (40.00)	23 (38.33)		
	University and above	26 (43.33)	26 (43.33)		

Data is expressed as n (%); or *mean ± SD.

ically adjusted the intake plan of nutritional preparations. Menglin Zhang was responsible for the analysis and detection of body composition one and three months after bariatric surgery, and used the questionnaire to issue the Dutch Eating Behavior Questionnaire (DEBQ) and the Bariatric Surgery Self-management Questionnaire (BSSQ) to understand the patients' dietary compliance and self-management ability. Lidan Zhao was responsible for the statistics, and the statistical data were entered and checked jointly by the two of them. The statistician did not participate in the design and implementation of the program.

(2) Oral nutritional supplement program after bariatric surgery. On the day of admission, the case manager measured the patient's height, weight, circumference and body composition, conducted preoperative diet education according to the measured results, and established the case file. One to two days after surgery, the nutrition specialist nurse instructed the patient to drink a small amount of water several times, and gave the patient warm water 20-30 mL/time, 3-5 times, once/h, and instructed the patient to drink slowly, 500 mL of water on the day and 1000 mL of water on the second day. Three to six days after surgery, the patient was given a bland liquid diet + whey protein powder (45 g/d). The patient was guided to drink 1500 mL of water, and the patient's energy intake was 600 kcal/d. One to two weeks after surgery, the patient was given a fluid diet + whey protein powder (60 g/d), and the patient's energy intake was 10 kcal (kg·d). Three to four weeks after surgery, the patient was given a semi-fluid diet + whey protein powder (60 g/d), and the patient's energy intake was 15 kcal (kg·d). Two to three months after surgery, the patient was given soft food + whey protein powder (60 g/d), and the patient's energy intake was 20 kcal (kg·d). Among them, the dietary requirements for one week to three months after surgery were 40% to 45% carbohydrates, 20% to 30% fat, 25% to 30% protein + weight loss special complex vitamins, and daily drinking water ≥ 2000 mL.

Control Group: Postoperative diet progression protocol

In this study, all patients followed a structured diet advancement protocol after bariatric surgery, beginning with clear fluids and gradually progressing to a soft diet. The dietary phases were as follows:

- Days 1–3 post-surgery: Clear fluids only
- Weeks 1–2: Bland liquid diet
- Weeks 3–4: Full fluid diet
- Weeks 5–6: Semi-fluid/pureed diet
- Weeks 7–12: Soft food diet
- After week 12: Transition to a low-calorie, balanced solid diet

This extended progression was based on institutional protocol, aimed at reducing the risk of early gastrointestinal intolerance and complications. Protein supplementation (minimum 60 g/day) was initiated during the fluid phase and continued throughout recovery. Patients were counselled to follow prescribed meal volumes, texture guidelines, and hydration targets (≥2000 mL/day).

All patients undergoing bariatric surgery were provided with standardized preoperative dietary guidance upon admission to the hospital. Specifically, patients were instructed to follow a low-calorie, high-protein, low-carbohydrate liquid diet for seven to ten days before surgery. This preoperative diet was designed to reduce liver volume, decrease visceral adiposity, and enhance surgical visibility and safety. The prescribed regimen typically included 800–1000 kcal/day, with at least 60–80 g of protein, and emphasized adequate fluid intake (≥1500 mL/day). Acceptable liquids included clear broths, low-fat dairy, protein shakes, and sugar-free beverages. Patients were advised to avoid solid foods, sugary drinks, carbonated beverages, and high-fat items. The case

management nurse conducted a brief in-hospital orientation session to reinforce dietary compliance, and adherence was monitored through verbal recall and written logs during preoperative assessments. Patients who demonstrated non-adherence were counselled and re-evaluated before surgical clearance.

In the present study, the phrase "dynamically adjust the intake plan of nutritional preparations" refers to the individualized modification of oral nutritional supplement (ONS) prescriptions based on the patients' daily energy and protein intake, as recorded through a dietary tracking app (Menthol Nutritionist). These adjustments were not related to food preparation, culinary menu design, or traditional meal planning, but rather to the quantitative regulation of supplement dosage—particularly whey protein powder—to ensure that nutritional intake aligned with the patient's postoperative recovery phase and ideal body weight. Specifically, adjustments targeted a protein intake of at least 60 g/day and an energy intake ranging from 10 to 20 kcal/kg/day, depending on the time elapsed since surgery. The data collected were reviewed weekly by the nutrition specialist nurse and supervising nutrition physician, who modified the amount and timing of ONS accordingly. While this nurse-led protocol provided a structured method for managing macronutrient intake, we acknowledge that it does not replace the comprehensive services of a registered dietitian formally trained to develop evidence-based individualized nutrition care plans. The absence of dietitian involvement represents a limitation and underscores the need for future studies to incorporate certified clinical dietitians as core members of the bariatric care team.

Observation indicators

(1) Patients were asked to weigh themselves on an empty stomach in the morning, wearing light clothes and bare feet. The test instrument was measured by an HCS-200RT weight scale, with kg as the unit of measurement, and the error was not more than 0.01 kg. A column height gauge measured the height; the waist and hip circumference were measured by a soft tape measure with cm as the unit of measurement, and the error should not exceed 0.01 cm. The Inbody 3.0 body composition analyzer was used to measure body composition. Body weight, BMI, FFM, body fat percentage (%), skeletal muscle mass and excess weight loss rate were recorded after the test.

(2) Nutritional indicators, including hemoglobin, albumin, and total protein, were compared between the two groups.

(3) The total incidence of postoperative complications, including abdominal hemorrhage, gastric fistula, vomiting, as well as anastomotic stenosis, was compared between the two groups.

(4) DEBQ was used to assess the postoperative eating behavior of patients in the two groups [22]. DEBQ included three dimensions: emotional, external, and restrained eating. 1 point represented "never," and 5 points represented "always." The higher the score, the higher the level of corresponding eating behavior.

(5) The Bariatric Surgery Self-Management Questionnaire (BSSQ) is a validated instrument designed to evaluate self-management behaviors critical to postoperative recovery and long-term success following bariatric surgery. The BSSQ consists of 33 items divided into multiple domains, including:

1. Dietary behaviors (e.g., protein intake, hydration, meal timing)
2. Physical activity adherence
3. Medication and supplement compliance
4. Self-monitoring behaviors (e.g., weight, symptoms, food logs)
5. Emotional coping and support-seeking behaviors

Each item is scored on a 5-point Likert scale ranging from "Never" (1) to "Always" (5), with higher scores indicating better adherence to recommended self-management practices. The total score ranges from 33 to 165, and in our study, it was rescaled to a 0–99 scale for comparative purposes. The BSSQ was administered postoperatively to both groups at one and three months by trained study personnel. Patients in the observation group were counselled more intensively on these domains as part of the case-management model, which may have contributed to their significantly higher BSSQ scores.

(6) The quality of life was assessed using the Short-Form 36 (SF-36) score [24], which included eight dimensions (physical function, social function, physical pain, emotional function, general health, mental health, role physical, and vitality), with a score of 0-100 for each dimension. The quality of life was positively correlated with the score.

(7) During hospitalization, the nursing satisfaction questionnaire made by our hospital was used to evaluate nursing satisfaction of patients, with a full score of 100. According to the score, it could be divided into satisfaction (score ≥80 points), basic satisfaction (60 points ≤ score <80 points) and dissatisfaction (score <60 points). Nursing satisfaction = (number of satisfaction cases + number of basic satisfaction cases)/total cases ×100%.

Assessment of dietary and vitamin intake compliance

Actual dietary intake—including protein, energy, fluid, and vitamin supplement consumption—was monitored using the Menthol Nutritionist app, where patients in both groups were instructed to record their 24-hour food and supplement intake. Compliance was assessed weekly by the case management team, with guidance provided for underreporting or deviations from the instructed plan. However, quantitative intake was only analyzed in the observation group, where the app data were actively used to tailor ONS dosages. In the control group, while intake logs were encouraged and verbally reviewed during follow-ups, no structured method was used to quantify or verify adherence to the prescribed dietary or vitamin regimen. Laboratory markers such as hemoglobin, albumin, and total protein were used as indirect indicators of nutritional adequacy, but specific micronutrient levels (e.g., iron, B12, vitamin D) were not assessed.

Micronutrient supplementation protocol

All patients were routinely prescribed a standardized bariatric multivitamin complex starting from the first week after surgery to address the risk of postoperative micronutrient deficiencies. The formulation used contained at minimum:

- Iron (≥45 mg)
- Vitamin B12 (≥350–500 mcg)
- Folic acid (400–800 mcg)
- Calcium citrate (≥1200–1500 mg) with Vitamin D3 (≥3000 IU)
- Vitamin A (≥5000 IU), Vitamin E, and Zinc in bariatric-recommended dosages

This formulation followed the guidelines established for post-bariatric patients to prevent common deficiencies in iron, B12, folate, calcium, and fat-soluble vitamins. Patients were advised to take divided doses (e.g., twice daily) and were monitored for adherence during follow-up visits. The same vitamin regimen was provided to the control and observation groups to avoid bias introduced by unequal micronutrient support.

Oral nutritional supplement program after bariatric surgery

Personalization of ONS Based on Ideal Body Weight and Energy Restriction in the observation group, oral nutritional supplementation (ONS) was tailored using a sim-

plified protocol based on each patient's ideal body weight (IBW) and postoperative energy restriction targets. IBW was calculated using the standard formula:

- IBW (kg) = 22 × height² (m²)
- Daily energy intake goals were set according to the postoperative phase:
- Week 1–2: 10 kcal/kg IBW/day
- Week 3–4: 15 kcal/kg IBW/day
- Week 5–12: 20 kcal/kg IBW/day

Protein requirements were uniformly set at a minimum of 60 g/day, adjusted upward if tolerated, particularly for patients with higher baseline BMI or physical activity levels.

All patients in the observation group received the same brand of whey protein powder (a medical-grade, high-biological-value supplement), but dosages were individualized to help patients reach their energy and protein targets when food intake was inadequate. The protein powder contained approximately 25 g of protein and 150 kcal per serving, and was administered in divided doses (1–3 servings/day) based on intake gaps identified through dietary logs. No flavor or formula variations were used, and micronutrient content was not adjusted individually—this was standardized and supplemented through bariatric multivitamin capsules given to all patients.

Specification of whey protein supplement used

All patients in the observation group received the same commercially available whey protein supplement, a whey protein isolate powder containing approximately 25 g of protein, 2 g of carbohydrates, 1 g of fat, and 150 kcal per 30 g serving. The supplement was not fortified with vitamins or minerals, and therefore did not serve as a complete meal replacement. It was used exclusively to meet daily protein intake targets (minimum of 60 g/day) and routine bariatric multivitamin supplementation. Patients consumed 1–3 servings daily based on their estimated protein gap from dietary intake, calculated using ideal body weight and reported food logs.

Statistical analysis

SPSS 24.0 statistical software was adopted for data analysis. Measurement data were expressed as $\bar{x}\pm SD$, and t-test and ANOVA were adopted for comparison. Count data were expressed as [n (%)], and the χ^2 test was adopted for comparison. $p<0.05$ represented that the difference was statistically significant.

RESULTS

Body composition of patients in the two groups

At one and three months after surgery, the body fat percentage, FFM, BMI and body weight in both groups were lower than baseline ($p<0.05$), while the skeletal muscle mass and excess weight loss rate in both groups were higher than baseline ($p<0.05$). Meanwhile, relative to the control group, the improvements of the above body composition in the observation group were more significant ($p<0.05$), as displayed in Fig. 1.

Nutritional status of patients in the two groups

At 1 and 3 months after surgery, the body fat percentage, albumin, hemoglobin and total protein levels in both groups were higher than baseline ($p<0.05$). Meanwhile, relative to the control group, the levels of albumin, hemoglobin, and total protein in the observation group were higher ($p<0.05$, Fig. 2).

Incidence of postoperative complications in the two groups

Relative to the control group, the total incidence of postoperative complications in the observation group was lower ($p<0.05$, Table 2).

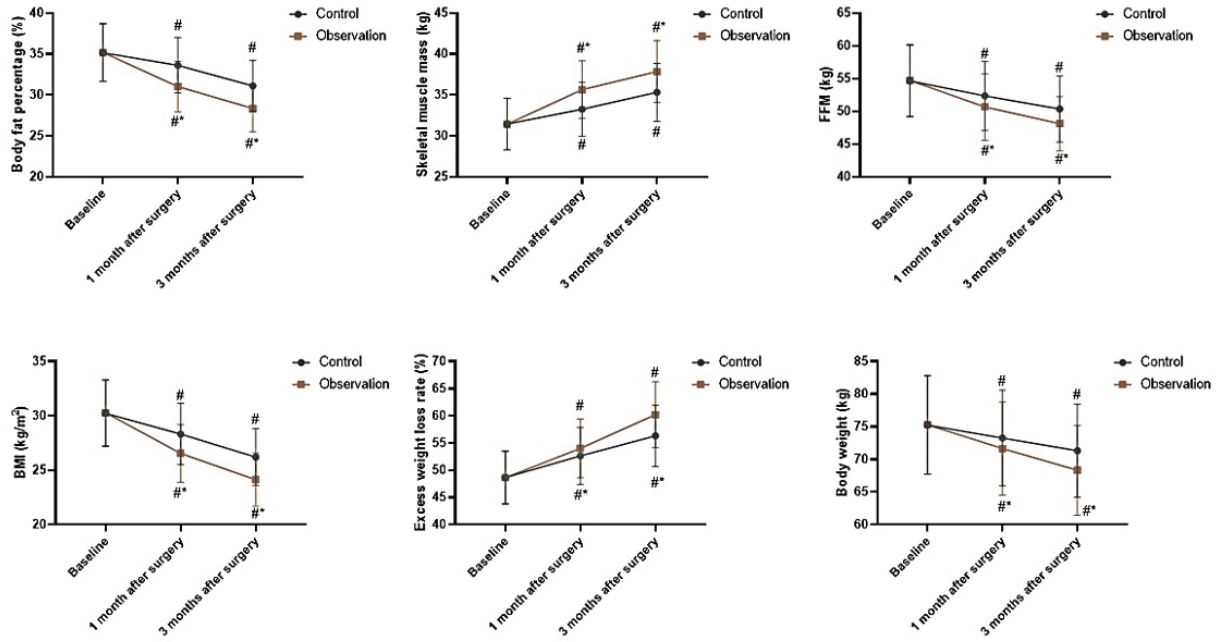

Fig. 1. Body composition of patients in the two groups. #p<0.05, vs baseline (ANOVA); *p<0.05, vs control group (t test).

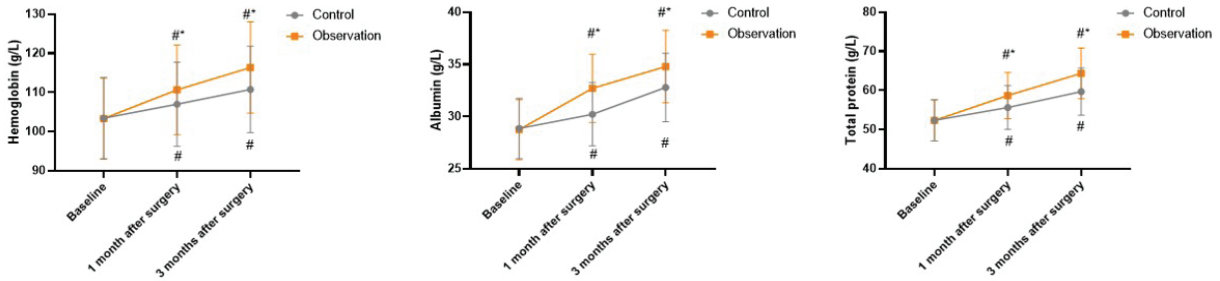

Fig. 2. Nutritional status of patients in the two groups. #p<0.05, vs baseline (ANOVA); *p<0.05, vs control group (t test).

Table 2. Incidence of postoperative complications in the two groups.

Groups	N	Abdominal hemorrhage	Gastric fistula	Vomiting	Anastomotic stenosis	Total incidence rate
Control group	60	3 (5.00)	2 (3.33)	3 (5.00)	3 (5.00)	11 (18.33)
Observation group	60	0 (0.00)	1 (1.67)	1 (1.67)	1 (1.67)	3 (5.01)
χ^2						5.175
p						0.022

Data is expressed as n (%).

Postoperative eating behavior of patients in the two groups

At 1 and 3 months after surgery, the scores of emotional eating and external eating in both groups were lower than baseline ($p<0.05$), while the score of restrained eating in both groups was higher than baseline ($p<0.05$). Meanwhile, relative to the control group, the improvements of the scores of emotional eating, external eating and restrained eating in the observation group were more significant ($p<0.05$), as displayed in Fig. 3.

Postoperative self-management behaviors of patients in the two groups

At 1 and 3 months after surgery, the BSSQ scores in both groups were higher than baseline ($p<0.05$), and relative to the control group, the BSSQ scores in the observation group were higher ($p<0.05$), as displayed in Fig. 4.

Quality of life in the two groups

At 1 and 3 months after surgery, the scores of physical function, social function, physical pain, emotional function, general health, mental health, role physical, and vitality in both groups were higher than baseline ($p<0.05$). Relative to the control group, the scores of physical function, social function, physical pain, emotional function, general health, mental health, role physical, and vitality in the observation group were higher ($p<0.05$), as displayed in Fig. 5.

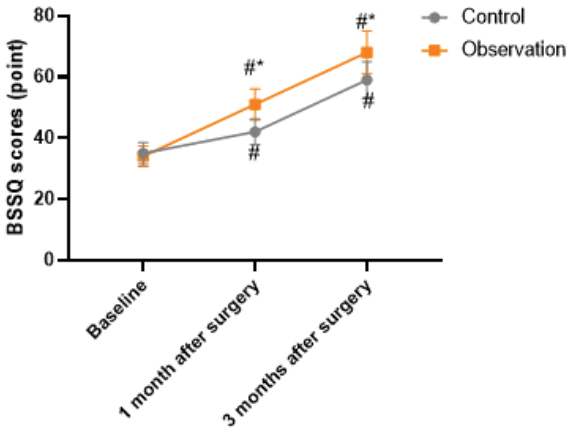

Fig. 4. Postoperative self-management behaviors of patients in two groups. #$p<0.05$, vs baseline (ANOVA); *$p<0.05$, vs control group (t test). #$p<0.05$, vs baseline; *$p<0.05$, vs control group.

Nursing satisfaction of patients the two groups

Relative to the control group, the total nursing satisfaction rate of patients in the observation group was higher ($p<0.05$, Table 3).

DISCUSSION

Obesity is a pathological condition in which fat accumulates excessively, usually caused by excessive nutrient intake [25]. Obesity is linked to an increased risk of hypertension, diabetes, lipid disorders, sleep disorders, coronary heart disease, and stroke [26]. Studies have shown that reducing weight

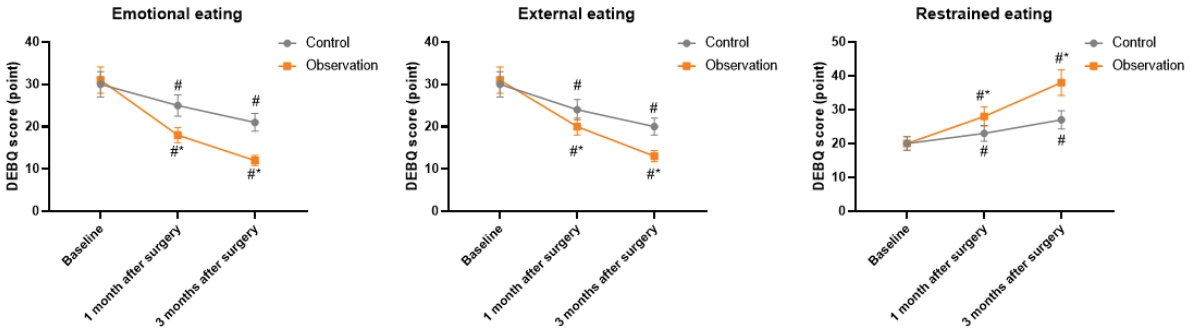

Fig. 3. Postoperative eating behavior of patients in the two groups. #$p<0.05$, vs baseline (ANOVA); *$p<0.05$, vs control group (t test).

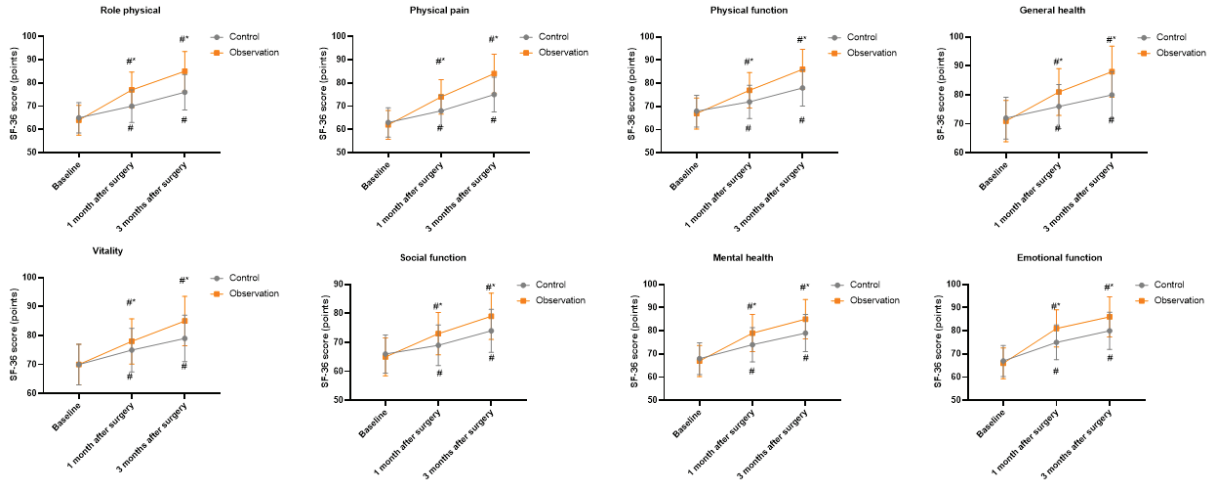

Fig. 5. Quality of life in the two groups. #p<0.05, vs baseline (ANOVA); *p<0.05, vs control group (t test). #p<0.05, vs baseline; *p<0.05, vs control group.

Table 3. Nursing satisfaction of patients in the two groups.

Groups	N	Satisfied	Barely satisfied	Dissatisfied	Total satisfaction
Control group	60	30 (50.00)	20 (33.33)	10 (16.67)	50 (83.33)
Observation group	60	35 (58.34)	23 (38.33)	2 (3.33)	58 (96.67)
χ^2					5.926
p					0.014

Data is expressed as n (%).

and fat accumulation can significantly extend national life expectancy and reduce the financial burden of health care [3]. Current approaches to weight loss include lifestyle interventions, medication, and surgery [27]. Some weight-loss medications, particularly older-generation agents, have been associated with neuropsychiatric side effects such as anxiety, insomnia, or mood changes, but these risks vary significantly depending on the specific drug and patient profile. Newer agents (e.g., GLP-1 receptor agonists) have shown a favorable safety profile in clinical trials, with few reports of severe mental health effects [28-31]. Protein isolates—particularly whey protein isolate—are known to provide highly bioavailable protein and have been shown to support muscle mass retention in postoperative patients. However, protein supplements' bioavailability and nutritional value vary considerably depending on their source, formulation, and protein concentration. For example, whey protein concentrates typically contain less protein and more lactose and fat than isolates, while protein waters may vary widely in their protein type and quantity. Most standard protein supplements also lack the comprehensive micronutrient profile found in complete protein meal replacements designed for bariatric patients. Therefore, accurate protein type and nutrient content specification is essential when interpreting their clinical impact.

However, after long-term practice, it has been found that many patients have reduced self-control after surgery and find it challenging to maintain good habits, which seriously affects the therapeutic effect of oral nutritional supplements [34]. The case-management model is a new nursing work and service concept that extends and continues the current holistic nursing model [35].

In the case-management model, the nurse plays the role of the person in charge of case management, is responsible for coordinating and communicating with doctors, medical teams and patients, formulating disease treatment plans and objectives, adjusting the plans based on the patient's situation, and constantly meeting the requirements of patients, so that they can achieve expectations within the scheduled period and have good clinical application effects [36].

Most anthropometric parameters, such as waist circumference, hip circumference, height, weight, and BMI, were used to assess the weight loss effect of patients after bariatric surgery. However, these indicators could not accurately reflect the body fat percentage and muscle content of obese patients, which had certain limitations [37]. The International Obesity Research Organization has indicated that the use of various tools to assess nutritional status, thereby improving treatment and medical nutritional support, is highly likely to decrease the morbidity burden of obese patients, so a growing number of studies have begun to focus on changes in body composition of patients after bariatric surgery [38]. After this procedure, changes in body composition, such as a sustained reduction in fat mass, are often associated with the inevitable loss of FFM [11]. Excessive loss of FFM is undesirable because FFM is responsible for most of the resting metabolic rate, regulating core body temperature, maintaining bone integrity, and maintaining function and quality of life as the body ages [39]. In our study, the results indicated that one and three months after surgery, the improvements of body fat percentage, FFM, BMI, body weight, skeletal muscle mass and excess weight loss rate in the observation group were more significant, suggesting that oral nutritional supplementation in the case management model could improve the body composition of patients after bariatric surgery. Consistently, Grupińska et al. suggested that oral nutritional supplements could improve body composition in women with breast cancer undergoing chemotherapy [40].

Moreover, our study also showed that at one and three months after the operation, relative to the control group, the improvements of the scores of emotional eating, external eating and restrained eating, as well as BSSQ scores in the observation group, were more significant. Meanwhile, at one and three months after the operation, relative to the control group, the scores of physical function, social function, physical pain, emotional function, general health, mental health, role physical, and vitality in the observation group were higher, suggesting that oral nutritional supplementation in the case management model could promote postoperative self-management ability, dietary compliance and quality of life in patients after bariatric surgery. In addition, we also found that oral nutritional supplementation in the case management model could enhance the nursing satisfaction of patients after bariatric surgery, which was in line with a study proposed by Dong et al. [46]. Although both groups received the same standard bariatric multivitamin complex, we acknowledge that the effects of vitamin supplementation could have interacted with or amplified the effects of oral nutritional supplements (ONS), particularly on markers of nutritional status such as hemoglobin, albumin, and protein levels. Therefore, while efforts were made to isolate the impact of ONS, micronutrient correction via vitamin intake may have contributed to improved outcomes, potentially confounding the degree to which results can be attributed to ONS alone. Future studies may consider a factorial design or biochemical monitoring of micronutrient levels to better disentangle these effects.

In conclusion, oral nutritional supplementation in the case-management model can improve body composition, promote nutritional status, reduce the incidence of complications, promote postoperative self-management ability, and enhance the quality of

life and nursing satisfaction in patients after bariatric surgery.

Recommendation

Future studies and clinical programs should prioritize the integration of registered clinical dietitians into case management models for postoperative bariatric patients. Including dietitians in multidisciplinary teams can ensure evidence-based, individualized nutritional care, leading to better outcomes in body composition, nutritional status, complication rates, and patient satisfaction. Institutional support to recruit and embed clinical dietitians into surgical and nutritional care pathways should be a strategic priority to align with international best practices.

Limitation

One notable limitation of our study is the prolonged timeline of postoperative diet advancement, with soft foods introduced only after six weeks postoperatively, lasting until week 12. This approach deviates from widely accepted post-bariatric surgery protocols in other regions, where soft foods are typically introduced by week 4, with transition to solid textures occurring by weeks 6–8. While our institution adopted a conservative progression to minimize gastrointestinal complications, this prolonged dietary restriction may have introduced confounding variables. Without personalized nutritional supplementation, patients in the control group may have experienced greater caloric deficits, reduced protein intake, and heightened dietary restraint—factors that could influence body composition, nutritional status, and psychological outcomes such as restrained eating. These effects may have amplified the observed benefits in the intervention group. Future studies should consider aligning with standard international diet progression guidelines to ensure broader generalizability and minimize the confounding impact of diet texture timelines.

A significant limitation of this study is the lack of objective, standardized tracking of dietary and vitamin intake in the control group. While the observation group utilized a digital app for real-time tracking and individualized ONS adjustments, intake data from the control group were based on self-reported logs and verbal follow-ups, which may introduce recall bias or underreporting. Furthermore, biochemical assessments of individual micronutrients were not conducted, limiting our ability to distinguish the effects of vitamin supplementation from the ONS protocol. This discrepancy in intake monitoring between groups may affect the accuracy of outcome comparisons.

ACKNOWLEDGMENTS

Thanks to Liping Su, Guodong Liu, Menglin Zhang and Lidan Zhao for their invaluable assistance.

Funding

This work received no funding.

Declaration of competing interest

The authors declare that they have no conflicts of interest.

Number ORCID of authors

- Juan Cheng: 0009-0008-3989-8416
- Yu Guo: 0009-0005-1230-5682

Credit authorship contribution statement

JC designed the study, collected data, and drafted the manuscript. YG performed data analysis, revised the manuscript, and drew figures.

REFERENCES

1. **Blüher M.** Obesity: global epidemiology and pathogenesis. Nat Rev Endocrinol 2019; 15(5): 288-298. *10.1038/s41574-019-0176-8.*
2. **Li J, Shi Q, Gao Q, Pan XF, Zhao L**, et al. Obesity pandemic in China: epidemiology, burden, challenges, and opportunities. Chin Med J (Engl) 2022; **135**(11): 1328-1330. *10.1097/cm9.0000000000002189.*
3. **Perdomo CM, Cohen RV, Sumithran P, Clément K, Frühbeck G.** Contemporary medical, device, and surgical therapies for obesity in adults. Lancet 2023; **401**(10382): 1116-1130. *10.1016/s0140-6736(22)02403-5.*
4. **Arterburn DE, Telem DA, Kushner RF, Courcoulas AP.** Benefits and Risks of Bariatric Surgery in Adults: A Review. Jama 2020; 324(9): 879-887. *10.1001/jama.2020.12567.*
5. **Nuzzo A, Czernichow S, Hertig A, Ledoux S, Poghosyan T, Quilliot D,** et al Le Gall M, Bado A, Joly F. Prevention and treatment of nutritional complications after bariatric surgery. Lancet Gastroenterol Hepatol 2021; 6(3): 238-251. *10.1016/s2468-1253(20)30331-9.*
6. **Mohapatra S, Gangadharan K, Pitchumoni CS.** Malnutrition in obesity before and after bariatric surgery. Dis Mon 2020; **66**(2): 100866. *10.1016/j.dis-amonth.2019.06.008.*
7. **Ikehata Y, Hachiya T, Kobayashi T, Ide H, Horie S**. Body composition and testosterone in men: a Mendelian randomization study. Front Endocrinol (Lausanne) 2023; **14**: 1277393. *10.3389/fendo.2023.1277393.*
8. **Chen L, Ming J, Chen T, Hébert JR, Sun P, Zhang L,** et al. Association between dietary inflammatory index score and muscle mass and strength in older adults: a study from National Health and Nutrition Examination Survey (NHANES) 1999-2002. Eur J Nutr 2022; **61**(8): 4077-4089. *10.1007/s00394-022-02941-9.*
9. **Fidilio E, Comas M, Giribés M, Cárdenas G, Vilallonga R, Palma F,** et al. Evaluation of Resting Energy Expenditure in Subjects with Severe Obesity and Its Evolution After Bariatric Surgery. Obes Surg 2021; 31(10): 4347-4355. *10.1007/s11695-021-05578-5.*
10. **Conte C, Hall KD, Klein S**. Is Weight Loss-Induced Muscle Mass Loss Clinically Relevant? Jama 2024; 332(1): 9-10. *10.1001/jama.2024.6586.*
11. **Nuijten MAH, Eijsvogels TMH, Monpellier VM, Janssen IMC, Hazebroek EJ, Hopman MTE**. The magnitude and progress of lean body mass, fat-free mass, and skeletal muscle mass loss following bariatric surgery: A systematic review and meta-analysis. Obes Rev 2022; 23(1): e13370. *10.1111/obr.13370.*
12. **Mikkola I, Jokelainen JJ, Timonen MJ, Härkönen PK, Saastamoinen E, Laakso MA,** et al. Physical activity and body composition changes during military service. Med Sci Sports Exerc 2009; 41(9): 1735-42. *10.1249/MSS.0b013e31819fcd3c.*
13. **Molero J, Olbeyra R, Flores L, Jiménez A, de Hollanda A, Andreu A,** et al. Prevalence of low skeletal muscle mass following bariatric surgery. Clin Nutr ESPEN 2022; 49: 436-441. *10.1016/j.clnesp.2022.03.009*.
14. **Thibault R, Huber O, Azagury DE, Pichard C.** Twelve key nutritional issues in bariatric surgery. Clin Nutr 2016; 35(1): 12-17. *10.1016/j.clnu.2015.02.012.*
15. **Andreu A, Flores L, Molero J, Mestre C, Obach A, Torres F,** et al. . Patients Undergoing Bariatric Surgery: a Special Risk Group for Lifestyle, Emotional and Behavioral Adaptations During the COVID-19 Lockdown. Lessons from the First Wave. Obes Surg 2022; 32(2): 441-449. *10.1007/s11695-021-05792-1.*
16. **Khanna D, Yalawar M, Saibaba PV, Bhatnagar S, Ghosh A, Jog P,** et al. Oral Nutritional Supplementation Improves Growth in Children at Malnutrition Risk and with Picky Eating Behaviors. Nutrients 2021; 13(10). *10.3390/nu13103590.*
17. **de Vet R, van Luijtelaar MJ, Brilleslijper-Kater SN, Vanderplasschen W, Beijersbergen MD, Wolf JR.** Effectiveness of case management for homeless per-

sons: a systematic review. Am J Public Health 2013; 103(10): e13-26. *10.2105/ajph.2013.301491.*

18. **Ji H, Chen R, Huang Y, Li W, Shi C, Zhou J**. Effect of simulation education and case management on glycemic control in type 2 diabetes. Diabetes Metab Res Rev 2019; 35(3): e3112. *10.1002/dmrr.3112.*
19. **Wu YL, Padmalatha KMS, Yu T, Lin YH, Ku HC, Tsai YT, Chang YJ, Ko NY.** Is nurse-led case management effective in improving treatment outcomes for cancer patients? A systematic review and meta-analysis. J Adv Nurs 2021; **77**(10): 3953-3963. *10.1111/jan.14874.*
20. **Burns T, Catty J, Dash M, Roberts C, Lockwood A, Marshall M.** Use of intensive case management to reduce time in hospital in people with severe mental illness: systematic review and meta-regression. Bmj 2007; 335(7615): 336. *10.1136/bmj.39251.599259.55.*
21. **Fabozzi G, Verdone G, Allori M, Cimadomo D, Tatone C, Stuppia L**, et al. Personalized Nutrition in the Management of Female Infertility: New Insights on Chronic Low-Grade Inflammation. Nutrients 2022; 14(9). *10.3390/nu14091918.*
22. **Arhire LI, Niță O, Popa AD, Gal AM, Dumitrașcu O, Gherasim A, Mihalache L, Graur M.** Validation of the Dutch Eating Behavior Questionnaire in a Romanian Adult Population. Nutrients 2021; 13(11). *10.3390/nu13113890.*
23. **Welch G, Wesolowski C, Piepul B, Kuhn J, Romanelli J, Garb J**. Physical activity predicts weight loss following gastric bypass surgery: findings from a support group survey. Obes Surg 2008; 18(5): 517-24. *10.1007/s11695-007-9269-x.*
24. **Lin Y, Yu Y, Zeng J, Zhao X, Wan C.** Comparing the reliability and validity of the SF-36 and SF-12 in measuring quality of life among adolescents in China: a large sample cross-sectional study. Health Qual Life Outcomes 2020; 18(1): 360. *10.1186/s12955-020-01605-8.*
25. **Piché ME, Tchernof A, Després JP.** Obesity Phenotypes, Diabetes, and Cardiovascular Diseases. Circ Res 2020; 126(11): 1477-1500. *10.1161/circresaha.120.316101.*
26. **Caballero B.** Humans against Obesity: Who Will Win? Adv Nutr 2019; 10(suppl_1): S4-s9. *10.1093/advances/nmy055.*
27. **Jackson VM, Breen DM, Fortin JP, Liou A, Kuzmiski JB, Loomis AK**, et al. Latest approaches for the treatment of obesity. Expert Opin Drug Discov 2015; 10(8): 825-39. *10.1517/17460441.2015.1044966.*
28. **Hunter E, Avenell A, Maheshwari A, Stadler G, Best D.** The effectiveness of weight-loss lifestyle interventions for improving fertility in women and men with overweight or obesity and infertility: A systematic review update of evidence from randomized controlled trials. Obes Rev 2021; 22(12): e13325. *10.1111/obr.13325.*
29. **Guglielmi V, Bettini S, Sbraccia P, Busetto L, Pellegrini M, Yumuk V,** et al. Beyond Weight Loss: Added Benefits Could Guide the Choice of Anti-Obesity Medications. Curr Obes Rep 2023; 12(2): 127-146. *10.1007/s13679-023-00502-7.*
30. **Sandoval DA, Patti ME**. Glucose metabolism after bariatric surgery: implications for T2DM remission and hypoglycaemia. Nat Rev Endocrinol 2023; 19(3): 164-176. *10.1038/s41574-022-00757-5.*
31. **Bal BS, Finelli FC, Shope TR, Koch TR.** Nutritional deficiencies after bariatric surgery. Nat Rev Endocrinol 2012; 8(9): 544-56. *10.1038/nrendo.2012.48.*
32. **Parrott JM, Craggs-Dino L, Faria SL, O'Kane M**. The Optimal Nutritional Programme for Bariatric and Metabolic Surgery. Curr Obes Rep 2020; 9(3): 326-338. *10.1007/s13679-020-00384-z.*
33. **Cawood AL, Burden ST, Smith T, Stratton RJ.** A systematic review and meta-analysis of the effects of community use of oral nutritional supplements on clinical outcomes. Ageing Res Rev 2023; 88: 101953. *10.1016/j.arr.2023.101953.*
34. **König L, Freire S, Gariani K, Karsegard J, Renaud C, Genton L, Collet TH.** [Management of type 2 diabetes on oral nutritional supplement]. Rev Med Suisse 2023; 19(829): 1072-1077. *10.53738/revmed.2023.19.829.1072.*

35. **Hernández-Zambrano SM, Mesa-Melgarejo L, Carrillo-Algarra AJ, Castiblanco-Montañez RA, Chaparro-Diaz L, Carreño-Moreno SP**,et al. Effectiveness of a case management model for the comprehensive provision of health services to multi-pathological people. J Adv Nurs 2019; 75(3): 665-675. *10.1111/jan.13892.*
36. **Perera S, Dabney BW.** Case management service quality and patient-centered care. J Health Organ Manag 2020; ahead-of-print(ahead-of-print). *10.1108/jhom-12-2019-0347.*
37. **Lugones-Sanchez C, Recio-Rodriguez JI, Agudo-Conde C, Repiso-Gento I, E GA, Ramirez-Manent JI**, et al. Long-term Effectiveness of a Smartphone App Combined With a Smart Band on Weight Loss, Physical Activity, and Caloric Intake in a Population With Overweight and Obesity (Evident 3 Study): Randomized Controlled Trial. J Med Internet Res 2022; 24(2): e30416. *10.2196/30416.*
38. **Gallagher D, Heymsfield SB, Heo M, Jebb SA, Murgatroyd PR, Sakamoto Y.** Healthy percentage body fat ranges: an approach for developing guidelines based on body mass index. Am J Clin Nutr 2000; 72(3): 694-701. *10.1093/ajcn/72.3.694.*
39. **Kyle UG, Schutz Y, Dupertuis YM, Pichard C**. Body composition interpretation. Contributions of the fat-free mass index and the body fat mass index. Nutrition 2003; 19(7-8): 597-604. *10.1016/s0899-9007(03)00061-3.*
40. **Grupińska J, Budzyń M, Maćkowiak K, Brzeziński JJ, Kycler W, Leporowska E,** et al. . Beneficial Effects of Oral Nutritional Supplements on Body Composition and Biochemical Parameters in Women with Breast Cancer Undergoing Postoperative Chemotherapy: A Propensity Score Matching Analysis. Nutrients 2021; 13(10). *10.3390/nu13103549.*
41. **Votto M, Bonitatibus G, De Filippo M, Pitigalage Kurera SA, Brambilla I, Guarracino C, De Amici M, Marseglia GL, Licari A.** Nutritional status in eosinophilic gastrointestinal disorders: A pediatric case-control study. Pediatr Allergy Immunol 2022; 33 Suppl 27(Suppl 27): 47-51. *10.1111/pai.13628.*
42. **Sherf-Dagan S, Sinai T, Goldenshluger A, Globus I, Kessler Y, Schweiger C, Ben-Porat T.** Nutritional Assessment and Preparation for Adult Bariatric Surgery Candidates: Clinical Practice. Adv Nutr 2021; 12(3): 1020-1031. *10.1093/advances/nmaa121.*
43. **Saxton R, McDougal OM.** Whey Protein Powder Analysis by Mid-Infrared Spectroscopy. Foods 2021; 10(5). *10.3390/foods10051033.*
44. **Li Y, Zhang ZH, Huang SL, Yue ZB, Yin XS, Feng ZQ, Zhang XG, Song GL**. Whey protein powder with milk fat globule membrane attenuates Alzheimer's disease pathology in 3×Tg-AD mice by modulating neuroinflammation through the peroxisome proliferator-activated receptor γ signaling pathway. J Dairy Sci 2023; 106(8): 5253-5265. *10.3168/jds.2023-23254.*
45. **Wobith M, Weimann A.** Oral Nutritional Supplements and Enteral Nutrition in Patients with Gastrointestinal Surgery. Nutrients 2021; 13(8). *10.3390/nu13082655.*
46. **Dong L, Pang K, Zeng Z, Tan L**. The impact of individual case management model on adherence to medical advice and Quality of Life in patients with diabetic nephropathy. Panminerva Med 2024. *10.23736/s0031-0808.24.05094-8.*

Invest Clin 66(2): 191 - 204, 2025 https://doi.org/10.54817/IC.v66n2a06

The p300-NF-κB pathway induces the activation of the NLRP3 inflammasome and the pyroptosis of neurons in an *in vitro* model of Alzheimer's disease.

Fengqin Sun and Wei Huang

Neurology Department, The Third People's Hospital of Yunnan Province, China.

Keywords: Alzheimer's disease; p300; pyroptosis; NLRP3 inflammasome.

Abstract. Inflammation-induced neuronal death is the primary cause of Alzheimer's disease (AD). p300 plays an important role in brain disorders. However, the role of p300 in AD remains unclear. This study aimed to investigate the potential of p300 in an *in vitro* model of AD. Protein expression was detected using western blotting. The mRNA levels were determined by reverse transcription-quantitative polymerase chain reaction. Cytokine release was detected using an enzyme-linked immunosorbent assay. Cellular function was determined using the cell counting kit-8, lactate dehydrogenase, and flow cytometry assays. Chromatin immunoprecipitation and luciferase assays verified the interaction between nuclear factor kappa B (NF-κB) and the NLR family pyrin domain containing 3 (NLRP3). E1A binding protein p300 (p300) was overexpressed in the $A\beta_{1-42}$ induced AD model in vitro. However, treatment with the p300 inhibitor (GNE-049) alleviated inflammation and $A\beta_{1-42}$-induced pyroptosis in the neurons. p300 activates NF-κB, which antagonizes the effects of GNE-049 and promotes neuronal pyroptosis. Moreover, NF-κB epigenetically activates the NLRP3 inflammasome. The p300/NF-κB pathway promotes neuronal pyroptosis in an *in vitro* AD model by activating the NLRP3 inflammasome. Therefore, the p300/NF-κB/NLRP3 signalling pathway may be a potential therapeutic target for AD.

Corresponding author: Wei Huang, Neurology Department, The Third people's Hospital of Yunnan Province, 292# Beijing Road, Guandu District, Kunming City, Yunnan Province 650000, China. Email: huangweidr@yeah.net

En el modelo in vitro de la enfermedad de Alzheimer, la vía p300 NF - Kappa B induce la activación del inflamasoma NLRP3 y la piroptosis neuronal en un modelo in vitro de la enfermedad de Alzheimer.

Invest Clin 2025; 66 (2): 191 – 204

Palabras clave: enfermedad de Alzheimer; P300; muerte por quemadura celular; cuerpo inflamatorio nlrp3.

Resumen. La muerte neuronal inducida por la inflamación es la principal causa de la enfermedad de Alzheimer (AD). El p300 juega un papel importante en las enfermedades cerebrales. Sin embargo, se desconoce el papel del p300 en la AD. El objetivo de este estudio es explorar el potencial del p300 en modelos in vitro de AD. Se utilizó Western blot para detectar la expresión de proteínas. Los niveles de ARNm se determinaron mediante la reacción cuantitativa en cadena de la polimerasa de transcripción inversa. Se utilizó la prueba de inmunoabsorción enzimática para detectar la liberación de citocinas. La función celular se determinó mediante el contador celular Kit - 8, la lactato deshidrogenasa y la medición con citometría de flujo. La interacción entre el factor nuclear Kappa b (nf - Kappa b) y el dominio Pirin 3 (nlrp3), que contiene la familia NLR, fue verificada por inmunoprecipitación de cromatina y detección de luciferasa. La proteína de unión a E1A p300 (p300) está sobreexpresada en un modelo de AD inducido por $A\beta_{1-42}$. Sin embargo, el tratamiento con un inhibidor del p300 (GNE - 049) redujo la inflamación y redujo la muerte por piroptosis neuronal inducida por $A\beta_{1-42}$. El p300 activa NF - Kappa b, que inhibe el efecto del GNE - 049 y promueve la muerte por piroptosis neuronal. Además, NF-κB epigeneticamentelly activa el NLRP3 inflamasoma Epigenética NF-Kappa B activa los cuerpos inflamatorios nlrp3. La vía p300 / NF - Kappa B promueve la muerte focal neuronal en modelos in vitro de AD activando el inflamasoma NLRP3. Por lo tanto, la transmisión de la señal p300/NF-Kappa B/NLRP3 puede ser un objetivo terapéutico potencial para la AD.

Received: 08-03-2025 Accepted: 10-05-2025

INTRODUCTION

Alzheimer's disease (AD) is a common neurodegenerative disorder [1]. The symptoms include apraxia, agnosia, aphasia, and emotional disturbance [2]. AD is the leading cause of dementia and accounts for > 60% of all cases [3]. Currently, nearly 50,000,000 people suffer from AD worldwide [4]. In China, among the 15.07 million people (≥60 years old) with dementia, 9.83 million (65.2%) were diagnosed with AD [5]. Moreover, the incidence of AD is increasing with an aging population[6]. However, the pathogenesis of AD is complex, and there are no effective prognostic biomarkers [7]. Therefore, identifying the potential molecular mechanisms underlying AD may provide novel therapeutic strategies.

Pyroptosis is a form of programmed cell death characterized by inflammasomes[8].

The NLR family pyrin domain containing 3 (NLRP3) is the main inflammasome expressed in brain tissues [9]. Stimuli-induced activation of NLRP3 inflammasomes cleaves caspase1 [10]. The cleaved caspase-1 then cleaves gasdermin D (GSDMD) and induces the accumulation of the N-terminus of GSDMD (GSDMD-N), which drives GSDMD to move to the cell membranes [11]. The enrichment of GSDMD-N in the cell membranes contributes to pore formation and subsequent relapse, releasing interleukin (IL)-1β and IL-18 [12,13]. The activation of the NLRP3 inflammasome is frequently observed in patients with AD. The NLRP3 inflammasome mediates neuroinflammation, cell senescence, and loss of neurons, which are key causes of AD [14-16]. However, inhibition of the NLRP3 inflammasome restores neuronal function and alleviates AD development [17].

Nuclear phosphoprotein E1A binding protein p300 (p300) is an acetyl transferase [18]. p300 regulates numerous biological processes such as proliferation, autophagy, apoptosis, and pyroptosis [19,20]. Increasing evidence has suggested that p300 is abnormally expressed in patients with brain disorders. For instance, p300 is downregulated in ischemia/reperfusion injury, whereas overexpressed p300 enhances the anti-apoptotic effects of myocardin-related transcription factor A [21]. However, p300 deficiency inhibits neuroepithelial cell proliferation in diabetes-induced tube defects [22]. Moreover, high levels of p300 in human brains with AD contribute to neuronal loss [23]. However, the role of p300 in AD has not yet been completely elucidated. In the present study, we investigated the potential role of p300 in an *in vitro* model of AD. We hypothesized that p300-mediated neuronal pyroptosis exacerbates the progression of AD.

MATERIALS AND METHODS

Cell culture

The mouse neuronal cell lines HT22 and HEK293T were obtained from ATCC (Manassas, VA, USA). The cells were cultured in Dulbecco's Modified Eagle's Medium supplemented with 10% fetal bovine serum (FBS). The cells were incubated at 37°C in a 5% CO_2.

HT22 cells were exposed to $A\beta_{1\text{-}42}$ (20 μM) and a p300 inhibitor (GNE-049, 500 nM) for 24 h. Cells in the control groups were cultured with FBS.

HT22 cells were transfected with small hairpin RNA shRNA) of nuclear factor kappa B (NF-κB) and overexpression plasmids or the control/vector using Lipofectamine 3000 (Invitrogen) according to the manufacturer's instructions.

Enzyme-linked immunosorbent assay (ELISA) assay

Cytokine levels were measured using ELISA kits (Abcam, Cambridge, USA), including IL-6, IL-1β, IL-18, tumor necrosis factor (TNF)-α, interferon (IFN)-γ, and IL-10.

Lactate dehydrogenase (LDH) assay

The release of LDH was determined using the corresponding LDH kit (Abcam, Cambridge, USA).

Reverse transcription-quantitative polymerase chain reaction (RT-qPCR)

Total RNA was extracted from the HT22 cells. A HiScript II 1st Strand cDNA Synthesis Kit (Vazyme, China) was used to synthesize the cDNA. PCR was performed using the HiScript II One-Step RT-PCR Kit (Vazyme, China) on an ABI 7900 system. Glyceraldehyde-3-phosphate dehydrogenase served as the loading control. The mRNA levels were calculated using the $2^{-\Delta\Delta CT}$ method.

Western blot

HT22 cells were harvested, and total protein was extracted. After centrifugation at 12000 × g, a BCA assay was performed to determine the protein concentration. Forty micrograms of protein were isolated using 10% Sodium dodecyl sulphate-polyacrylamide gel electrophoresis. Proteins were transferred to polyvinylidene fluoride membranes. After sealing with 5% skim milk, the membranes

were incubated with primary antibodies, including anti-p300 (ab275378; 1: 1000, Abcam, UK), anti-p-p65 (ab32536; 1: 2000, Abcam, UK), and anti-GAPDH (ab9485; 1: 2500, Abcam, UK) and then with goat anti-rabbit IgG H&L (ab205718; 1: 10000, Abcam, UK). Subsequently, the bands were imaged using an enhanced chemiluminescence kit (6104-58-1; Sigma-Aldrich, Germany).

Luciferase assay

JASPAR (https://jaspar.elixir.no/) was used to predict the binding sites between NF-κB and the promoter of NLRP3. Binding was amplified and inserted into the pMIR-GLOTM luciferase vector (Promega). HEK293T cells were transfected with wild-type (WT)/mutant type (MUT) of NLRP3 and NF-κB shRNA/overexpression plasmids. After 48 h, luciferase activity was detected using a kit (Promega).

Chromatin immunoprecipitation (ChIP) assay

A ChIP assay was conducted on HT22 cells using a ChIP kit (Sigma-Aldrich). Briefly, cells were crosslinked with 1% formalin, afterwards, cells were lysed and sonicated. The sonicated chromatin was incubated with antibodies, including anti-NF-κB (ab32536; 1: 30, Abcam, UK) and anti-IgG (ab172730; 1: 50, Abcam, UK) using Protein G magnetic beads. Finally, the DNA fragments were analyzed by RT-qPCR.

Cell counting kit-8 (CCK-8) assay

The cells were seeded in a 6-well plate (4000 cells/well) and cultured for 0, 24, 48, and 72 h. The cells were then supplemented with CCK-8 reagent. Finally, cell viability was determined using a microplate reader at an absorbance of 450 nm.

Flow cytometry

Neuronal pyroptosis was detected using flow cytometry with propidium iodide (PI) and caspase-1 staining. Briefly, neurons were digested with ethylenediamine tetraacetic acid-free trypsin. Then, the cells were harvested by centrifugation at 1000 rpm for 5 min. Afterwards, cells were resuspended and washed with PBS twice. The cells were incubated in the dark with FAM FLICA™ Caspase-1 Kit (ICT098; Bio-Rad, USA) and PI (4 μL). The results were analyzed using a flow cytometer (Biosciences, USA).

Statistical analysis

Each independent experiment was performed in triplicate. Graphpad v.8. software was used to analyze the data. Data are presented as the mean±SD. Student's t-test and ANOVA were used to analyze differences. $p<0.05$ was considered statistically significant.

RESULTS

p300 is upregulated in an in vitro model of AD

p300 is frequently upregulated in patients. Therefore, we determined the p300 expression in an AD model *in vitro*. We found that p300 mRNA expression in HT-22 cells exposed to $A\beta_{1\text{-}42}$ was markedly increased compared with that in the control group (Fig. 1A). This finding was consistent with the Western blot results. $A\beta_{1\text{-}42}$ treatment markedly increased the protein expression of p300 (Fig. 1B).

p300 deficiency inhibits neuroinflammation

p300 is a key regulator of the inflammatory response and mediates cerebral injury by activating inflammation-related signalling. Therefore, we hypothesized that p300 promotes AD pathogenesis by inducing neuroinflammation. As shown in Fig. 2A-E, the release of proinflammatory cytokines, such as IL-6, IL-1β, IL-18, tumor necrosis factor (TNF)-α, and interferon (IFN)-γ, was significantly increased after $A\beta_{1\text{-}42}$ exposure, whereas IL-10 was markedly decreased (Fig. 2F). However, GNE-049 treatment significantly alleviated the effects of $A\beta_{1\text{-}42}$, inhibited the release of IL-6, IL-1β, IL-18, TNF-α, and IFN-γ, and increased the release of IL-

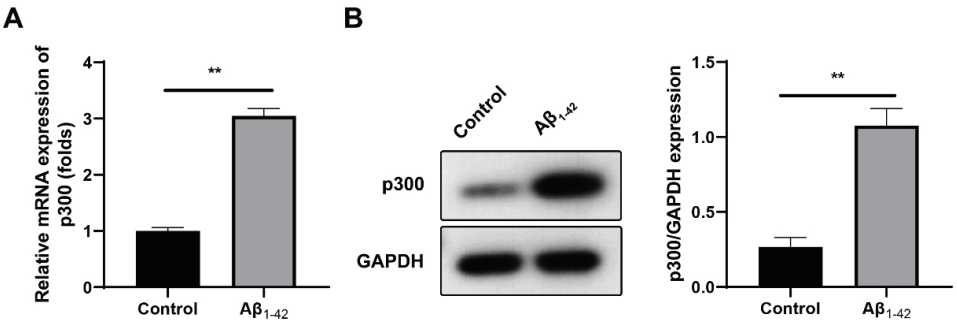

Fig. 1. The expression of p300 in in vitro model of AD.
(A) RT-qPCR was conducted to detect p300 mRNA expression in HT-22 cells exposed to $A\beta_{1\text{-}42}$. (B) Western blot was conducted to detect p300 protein expression in HT-22 cells exposed to $A\beta_{1\text{-}42}$. The difference in comparison was analyzed using the Student t-test. AD: Alzheimer's disease; p300: E1A binding protein p300; GAPDH: glyceraldehyde-3-phosphate dehydrogenase; RT-qPCR: reverse transcription-quantitative polymerase chain reaction. $^{**}p<0.01$.

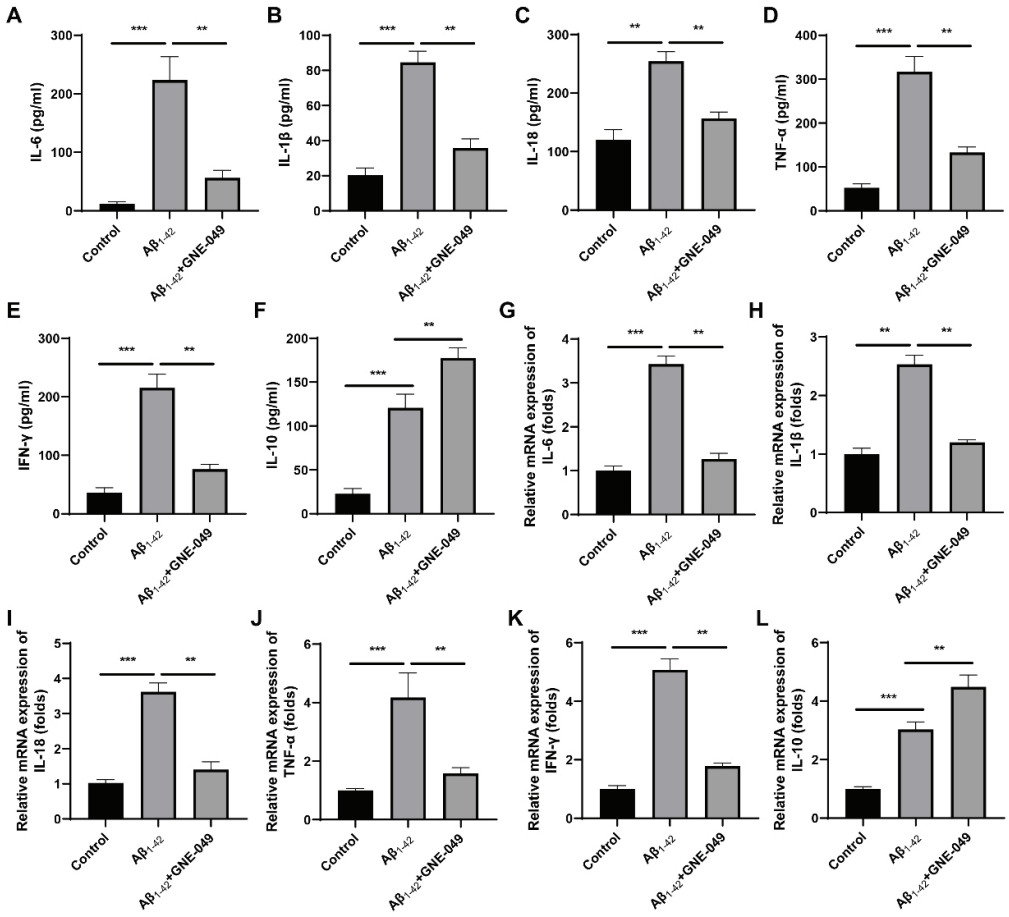

Fig. 2. p300 deficiency inhibits neuroinflammation.
(A-F) ELISA was used to detect the release of cytokines in HT-22 cells. (G-L) RT-qPCR was conducted to detect cytokine mRNA expression in HT-22 cells. Comparison difference was analyzed using one-way ANOVA. p300: E1A binding protein p300; IL-6: interleukin 6; IL-1β: interleukin 1β; IL-18: interleukin 18, TNF-α: tumor necrosis factor α; IFN-γ: interferon γ; IL-10: interleukin 10. ELISA: enzyme-linked immunosorbent assay; RT-qPCR: reverse transcription-quantitative polymerase chain reaction. $^{**}p<0.01$, $^{***}p<0.001$.

10. This finding is consistent with the RT-qPCR results. GNE-049 treatment suppressed the mRNA expression of IL-6, IL-1β, IL-18, TNF-α, and IFN-γ (Fig. 2 G-K), while increasing IL-10 mRNA expression (Fig. 2 L). These findings suggest that the inhibition of p300 expression suppresses neuroinflammation.

p300 deficiency inhibits the pyroptosis of neurons

Inflammation-induced pyroptosis, which is characterized by the activation of the inflammasome and an increase in cytotoxicity and death, is a key cause of AD. p300 protein expression was markedly reduced by GNE-049 treatment (Fig. 3A). $A\beta_{1-42}$ exposure markedly increased LDH release (Fig. 3B), which was antagonized by GNE-049 treatment. Moreover, GNE-049 treatment promoted neuronal viability (Fig. 3C). GNE-049 treatment markedly alleviated the pyroptosis in the neurons induced by $A\beta_{1-42}$ exposure (Fig. 3D). Additionally, GNE-049 treatment suppressed the mRNA expression of NLRP3, PYD and CARD domain containing (ASC), and caspase-1 (Fig. 3E). These findings suggested that p300 inhibition alleviates neuronal pyroptosis in AD.

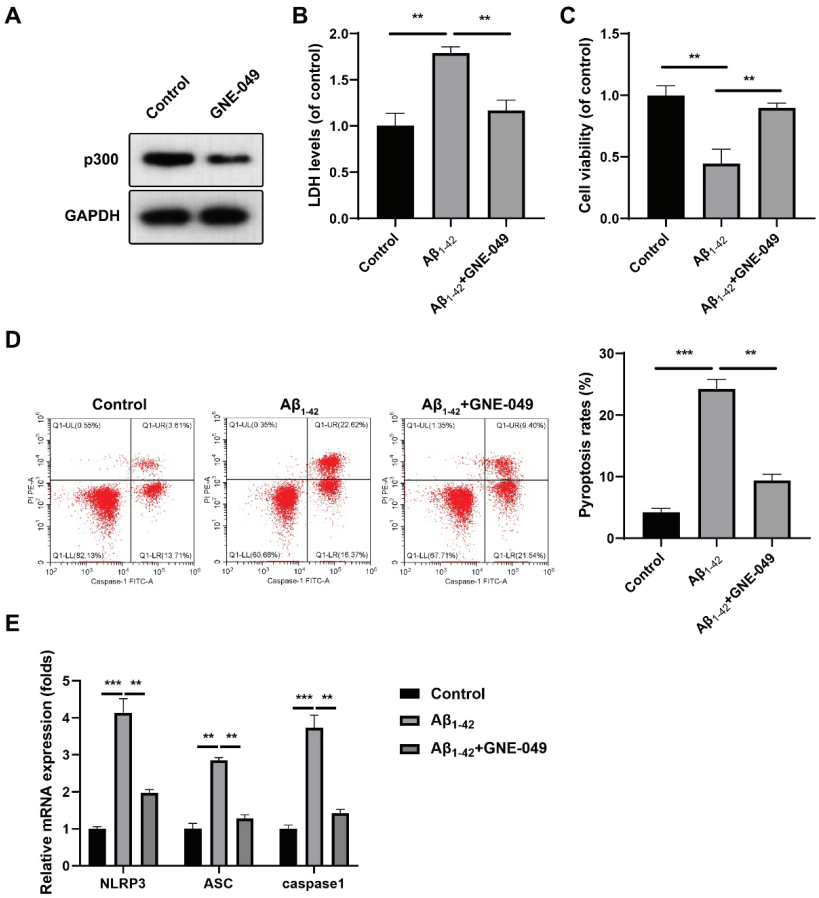

Fig. 3. p300 deficiency inhibits the pyroptosis of neurons.
(A) p300 protein expression was detected using Western blot. (B) LDH assay was conducted to detect cytotoxicity of HT-22 cells. (C) CCK-8 was performed to determine the cell viability of HT-22 cells. (D) Flow cytometry was used to detect the pyroptosis of HT-22 cells. (E) RT-qPCR was conducted to detect mRNA expression in HT-22 cells. Comparison difference was analyzed using one-way ANOVA. p300: E1A binding protein p300; NLRP3: NLR family pyrin domain containing 3; ASC: PYD and CARD domain containing; LDH: lactate dehydrogenase; RT-qPCR: reverse transcription-quantitative polymerase chain reaction. $^{**}p<0.01$, $^{***}p<0.001$.

p300 activates NF-κB signaling

p300 participates in the inflammatory response by activating inflammatory signalling. Therefore, we hypothesized that p300 mediates neuroinflammation by activating NF-κB signaling. $A\beta_{1\text{-}42}$ exposure significantly increased the protein expression of p-p65 (Fig. 4), which GNE-049 alleviated.

p300 induces neuroinflammation via activating NF-κB signaling

To verify the role of NF-κB in AD, neurons were transfected with an NF-κB-overexpression plasmid. We found that overexpression of NF-κB alleviated the effects of GNE-049 and promoted the release of IL-6, IL-1β, IL-18, TNF-α, and IFN-γ, as well as decreased IL-10 (Fig.5A-F). Moreover, overexpression of NF-κB markedly increased the mRNA expression of IL-6, IL-1β, IL-18, TNF-α, and IFN-γ (Fig. 5G-K), but decreased IL-10 mRNA expression (Fig. 5L).

p300 induces pyroptosis via activating NF-κB signaling

A rescue assay was conducted to confirm further the role of p300/NF-κB signaling in AD. We found that overexpression of NF-κB markedly alleviated the effects of GNE-049 and promoted neuronal cytotoxicity (Fig. 6A). However, NF-κB overexpression suppressed neuronal viability (Fig. 6B). Overexpression of NF-κB alleviated the effects of GNE-049 and promoted pyroptosis in neurons (Fig. 6C). Moreover, overexpression of NF-κB markedly increased the mRNA expression of NLRP3, ASC, and caspase-1 (Fig. 6D). These findings suggest that p300 regulates neuronal pyroptosis by activating NF-κB signaling.

p300-dependent activation of NF-κB epigenetically activates NLRP3.

NF-κB, a key transcription factor in inflammatory signalling, participates in biological processes via its downstream regulation. We found that NLRP3 mRNA expression was markedly increased by p300 overexpression and returned to normal levels after transfection with NF-κB shRNA (Fig. 7A). NF-κB regulates its downstream activity by binding to the promoters of its target genes. Therefore, we hypothesized that NF-κB binds to the NLRP3 promoter (Fig. 7 B). Fig. 7C shows the binding motif for NF-κB. Four binding sites were identified in the promoter of NLRP3 (Fig. 7c). Overexpression of p300 and NF-κB markedly enhanced the transcription of NLRP3 (Fig. 7D). To identify the site that binds NF-κB, the 3'-UTR of the binding

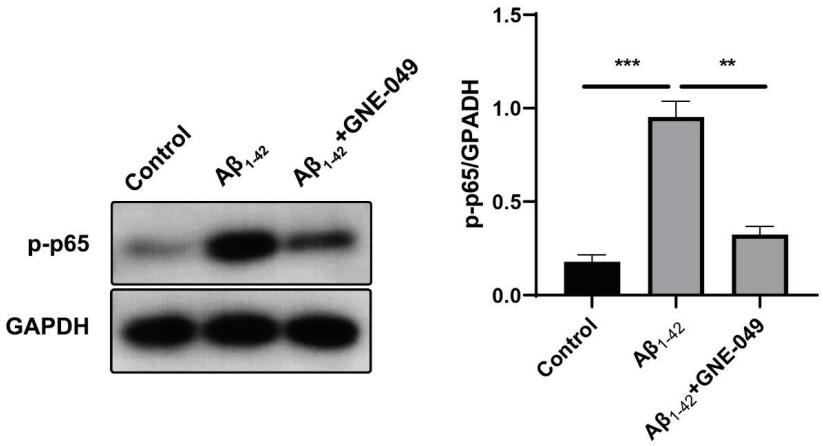

Fig. 4. p300 activates NF-κB signaling.
Western blot was performed to detect the p-p65 protein expression in HT-22 cells. Comparison difference was analyzed using one-way ANOVA. p300: E1A binding protein p300; GAPDH: glyceraldehyde-3-phosphate dehydrogenase. $^{**}p<0.01$, $^{***}p<0.001$.

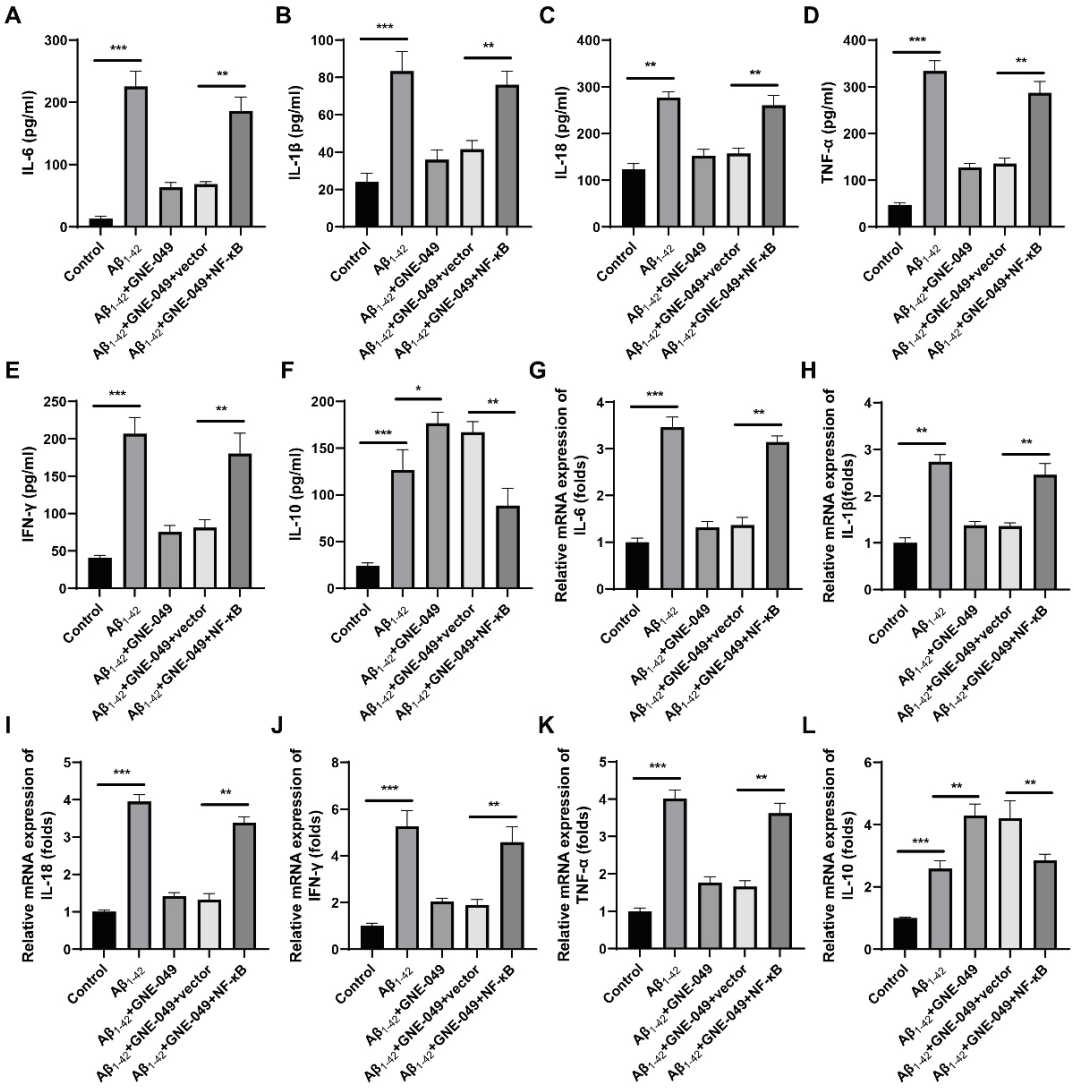

Fig. 5. p300 induces neuroinflammation via activating NF-κB signalling.
(A-F) ELISA was used to detect the release of cytokines in HT-22 cells. (G-L) RT-qPCR was performed to detect the p300 mRNA expression in HT-22 cells. Comparison difference was analyzed using one-way ANOVA. p300: E1A binding protein p300; IL-6: interleukin 6; IL-1β: interleukin 1β; IL-18: interleukin 18, TNF-α: tumor necrosis factor α; IFN-γ: interferon γ; IL-10: interleukin 10. ELISA: enzyme-linked immunosorbent assay; RT-qPCR: reverse transcription-quantitative polymerase chain reaction. $^{*}p<0.05$, $^{**}p<0.01$, $^{***}p<0.001$.

sites was mutated and inserted into luciferase reporters. Co-transfection with p300 and NF-κB significantly increased luciferase activity (Fig. 7E). Moreover, luciferase activity was markedly increased in MUT1/3/4 cells after $A\beta_{1\text{-}42}$ exposure, which was antagonized by GNE-049 treatment (Fig. 7F), whereas there was no significant alteration in MUT2. Additionally, p300 deficiency markedly suppressed the co-occupancies of site2 in HEK293T cells (Fig. 7G-H). These findings suggest that the p300-mediated activation of NF-κB epigenetically upregulates NLRP3 expression.

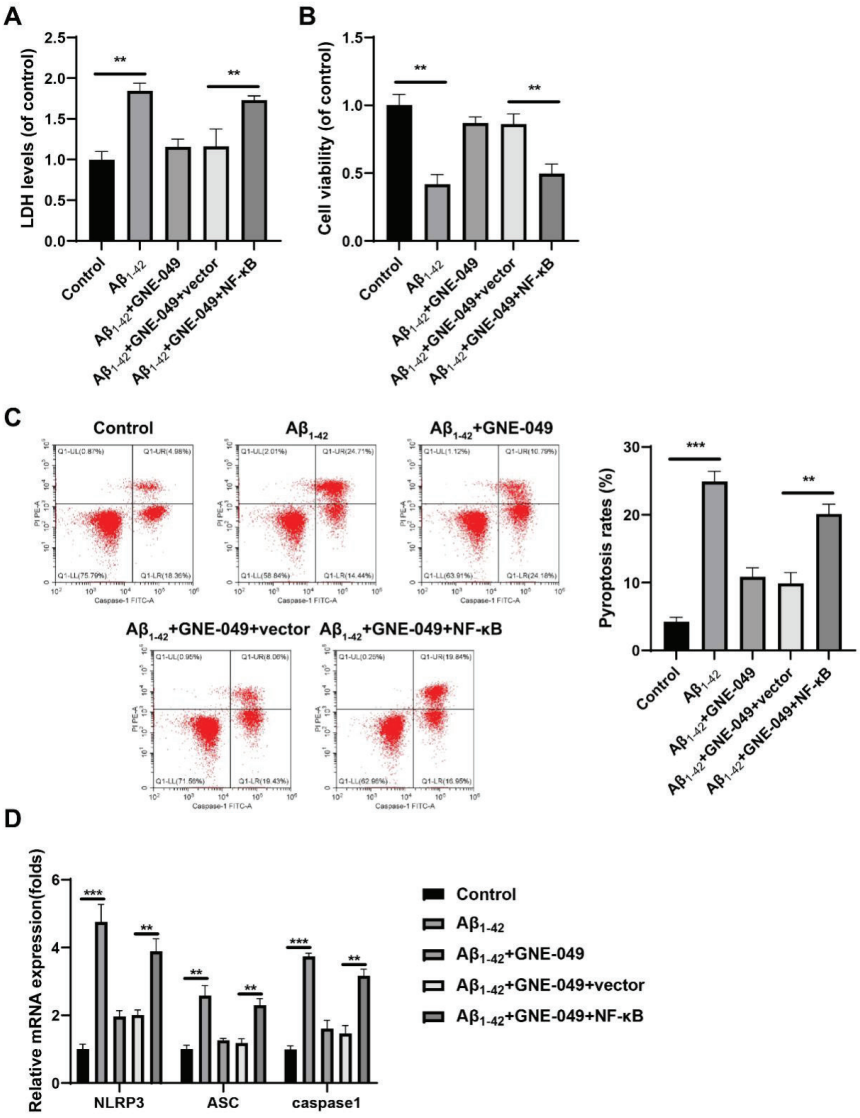

Fig. 6. p300 induces pyroptosis via activating NF-κB signaling.
(A) The LDH assay detected cytotoxicity in HT-22 cells. (B) The CCK-8 assay was performed to determine the viability of HT-22 cells. (C) Flow cytometry was used to detect pyroptosis in the HT-22 cells. (D) RT-qPCR was performed to detect the mRNA expression in HT-22 cells. Comparison difference was analyzed using one-way ANOVA. p300: E1A binding protein p300; NLRP3: NLR family pyrin domain containing 3; ASC: PYD and CARD domain containing; LDH: lactate dehydrogenase; RT-qPCR: reverse transcription-quantitative polymerase chain reaction. $^{**}p<0.01$, $^{***}p<0.001$.

DISCUSSION

In this study, p300 was upregulated in *an in vitro* model of AD. Interestingly, p300 deficiency inhibits neuroinflammation and suppresses pyroptosis in the neurons. Moreover, p300 activates NF-κB, and its overexpression promotes pyroptosis in neurons. Additionally, the p300-mediated activation of NF-κB epigenetically upregulates NLRP3, which induces pyroptosis in neurons. Therefore, the p300/NF-κB/NLRP3 pathway may be a potential target in AD.

p300 is aberrantly expressed in several brain disorders. Chatterjee et al.[24] revealed that CBP/p300 activation enhances neuro-

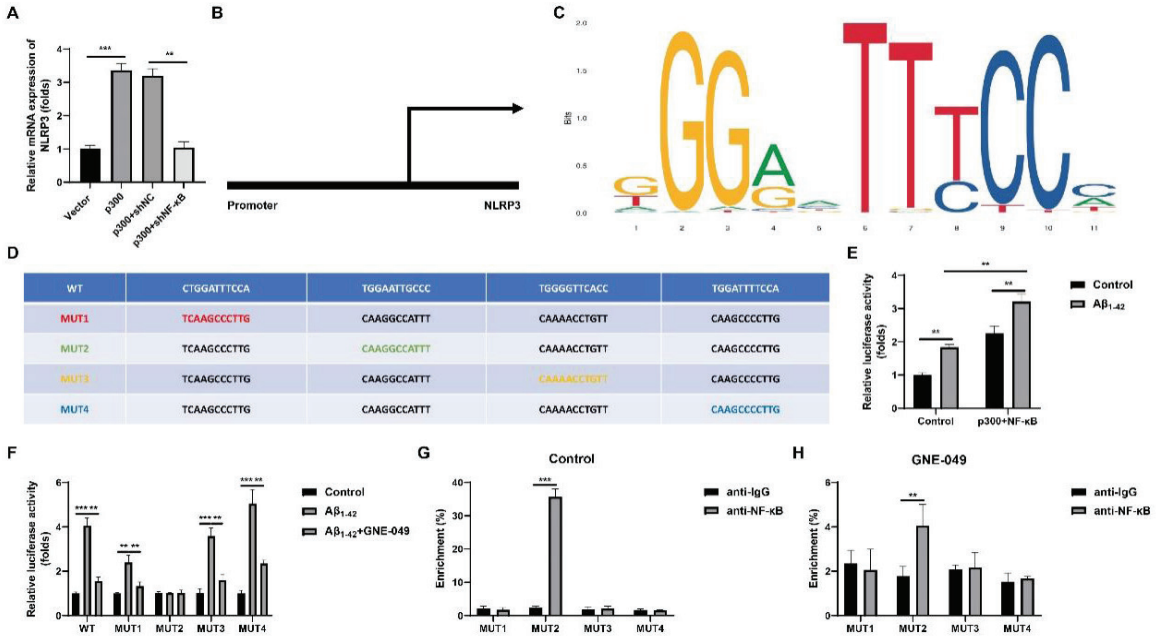

Fig. 7. p300-depedent activation of NF-κB epigenetically activates NLRP3.
(A) RT-qPCR was conducted to detect mRNA expression in HT-22 cells. (B) A hypothesis of NF-κB/NLRP3 signalling. (C) JASPAR was used to analyze the binding motif of NF-κB. (D) JASPAR was used to analyze the binding sites between NF-κB and the promoter of NLRP3. (E) Luciferase assay was conducted to confirm that the p300/NF-κB promoted the transcription of NLRP3 in HEK293T cells. (F) Luciferase assay was performed to verify the exact binding site between NF-κB and the promoter of NLRP3 in HEK293T cells. (G-H) ChIP assay was performed to verify the binding sites in HEK293T cells. The difference in comparison was analyzed using one-way or two-way ANOVA. p300: E1A binding protein p300; NLRP3: NLR family pyrin domain containing 3; WT: wild type; MUT: mutant type; RT-qPCR: reverse transcription-quantitative polymerase chain reaction. ChIP: chromatin immunoprecipitation. $^{**}p<0.01$, $^{***}p<0.001$.

genesis and prolongs memory duration, and maturation, and differentiation of adult neuronal progenitors. However, hyperactivation of p300 contributes to tauopathy pathogenesis [25]. Therefore, p300 may play protective and passive roles in brain disorders. This may be because the roles of p300 vary with disease subtype and signalling. Therefore, it is crucial to identify the role of p300 in AD, which is very important. CBP/p300 activation-mediated acetylation of tau exacerbates traumatic brain injury, which is the most significant non-genetic, non-aging-related risk factor for AD [26]. Moreover, p300-mediated autophagy promoted neuronal damage and inflammation in AD [27]. Therefore, p300 may promote the pathogenesis of AD. In this study, p300 was upregulated in an in vitro AD model. Targeting p300 may be an effective strategy for alleviating AD [25,26]. In this study, p300 deficiency induced by a specific inhibitor suppressed neuroinflammation and pyroptosis in the neurons. These findings suggest that p300 inhibition may alleviate neuronal loss during AD pathogenesis, consistent with previous studies.

p300, an acetyl transferase, has no DNA-binding domain [28]. p300 regulates gene expression by interacting with transcription factors. For instance, Sox8 induces the activation of the LIF interleukin 6 family cytokine downstream transcription factor signal transducer and activator of transcription 3 via p300 to promote astrocytic differentia-

tion [29]. Moreover, REST recruits CBP/p300 to the EAAT2 promoter to alleviate manganese-induced excitotoxicity [30]. Geong et al. [31] reported that p300/NF-κB promotes microglial activation and neuroinflammation. In the present study, p300 activated NF-κB. NF-κB is a key regulator of inflammatory signalling. NF-κB is a key mediator of brain inflammation in AD [32]. Activating NF-κB signaling stimulates the innate immune system and induces neurodegeneration and neuronal loss [33-35]. In this study, overexpression of NF-κB antagonized the effects of GNE-049 and promoted neuroinflammation and neuronal death.

Pyroptosis is a type of inflammation-related cell death process. Inflammation also induces necroptosis [36]. Although pyroptosis and necroptosis share some properties, such as lytic and inflammatory types of programmed cell death and releasing damage-associated molecular patterns, pyroptosis is differentiated from necroptosis, a backup cell death defense mechanism. In contrast, pyroptosis is a primary cellular response after sensing potentially damaging insults[37]. Necroptosis is characterized by the activation of receptor-interacting serine/threonine kinase 3/mixed lineage kinase domain-like pseudokinase signalling, whereas pyroptosis is characterized by the activation of inflammasomes and executed by GSDMD[38]. In this study, p300-dependent upregulation of NF-κB activated the NLRP3 inflammasome and increased the release of IL-1β and IL-18 after $A\beta_{1-42}$ exposure. Therefore, the p300/NF-κB/NLRP3 pathway-mediated neuronal death occurred via pyroptosis.

In conclusion, p300 was upregulated in an *in vitro* model of AD. p300-mediated upregulation of NF-κB epigenetically activates the NLRP3 inflammasome and pyroptosis in neurons. However, p300 inhibition alleviated neuroinflammation and neuronal pyroptosis. Therefore, targeting p300/NF-κB/NLRP3 may be a promising strategy for alleviating AD.

Ethics approval and consent to participate

This study was approved by the Ethics Committee of the Third People's Hospital of Yunnan Province. All experimental animal procedures followed the Guidelines for the Care and Use of Laboratory Animals formulated by China's Ministry of Science and Technology.

Funding

Not applicable.

Consent for publication

Not applicable.

Availability of data and material

The datasets used and/or analyzed during the current study are available from the corresponding author upon reasonable request.

Competing interests

Not applicable.

Number ORCID of authors

- Fengqin Sun (FQS): 0009-0009-0865-8011
- Wei Huang (WH): 0009-0008-9840-1633.

Author contributions

FQS performed data analysis and drafted the manuscript. FQS and WH conceived and supervised the study and reviewed the manuscript. FQS and WH ran the software and modified the code. FQS and WH were involved in the study design and contributed to the data collection procedure and interpretation.

ACKNOWLEDGEMENTS

Not applicable.

Conflicts of interest

The authors declared that they have no conflicts of interest regarding this work.

REFERENCES

1. **Scheltens P, De Strooper B, Kivipelto M, Holstege H, Chetelat G, Teunissen CE**, et al. Alzheimer's disease. Lancet. 2021;397(10284):1577-90. *doi: 10.1016/S0140-6736(20)32205-4.*
2. **Porsteinsson AP, Isaacson RS, Knox S, Sabbagh MN, Rubino I**. Diagnosis of Early Alzheimer's Disease: Clinical Practice in 2021. J Prev Alzheimers Dis. 2021;8(3):371-86. *doi: 10.14283/jpad.2021.23.*
3. **2023 Alzheimer's disease facts and figures.** Alzheimers Dement. 2023;19(4):1598-695. doi: *10.1002/alz.13016*.
4. **Graff-Radford J, Yong KXX, Apostolova LG, Bouwman FH, Carrillo M, Dickerson BC,** et al. New insights into atypical Alzheimer's disease in the era of biomarkers. Lancet Neurol. 2021;20(3):222-34. *doi: 10.1016/S1474-4422(20)30440-3.*
5. **Wang Q, Gao F, Dai LN, Zhang J, Bi D, Shen Y**. Clinical Research Investigating Alzheimer's Disease in China: Current Status and Future Perspectives Toward Prevention. J Prev Alzheimers Dis. 2022;9(3):532-41. *doi: 10.14283/jpad.2022.46.*
6. **Fan R, Peng X, Xie L, Dong K, Ma D, Xu W**, et al. Importance of Bmal1 in Alzheimer's disease and associated aging-related diseases: Mechanisms and interventions. Aging Cell. 2022;21(10):e13704. *doi: 10.1111/acel.13704.*
7. **Chen P, Guo Z, Zhou B**. Insight into the role of adult hippocampal neurogenesis in aging and Alzheimer's disease. Ageing Res Rev. 2023;84:101828. *doi: 10.1016/j.arr.2022.101828.*
8. **Yang F, Bettadapura SN, Smeltzer MS, Zhu H, Wang S.** Pyroptosis and pyroptosis-inducing cancer drugs. Acta Pharmacol Sin. 2022;43(10):2462-73. *doi: 10.1038/s41401-022-00887-6.*
9. **Moonen S, Koper MJ, Van Schoor E, Schaeverbeke JM, Vandenberghe R, von Arnim CAF,** et al. Pyroptosis in Alzheimer's disease: cell type-specific activation in microglia, astrocytes and neurons. Acta Neuropathol. 2023;145(2):175-95. *doi: 10.1007/s00401-022-02528-y.*
10. **Zhou J, Qiu J, Song Y, Liang T, Liu S, Ren C**, et al. Pyroptosis and degenerative diseases of the elderly. Cell Death Dis. 2023;14(2):94. *doi: 10.1038/s41419-023-05634-1.*
11. **Elias EE, Lyons B, Muruve DA.** Gasdermins and pyroptosis in the kidney. Nat Rev Nephrol. 2023;19(5):337-50. *doi: 10.1038/s41581-022-00662-0.*
12. **Li Z, Ji S, Jiang ML, Xu Y, Zhang CJ.** The Regulation and Modification of GSDMD Signaling in Diseases. Front Immunol. 2022;13:893912. *doi: 10.3389/fimmu.2022.893912.*
13. **Huang Y, Xu W, Zhou R.** NLRP3 inflammasome activation and cell death. Cell Mol Immunol. 2021;18(9):2114-27. *doi: 10.1038/s41423-021-00740-6.*
14. **Yao H, Zhang D, Yu H, Yuan H, Shen H, Lan X**, et al. Gut microbiota regulates chronic ethanol exposure-induced depressive-like behavior through hippocampal NLRP3-mediated neuroinflammation. Mol Psychiatry. 2023;28(2):919-30. *doi: 10.1038/s41380-022-01841-y.*
15. **Hou Y, Wei Y, Lautrup S, Yang B, Wang Y, Cordonnier S, et al**. NAD(+) supplementation reduces neuroinflammation and cell senescence in a transgenic mouse model of Alzheimer's disease via cGAS-STING. Proc Natl Acad Sci U S A. 2021;118(37). *doi: 10.1073/pnas.2011226118.*
16. **Han YH, Liu XD, Jin MH, Sun HN, Kwon T**. Role of NLRP3 inflammasome-mediated neuronal pyroptosis and neuroinflammation in neurodegenerative diseases. Inflamm Res. 2023;72(9):1839-59. *doi: 10.1007/s00011-023-01790-4.*
17. **Cai Y, Chai Y, Fu Y, Wang Y, Zhang Y, Zhang X, et al.** Salidroside Ameliorates Alzheimer's Disease by Targeting NLRP3 Inflammasome-Mediated Pyroptosis. Front Aging Neurosci. 2021;13:809433. *doi: 10.3389/fnagi.2021.809433.*

18. **Chakraborty R, Ostriker AC, Xie Y, Dave JM, Gamez-Mendez A, Chatterjee P,** et al. Histone Acetyltransferases p300 and CBP Coordinate Distinct Chromatin Remodeling Programs in Vascular Smooth Muscle Plasticity. Circulation. 2022;145(23):1720-37. *doi: 10.1161/CIRCULATIONAHA.121.057599.*
19. **Xu Y, Wan W.** Acetylation in the regulation of autophagy. Autophagy. 2023;19(2):379-87. *doi: 10.1080/15548627.2022.2062112.*
20. **Chen Q, Yang B, Liu X, Zhang XD, Zhang L, Liu T.** Histone acetyltransferases CBP/p300 in tumorigenesis and CBP/p300 inhibitors as promising novel anticancer agents. Theranostics. 2022;12(11):4935-48. *doi: 10.7150/thno.73223.*
21. **Cao W, Feng Z, Zhu D, Li S, Du M, Ye S, et al**. The Role of PGK1 in Promoting Ischemia/Reperfusion Injury-Induced Microglial M1 Polarization and Inflammation by Regulating Glycolysis. Neuromolecular Med. 2023;25(2):301-11. *doi: 10.1007/s12017-023-08736-3.*
22. **Bai B, Zhang Q, Wan C, Li D, Zhang T, Li H.** CBP/p300 inhibitor C646 prevents high glucose exposure induced neuroepithelial cell proliferation. Birth Defects Res. 2018;110(14):1118-28. *doi: 10.1002/bdr2.1360.*
23. **Cintra MTG, Avila RT, Soares TO, Cunha LCM, Silveira KD, de Moraes EN,** et al. Increased N200 and P300 latencies in cognitively impaired elderly carrying ApoE epsilon-4 allele. Int J Geriatr Psychiatry. 2018;33(2):e221-e7. *doi: 10.1002/gps.4773.*
24. **Chatterjee S, Mizar P, Cassel R, Neidl R, Selvi BR, Mohankrishna DV, et al**. A novel activator of CBP/p300 acetyltransferases promotes neurogenesis and extends memory duration in adult mice. J Neurosci. 2013;33(26):10698-712. *doi: 10.1523/JNEUROSCI.5772-12.2013.*
25. **Chen X, Li Y, Wang C, Tang Y, Mok SA, Tsai RM, et al.** Promoting tau secretion and propagation by hyperactive p300/CBP via autophagy-lysosomal pathway in tauopathy. Mol Neurodegener. 2020;15(1):2. *doi: 10.1186/s13024-019-0354-0.*
26. **Shin MK, Vazquez-Rosa E, Koh Y, Dhar M, Chaubey K, Cintron-Perez CJ, et a**l. Reducing acetylated tau is neuroprotective in brain injury. Cell. 2021;184(10):2715-32 e23. *doi: 10.1016/j.cell.2021.03.032.*
27. **Wu J, Han Y, Xu H, Sun H, Wang R, Ren H, et al.** Deficient chaperone-mediated autophagy facilitates LPS-induced microglial activation via regulation of the p300/NF-kappaB/NLRP3 pathway. Sci Adv. 2023;9(40):eadi8343. *doi: 10.1126/sciadv.adi8343.*
28. **Kikuchi M, Morita S, Wakamori M, Sato S, Uchikubo-Kamo T, Suzuki T, et** al. Epigenetic mechanisms to propagate histone acetylation by p300/CBP. Nat Commun. 2023;14(1):4103. *doi: 10.1038/s41467-023-39735-4.*
29. **Takouda J, Katada S, Imamura T, Sanosaka T, Nakashima K.** SoxE group transcription factor Sox8 promotes astrocytic differentiation of neural stem/precursor cells downstream of Nfia. Pharmacol Res Perspect. 2021;9(6):e00749. *doi: 10.1002/prp2.749.*
30. **Pajarillo E, Digman A, Nyarko-Danquah I, Son DS, Soliman KFA, Aschner M, et al.** Astrocytic transcription factor REST upregulates glutamate transporter EAAT2, protecting dopaminergic neurons from manganese-induced excitotoxicity. J Biol Chem. 2021;297(6):101372. *doi: 10.1016/j.jbc.2021.101372.*
31. **Jeong GW, Lee HH, Lee-Kwon W, Kwon HM.** Microglial TonEBP mediates LPS-induced inflammation and memory loss as transcriptional cofactor for NF-kappaB and AP-1. J Neuroinflammation. 2020;17(1):372. *doi: 10.1186/s12974-020-02007-9*.
32. **Chen S, Liu H, Wang S, Jiang H, Gao L, Wang L, et** al. The Neuroprotection of Verbascoside in Alzheimer's Disease Mediated through Mitigation of Neuroinflammation via Blocking NF-kappaB-p65 Signaling. Nutrients. 2022;14(7). *doi: 10.3390/nu14071417.*
33. **Zhou L, Kong G, Palmisano I, Cencioni MT, Danzi M, De Virgiliis F, et al**. Reversible CD8 T cell-neuron cross-talk causes

aging-dependent neuronal regenerative decline. Science. 2022;376(6594):eabd5926. *doi: 10.1126/science.abd5926.*

34. **Yu CH, Davidson S, Harapas CR, Hilton JB, Mlodzianoski MJ, Laohamonthonkul P, et al**. TDP-43 Triggers Mitochondrial DNA Release via mPTP to Activate cGAS/STING in ALS. Cell. 2020;183(3):636-49 e18. *doi: 10.1016/j.cell.2020.09.020.*
35. **Jung BK, Park Y, Yoon B, Bae JS, Han SW, Heo JE, e**t al. Reduced secretion of LCN2 (lipocalin 2) from reactive astrocytes through autophagic and proteasomal regulation alleviates inflammatory stress and neuronal damage. Autophagy. 2023;19(8):2296-317. *doi: 10.1080/15548627.2023.2180202.*
36. **Chen S, Guan S, Yan Z, Ouyang F, Li S, Liu L, et al.** Role of RIPK3–CaMKII–mPTP signaling pathway–mediated necroptosis in cardiovascular diseases (Review). Int J Mol Med. 2023;52(4). *doi: 10.3892/ijmm.2023.5301.*
37. **Frank D, Vince JE.** Pyroptosis versus necroptosis: similarities, differences, and crosstalk. Cell Death Differ. 2019;26(1):99-114. *doi: 10.1038/s41418-018-0212-6.*
38. **Gao W, Wang X, Zhou Y, Wang X, Yu Y.** Autophagy, ferroptosis, pyroptosis, and necroptosis in tumor immunotherapy. Signal Transduct Target Ther. 2022;7(1):196. *doi: 10.1038/s41392-022-01046-3.*

Invest Clin 66(2): 205 - 216, 2025 https://doi.org/10.54817/IC.v66n2a07

Lycopene regulates the formation of calcium oxalate kidney stones by modulating reactive oxygen species(ROS) and NF-κB pathways.

Liangwen Ye, Yuhang Tang, Zhijie Zhang, Xiangyi Hou, Wei Xu, Xianghui Suo and Li Zhang

The First Clinical Medical College, Nanjing University of Chinese Medicine, Nanjing City, Jiangsu province, China.

Keywords: lycopene; renal tubular epithelial cells; oxalic acid; reactive oxygen species; apoptosis.

Abstract. This study aims to determine whether lycopene can reduce oxidative stress and inflammatory damage in HK-2 cell cultures induced by calcium oxalate crystallization through the modulation of reactive oxygen species (ROS) and the NF-κB signalling pathway. Cell cultures were divided into four groups: The control group, the Model group (COM + oxalic acid), and two Lycopene intervention groups (COM + oxalic acid + 5/10 μmol/L lycopene). After 24 hours of culture, viability, LDH, oxidative and anti-oxidative parameters, mitochondrial membrane potential, MCP-1, IL-6, apoptosis and related proteins, and activation and expression of NF-κB were determined by adequate methods. When compared to the control group, the model group exhibited decreased cell activity ($p<0.001$) and GSH and SOD antioxidant capacity ($p<0.05$), alongside a significant rise in LDH, MDA, and the release of inflammatory mediators MCP-1 and IL-6 ($p<0.05$). The levels of protein expression for NF-κB, OPN, Bax, Cyt C, and active Caspase-3 were increased ($p<0.05$), whereas Bcl-2 protein expression significantly diminished ($p<0.05$). The mitochondrial membrane potential decreased. Lycopene intervention reduced the damage to HK-2 cells ($p<0.05$), accompanied by decreased levels of LDH, MDA, and inflammatory factors MCP-1 and IL-6 ($p<0.05$), and increased GSH and SOD antioxidant capacity ($p<0.05$). The mitochondrial membrane potential was observed to increase. No significant changes were observed in the expression of NF-κB. The expressions of OPN, Bax, Cyt C, and Caspase-3 decreased ($p<0.05$), whereas the level of Bcl-2 protein expression increased. In conclusion, lycopene decreases cellular damage by inhibiting lipid peroxidation induced by calcium oxalate crystals and oxalate, enhancing intracellular antioxidant enzyme activity, modulating ROS and NF-κB inflammatory pathways, improving mitochondrial integrity, and exerting anti-inflammatory effects through the inhibition of the mitochondrial-mediated Bax/Caspase-3 signalling pathway.

Corresponding author: Li Zhang. The First Clinical Medical College. Nanjing University of Chinese Medicine. No. 138, Xianlin Road, Qixia District. Nanjing City 210023, Jiangsu Province, China. Tel: +86 13952009414. Email: LiiZZhang@outlook.com

El licopeno regula la formación de cálculos renales de oxalato cálcico modulando las vías de especies reactivas de oxígeno (ROS) y NF-κB.

Invest Clin 2025; 66 (2): 205 – 216

Palabras clave: licopeno; células epiteliales tubulares renales; ácido oxálico; especies reactivas de oxígeno; apoptosis.

Resumen. Este estudio tiene como objetivo determinar si el licopeno puede reducir el estrés oxidativo y el daño inflamatorio inducidos por la cristalización de oxalato de calcio en cultivos de células HK-2 a través de la modulación de especies reactivas de oxígeno (ROS) y las vías de señalización de NF-κB. Los cultivos celulares se dividieron en cuatro grupos: grupo control, grupo modelo (COM + ácido oxálico) y dos grupos de intervención con licopeno (COM + ácido oxálico + 5/10 μmol/L de licopeno). Después de 24 horas de cultivo, se determinaron la viabilidad, la LDH, los parámetros oxidativos y antioxidantes, el potencial de membrana mitocondrial, MCP-1, IL-6, la apoptosis y proteínas relacionadas, y la activación y expresión de NF-κB mediante métodos adecuados. En comparación con el grupo control, el grupo modelo mostró una actividad celular ($p<0,001$) y una capacidad antioxidante de GSH y SOD ($p<0,05$) disminuidas, junto con aumento significativo de LDH, MDA y la liberación de mediadores inflamatorios MCP-1 e IL-6 ($p<0,05$). Los niveles de expresión de proteínas para NF-κB, OPN, Bax, Cyt C y Caspasa-3 activa aumentaron ($p<0,05$), mientras que la expresión de la proteína Bcl-2 disminuyó significativamente ($p<0,05$). El potencial de membrana mitocondrial disminuyó. La intervención con licopeno redujo el daño celular ($p<0,05$), acompañada de una disminución de los niveles de LDH, MDA y los factores inflamatorios MCP-1 e IL-6 ($p<0,05$), y un aumento de la capacidad antioxidante de GSH y SOD ($p<0,05$). Se observó un aumento del potencial de membrana mitocondrial. No se observaron cambios significativos en la expresión de NF-κB. La expresión de OPN, Bax, Cyt C y Caspasa-3 disminuyó ($p<0,05$), mientras que la expresión de la proteína Bcl-2 aumentó. En conclusión, el licopeno disminuyó el daño celular al inhibir la peroxidación lipídica inducida por cristales de oxalato de calcio y oxalato, potenciar la actividad enzimática antioxidante intracelular, modular las vías inflamatorias de ROS y NF-κB, mejorar la integridad mitocondrial y ejercer efectos antiinflamatorios mediante la inhibición de la vía de señalización Bax/Caspasa-3 mediada por mitocondrias.

Received: 25-03-2025 *Accepted: 27-04-2025*

INTRODUCTION

Kidney stones constitute a common issue encountered in the urology field. Their widespread occurrence, high rates of recurrence, and the financial burden of treatment have significant implications for individuals and society [1]. One key factor contributing to kidney stone formation is the harm inflicted on renal tubular epithelial cells due to increased oxalate levels, with hyperoxaluria identified as a significant risk fac-

tor for developing urinary stones [2]. Exposure to elevated concentrations of oxalic acid over extended periods can trigger oxidative stress in these cells, leading to an overproduction of reactive oxygen species. This process may cause cellular harm, such as cell degeneration, apoptosis, and the exposure of the basement membrane of renal tubular epithelial cells [3], potentially worsening subsequent injuries. Following this, a series of cellular lipid peroxidation and inflammatory responses may occur [4]; as a result, antioxidants and anti-inflammatory medications are commonly employed to avert renal injury and the formation of kidney stones.

Lycopene (LYC), a vital carotenoid that falls under the classification of isoprenoid compounds, demonstrates properties such as anti-inflammatory, antioxidant, free radical scavenging, and immune modulation [5, 6]. Research indicates that lycopene may aid in relieving chronic prostatitis/chronic pelvic pain syndrome through its ability to diminish inflammation and oxidative stress by engaging the NF-κB, Nrf2, and MAPKs signalling pathways [7]. Nonetheless, no prior investigations have directly examined its protective effects against kidney damage caused by calcium oxalate stones. This study intends to explore the role and associated molecular mechanisms of LYC in the damage inflicted on renal tubular epithelial cells by oxalic acid and calcium oxalate crystals in vitro, thereby providing a theoretical foundation for utilizing anti-inflammatory and antioxidant agents, such as LYC, in the prevention and management of kidney stone disorders.

MATERIAL AND METHODS

Cells. HK-2 cells (purchased from BOSTER, catalogue number CX0044) were passed to the ninth passage.

Drugs and Reagents. *Lycopene* (Shanghai Yuanye Biotechnology Co., Ltd., product number B20378, purity ≥90%), *oxalic* (Shanghai Macklin Biochemical Technology Co., Ltd., product number O871905), *DMEMF-12* (1:1) basic medium (Gibco, USA, product number C11330500BT), *Cell Counting Kit-8* (Biosharp, product number BS350B), *Reduced glutathione* (GSH) assay kit, *Lactate dehydrogenase* (LDH) assay kit (Nanjing Jiancheng Bioengineering Institute Co., Ltd., product numbers A006-2-1 and A020-2-2), *Malondialdehyde* (MDA) Colorimetric Assay Kit, *Total Superoxide Dismutase* (T-SOD) Activity Assay Kit (Wuhan Elabscience Biotechnology Co., Ltd., product numbers E-BC-K028-M and E-BC-K020-M), In this study, we employed the *human IL-6 ELISA* kit and the *human MCP-1 ELISA* kit (Quanzhou Ruixin Biotechnology Co., Ltd., product numbers RX106126H and RX106032H), *Reactive oxygen species* (ROS) detection kit(Shanghai beyotimeBiotechnology Co., Ltd., product numbers S0033S). Additionally, *rabbit-derived antibodies* include *NF-κB p65*, *Osteopontin* (OPN), *Bax, Bcl-2, cytochrome C* (Cyt C), and *active-Caspase3*. *Secondary antibodies* include an *anti-mouse antibody* from Shanghai Beyotime Biotechnology Co., Ltd. (product numbers: AF5243, AF7662, A0216) and a *secondary rabbit antibody* from Proteintech Group, Inc. (batch numbers: 50599-2-Ig, 26593-1-AP, SA00001-2). Furthermore, a *mouse-derived GAPDH* antibody from BOSTER is identified by product numbers: PB9334, BM3937, and BM3876.

Instrumentation

In this research, the equipment used included the Series II Water Jacket CO2 cell culture incubator, the Infinite M1000 Pro full-wavelength microplate reader (Tecan, Switzerland), the Axio Vert A1 inverted fluorescence microscope (Zeiss, Germany), the Mini-Protean 3 Dodeca electrophoresis system, the ChemiDoc XPS+ all-in-one gel imaging system (Bio-Rad Company, USA), and the MoFlo XDP ultra-fast flow cytometer (BD Company, USA).

Method

LYC was dissolved in DMSO, and a blank culture medium was subsequently introduced

to formulate a storage solution with a concentration of 1000 μmol/L. The solution was passed through a microporous filter with a pore size of 0.22 μm and kept in a refrigerator at 4°C. Before beginning the experiment, the prepared LYC solution was administered to cultured cells in increasing concentrations (5, 10, 20, 40, 80, 100, 200, 500 μmol/L) to identify LYC's effective concentration and toxicity range. In a 96-well plate populated with HK-2 cells (1×10^4 cells x well), the effects of different LYC concentrations on HK-2 cytotoxicity were evaluated using the CCK-8 kit, with assessments made 24 hours after administration (refer to Table 1). Ultimately, lycopene concentrations of 5 μM and 10 μM were chosen for further experiments.

"A" Experimental grouping and intervention

The experimental groups were defined as follows: 1) Control group: cultured in basal medium for 24 hours; 2) Model group: cultured in basal medium containing oxalic (2 mmol/L) and COM (100 μg/mL) for 24 hours; 3) LYC I (5 μmol/L) group: treated with 5 μmol/L (LYC) in addition to the model group; 4) LYC II (10 μmol/L) group: treated with 10 μmol/L LYC in addition to the model group. These groups were utilized for subsequent experiments, including cell viability assessments, antioxidant capacity, inflammatory factors, reactive oxygen species, and Western blot analysis. Before the experiments, the original medium in the culture wells was removed, and serum-free medium was added to minimize the influence of proteins present in fetal bovine serum (FBS) on the experimental outcomes.

"B" CCK-8 assay to detect cell activity

HK-2 cells were plated in a 96-well plate at a density of 1×10^4 cells x well. After over 18 hours for complete attachment, the cells were allocated into groups for experimental interventions as specified in Section "A". Once the interventions were completed, the original culture medium was discarded and substituted with serum-free medium in every well. Subsequently, 100 μL of newly prepared culture medium and 10 μL of CCK-8 reagent were added, and the plate was incubated at 37°C for three hours. The absorbance (Ab) at 450 nm was recorded using a microplate reader. Each condition was evaluated in parallel within six replicate wells, and the experiment was conducted three times. The average value of Ab was computed, and cell activity was evaluated using the formula: Ab (experimental group) / Ab (control group) × 100%.

"C" Measurement of indicators related to antioxidant capacity

Cells were plated in a 6-well culture plate at a density of 2×10^5 cells per well until they adhered properly. The experimental groups aligned with those described previously (Experimental grouping). After a 24-hour incu-

Table 1. Effect of different concentrations of Lycopene on HK-2 cell activity.

Groups	Concentration /μmol/L	Relative cellular activity / %
Control group	0	100 ± 15.92
Lycopene group	5	98.26 ± 1.09
	10	94.75 ± 0.84
	20	88.13 ± 2.12
	40	86.92 ± 2.75
	80	85.02 ± 2.47
	100	79.82 ± 2.34
	200	69.27 ± 4.76
	500	31.39 ± 2.42

Data is expressed as $\bar{x} \pm$ sd, n=3.

bation, cells from each group were collected, and the protein concentration was measured in centrifuge tubes. The instructions of the kit were followed to operate. Finally, the contents of lactate dehydrogenase(LDH), malondialdehyde (MDA), glutathione(GSH), and total superoxide dismutase(T-SOD) were measured in the cells using a Microplate reader at wavelengths of 450, 532, 405, and 450 nm and an ELISA kit was used for detection of IL-6, MCP-1 secretion.

"D" Cells were plated in a 6-well culture plate at a density of 2 x 10^5 cells per well until they adhered properly. The experimental groups aligned with those described in section "A". After a 24-hour incubation, the supernatant from each cell group was gathered into centrifuge tubes. Next, 50 μL from each group was transferred to the enzyme plate, following the instructions provided with the kit. Essential procedures included preparing three duplicate wells for every cell group, with the experiment conducted three times. The absorbance (Ab) measurement was taken at a wavelength of 450 nm to assess the levels of the inflammatory cytokines IL-6 and MCP-1.

"E" Observation of cellular ROS

Cells were plated in a 6-well culture dish at a density of 2 x 10^5 cells per well, adhering to the group allocations outlined before (A). After a 24-hour culture period, a ROS detection kit was utilized to evaluate the levels of intracellular ROS. Specifically, 10 μmol/L DCFH-DA, which was diluted in serum-free culture medium, was introduced in a dark environment. One mL of this fluorescent probe was administered, and the cells were incubated for 20 minutes. After incubation, the cells underwent three washes with 1 mL of serum-free culture medium, after which images were taken using an inverted fluorescence microscope.

"F" Western blot for protein expression in HK-2 cells

Cells were planted in a 6-well plate according to the method described in Section "D", then collected and denatured at high temperature. Electrophoresis was performed using the SDS gel system, followed by transfer to a PVDF membrane. The membrane was blocked with 5% skim milk at room temperature for 2 hours. The primary antibodies (NF-κB p65, OPN, Bax, Bcl-2, Cyt C, active-Caspase3, and GAPDH) were added and incubated at 4°C overnight. Subsequently, they were incubated with a secondary antibody at room temperature for 1.5 hours. The developing agent was added, and images were captured using an automatic gel imager. The ImageJ software was used to measure the gray value of each band and calculate the relative expression of target proteins in each group.

Statistical methods

All data were analyzed statistically with the use of GraphPad Prism 8.0.1 software. The outcomes are represented as $\bar{x} \pm SD$. A one-way ANOVA was utilized to compare several groups. A p-value lower than 0.05 was considered a statistically significant difference.

RESULTS

Comparison of cell activity and LDH in each group

Following 24 hours of treatment in the culture medium, the viability of cells in each group was assessed. The findings indicated a notable reduction in cell viability within the model group when juxtaposed with the control group ($p<0.001$), alongside a significant elevation in LDH levels ($p<0.001$). Conversely, cell viability in the LYC groups (5 μM, 10 μM) exhibited a marked increase compared to the model group ($p<0.05$), while LDH levels showed a significant decrease ($p<0.05$) (Table 2).

Comparison of antioxidant and anti-inflammatory capacities of HK-2 cells

The findings from the biochemical index assessments indicated a notable reduction in GSH levels within the model group when contrasted with the control group

Table 2. Comparison of cellular activity and intracellular lactate dehydrogenase content in each group.

Items	Control group	Model group	LYC (5μM)	LYC (10μM)
Cellular activity (%)	100	42±2.98[a]	60.37±3.44[b]	51.79±1.88[b]
LDH (U/g prot)	369.9±41.43	906±79.97[a]	483.7±70.8[b]	588.8±33.56[b]

Note: [a] is $p<0.001$ compared with the control group, and [b] is $p<0.05$ compared with the model group; as x, $\bar{x} \pm sd$, n=3. LDH: lactate dehydrogenase; LYC: Lycopene.

($p<0.05$). Conversely, MDA levels were found to have increased markedly ($p<0.05$). MDA levels saw a significant decline due to LYC treatment ($p<0.001$) (Table 3). Furthermore, when examining the model group, there was a notable surge in inflammatory cytokines IL-6 and MCP-1 compared to the control group ($p<0.05$). LYC administration at doses of 5 μM and 10 μM demonstrated an inhibitory effect on the secretion of IL-6 and MCP-1 relative to the model group ($p<0.05$) (Table 4).

Changes in intracellular ROS, mitochondrial membrane potential and apoptosis across different cell groups

In comparison to the control group, the model group exhibited enhanced green fluorescence and a reduced mitochondrial membrane potential. Following intervention with LYC (5 μM, 10 μM), the model group showed an increase in red fluorescence, a decrease in green fluorescence, and an improvement in mitochondrial membrane potential. Moreover, the generation of ROS was increased in the model group compared to the control group. However, after LYC intervention (5 μM, 10 μM), the model group demonstrated a decrease in ROS production (see Fig. 1 and Fig. 2). PI and Hoechst staining indicated that, in contrast to the control group, there was a rise in apoptotic cells within the model group, evidenced by intensified blue fluorescence. In comparison to the model group, treatment with LYC (5 μM, 10 μM) resulted in an improvement and a reduction in cell apoptosis, as shown by diminished blue fluorescence (Fig. 3).

Expression of inflammation and apoptosis-related proteins

The levels of NF-κB p65 and OPN in the model group were significantly elevated ($p<0.05$) compared to the control group, whereas LYC (5 μM, 10 μM) led to a decrease relative to the model group (Fig. 4). The expression levels of Bax, CytC, and active caspase3 were markedly increased ($p<0.05$) in the model group when compared to the control group, while Bcl-2 expression was significantly decreased ($p<0.05$). The LYC (5 μM, 10 μM) treatment group exhibited a downregulation in Bax, CytC, and active caspase3 expression, along with an upregulation in Bcl-2 expression compared to the model group (Table 5, Fig. 5).

DISCUSSION

The main goals in treating kidney stones include removing the stones, protecting kidney function, and tackling the root causes to reduce the likelihood of recurrence [8]. Thus, it is vital to identify specific pharmacological agents that target the condition's etiology for preventing and treating stones. The formation of kidney stones is a complicated process that entails the supersaturation of factors contributing to urolithiasis, harm to renal tubular epithelial cells, and the mechanisms of crystal adhesion, aggregation, nucleation, and growth [9]. A significant contributor to the development of kidney stones is oxalic acid. Elevated concentrations of oxalic acid may result in oxidative damage and initiate an inflammatory reaction in renal tubular epithelial cells [10].

Table 3. Comparison of indicators related to intracellular antioxidant capacity in each group.

Items	Control group	Model group	Lycopene (5μM)	Lycopene (10μM)
Glutathione (GSH, umol/g protein)	327.4±29.98	111.8±11.71[a]	212.1±21.1[b]	201.2±22.19[b]
Total superoxide dismutase (T-S0D, U/mg protein)	13.54±0.70	11.57±1.61	15.03±2.56	14.59±2.29
Malondialdehyde (MDA, nmol/mg protein)	2.166±0.3	22.89±0.441[a]	14.68±1.72[b]	15.43±0.85[b]

Note: [a] is $p<0.001$ compared with the control group, and [b] is $p<0.05$ compared with the model group. The above data was analyzed using one-way ANOVA. $\bar{x} \pm sd$, n=3.

Table 4. Effect of Lycopene on Interleukin-6 (IL-6) and Monocytechemotactic protein-1 (MCP-1) released from oxalic acid/calcium oxalate-induced HK-2 cells.

Groups	IL-6 (pg/mL)	MCP-1(pg/mL)
Control group	4.49 ± 0.44	9.78 ± 1.38
Model group	9.25 ± 0.46[a]	29.38 ± 3.51[a]
Lycopene (5μM)	5.42 ± 1.49[b]	7.71 ± 6.10[b]
Lycopene (10μM)	5.28 ± 1.51[b]	11.84 ± 4.85[b]

Note: [a] is $p<0.001$ compared with the control group, and [b] is $p<0.05$ compared with the model group. The above data was analyzed using one-way ANOVA; ($\bar{x} \pm sd$, n=3).

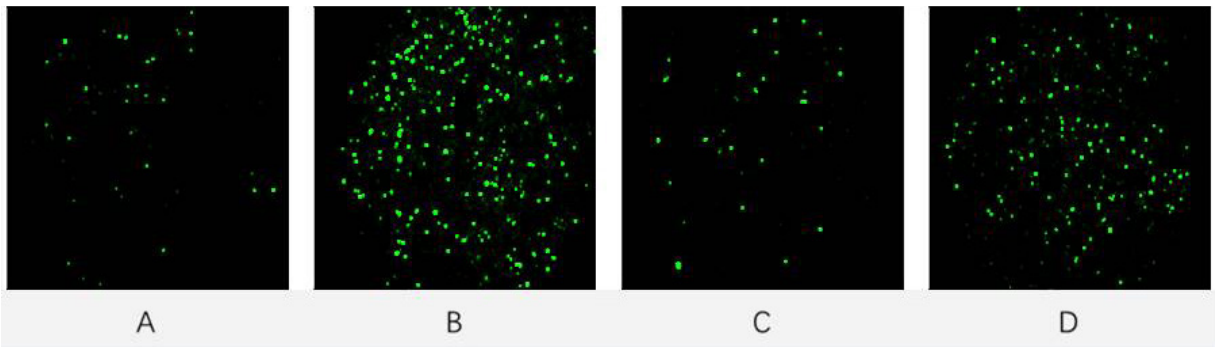

Fig. 1. Effect of LYC on oxalic acid/calcium oxalate crystal-induced intracellular reactive oxygen species ROS in HK-2 cells. A. control group; B. model group; C. LYC (5 μM); D. LYC (10 μM) group (Immunofluorescence, x100).

An expanding array of studies has demonstrated a relationship between inflammation, oxidative stress, and kidney stone formation [4, 11]. Hence, investigating effective anti-inflammatory and antioxidant mechanisms is crucial for alleviating kidney injury associated with calcium oxalate stones.

Malondialdehyde (MDA) is the end product generated from the peroxidation of cellular lipids. The levels of MDA offer valuable information regarding the degree of lipid peroxidation in the body, thereby acting as an indirect indicator of cellular damage.

Although free radicals can inflict considerable harm, human cells also harbor substances that neutralize these free radicals. Among these protective agents, super-

oxide dismutase (SOD) stands out as a key antioxidant enzyme that aids in reducing the damage inflicted by oxygen-derived free radicals [12]. A reduction in SOD activity indicates a lower ability of the organism to combat free radical-induced damage, implying that the organism may be undergoing oxidative stress. For example, continuous exposure to elevated levels of oxalic acid can promote the production of free radicals, which initiate lipid peroxidation within biological membranes.

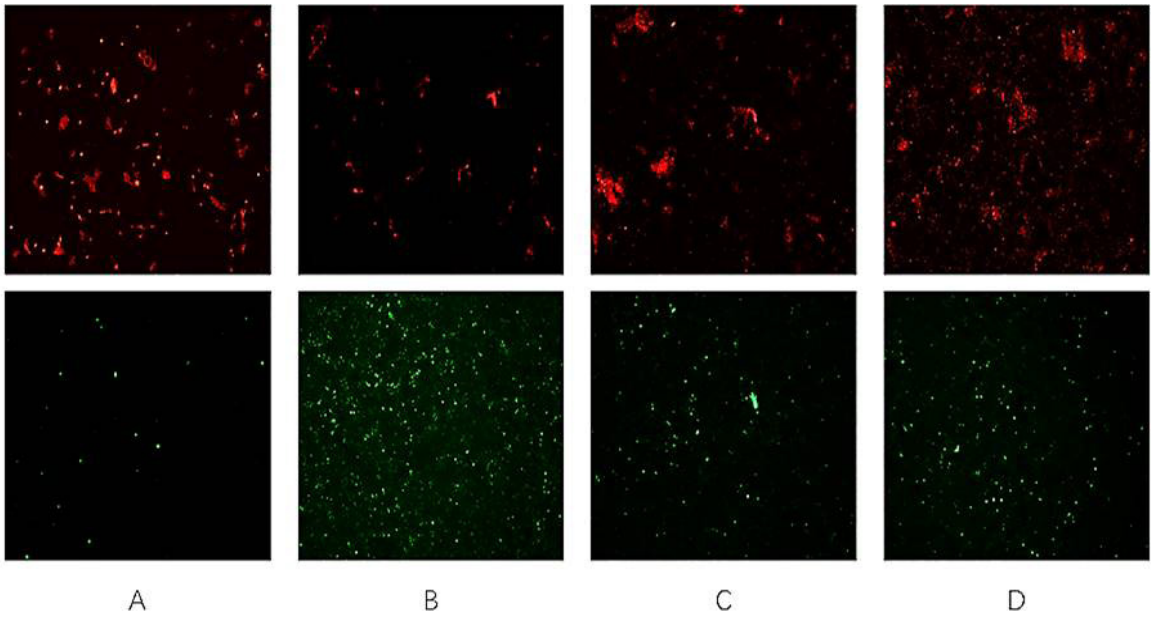

Fig. 2. Effect of LYC on mitochondrial membrane potential induced by oxalic acid/calcium oxalate crystals in HK-2 cells. A. control group; B. model group; C. LYC (5 μM); D. LYC (10 μM) group (Immunofluorescence, x100).

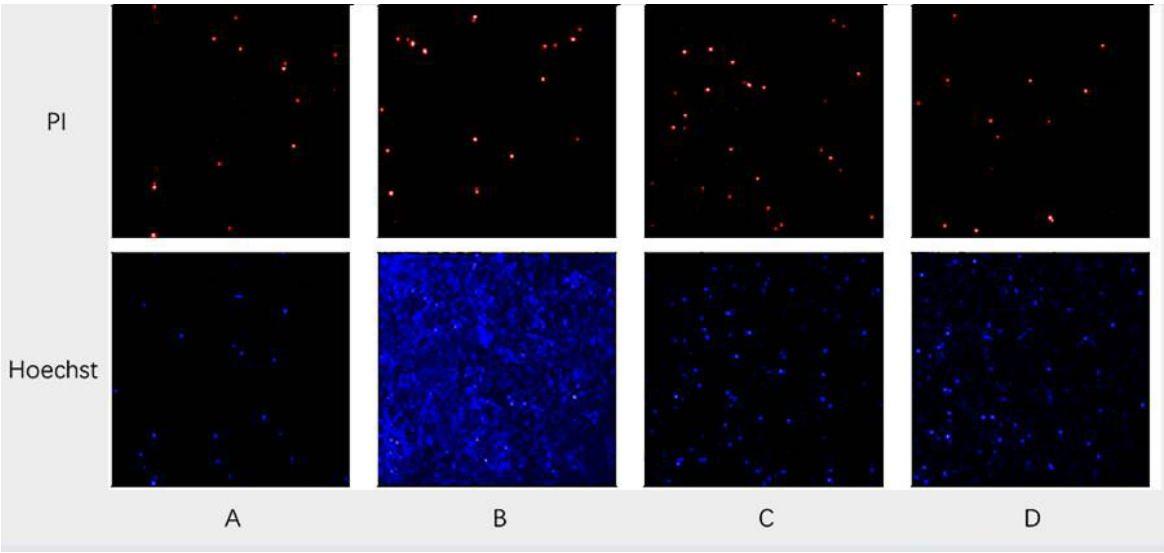

Fig. 3. Effect of LYC on the apoptotic profile of HK-2 cells induced by oxalic acid/calcium oxalate crystals. A. control group; B. model group; C. LYC (5 μM); D. LYC (10 μM) group. PI: propidium iodide (Immunofluorescence, x100).

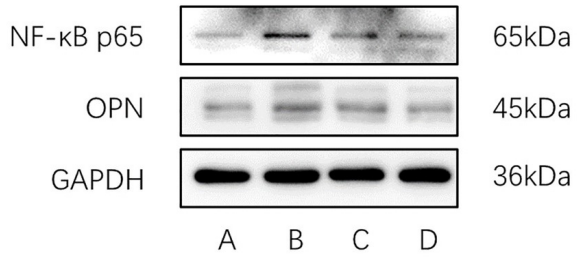

Fig. 4. LYC ameliorates oxalic acid/calcium oxalate crystal-induced changes in inflammation-associated protein levels in HK-2 cell injury.

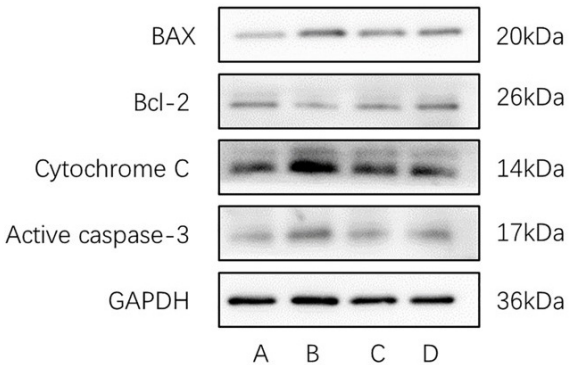

Fig. 5. Changes in the levels of mitochondrial damage-related proteins in HK-2 cells.

Table 5. Relative expression of proteins related to inflammation and mitochondrial damage in cells of each group.

Items	Control group	Model group	Lycopene (5μM)	Lycopene(10μM)
P65	0.708±0.077	1.014±0.053[a]	0.807±0.163	0.782±0.229
Osteopontin (OPN)	0.546±0.70	0.864±0.006[a]	0.746±0.260	0.642±0.127[b]
BAX	0.427±0.062	1.109±0.205[a]	0.734±0.221	0.542±0.203[b]
Bcl-2	1.13±0.301	0.466±0.228[a]	0.536±0.261	0.544±0.245
Cytochrome C (Cyt C)	0.539±0.066	2.242±0.428[a]	0.930±0.264[b]	0.775±0.490[b]
Active caspase3	0.355±0.155	1.16±0.231[a]	0.585±0.212[b]	0.771±0.165

Note: [a] is $p<0.001$ compared with the control group, and [b] is $p<0.05$ compared with the model group. The above data was analyzed using one-way ANOVA.

This chain of events may result in changes to the ultrastructural integrity of cell membranes, enable cellular penetration, inflict harm on mitochondria and DNA, and ultimately lead to cell necrosis and apoptosis[13]. These experimental findings reveal that the oxidative damage to HK-2 cells induced by oxalic acid/calcium oxalate is significant, as evidenced by compromised cell proliferation, decreased cell viability, heightened release of lipid peroxidation byproducts like MDA and LDH, along with lower levels of antioxidant enzymes such as SOD and GSH. Following treatment with LYC, we noted an enhancement in cell viability, reduced oxidative injury, and increased antioxidant activity.

Reactive oxygen species (ROS) are recognized as primary regulators of oxidative stress and identified as significant contributors to the damaging effects of pathological stone formation [14]. The role of the NF-κB signaling pathway is critical in facilitating intrarenal inflammation mediated by oxidative stress [15]. The significant production of ROS caused by oxidative stress can additionally activate various signalling pathways associated with inflammation, creating diverse inflammatory mediators and promoting the buildup of inflammatory cells, thus triggering and enhancing the inflammatory response. Studies show that heightened oxalic acid levels can provoke the activation of the NF-κB intracellular signalling pathway, which leads to an increased expression of inflammatory factors like OPN and MCP-1/IL-6, ultimately resulting in the infiltration of inflammatory cells and causing interstitial damage [4]. Monocyte chemotactic protein-1 is an essential inflammatory mediator contributing to the inflammatory

reactions linked to calcium oxalate kidney stones. Under standard physiological conditions, renal tissue cells only produce a minimal amount of MCP-1. However, when oxalic acid or calcium oxalate crystals precipitate in urine due to supersaturation, these substances can damage and stimulate these cells, leading to a substantial increase in MCP-1 production, subsequently attracting monocytes into the inflamed tissue [16]. Boonla et al. [17] compared MCP-1 and IL-6 mRNA expression levels in kidney tissues adjacent to stones and those in normal kidneys. Their findings indicated more severe tubular damage in the tissues surrounding the stones and significantly reduced expression levels of MCP-1 and IL-6 compared to normal kidney tissues. This observation implies that MCP-1 and IL-6 may be involved in advancing kidney stone disease.

Furthermore, during cellular damage, various negatively charged molecules—including osteopontin (OPN), hyaluronic acid (HA), and CD44 [18]—are showcased on the cell surface. These molecules can bind to Ca2+ ions and attach to positively charged calcium oxalate crystals. The adhering crystals can trigger cellular production of free radicals, further harming the renal epithelium via lipid peroxidation, thus heightening the possibility of kidney stone formation. The study utilized ELISA experiments to show that MCP-1 and IL-6 release were elevated in the model group, while LYC was found to have a protective effect. Western blot analyses indicated that NF-κB and OPN levels were upregulated in the model group relative to the control group; however, their expression was reduced after LYC treatment. In addition, a combined analysis of reactive oxygen species levels in cells revealed that LYC could ameliorate the intrarenal ROS levels triggered by oxalic acid/calcium oxalate crystals in HK-2 cells, effectively inhibiting the NF-κB signalling pathway and thereby diminishing the intrarenal inflammatory response.

The deposition of calcium oxalate crystals may also cause damage to mitochondria by increasing cellular ceramide levels. Mitochondrial abnormalities or oxidative stress can trigger the initiation of cell apoptosis programs. The family of Bcl-2 proteins is crucial in governing mitochondrial permeability to various proteins and the permeabilization of the outer mitochondrial membrane, playing an essential role in the intrinsic apoptosis pathway. Bax and Bcl-2 are pro-apoptotic and anti-apoptotic agents, respectively [19]. While Bcl-2 shields cells from mitochondrial injury and suppresses apoptosis, Bax enhances the permeability of the mitochondrial membrane, facilitating the release of cytochrome C (Cyt C) [20]. This sequence of events leads to an increase in hydrogen peroxide production, a decrease in glutathione peptide levels, and a drop in mitochondrial membrane potential, coupled with the liberation of apoptotic factors into the cytosol, which ultimately activates caspase-3 and induces cell death [21]. The expression levels of proteins associated with the mitochondrial pathway were evaluated in this study.

Results indicate that treatment with oxalic acid/calcium oxalate crystals led to an upregulation of Bax, Cyt C, and active-caspase3, while a downregulation of Bcl-2 was observed. Following the intervention with LYC, improvements in cell apoptosis were noted. These findings imply that LYC may mitigate HK-2 cell apoptosis by inhibiting the Bax/caspase3 signalling pathway.In conclusion, LYC demonstrates a significant ability to reduce oxidative stress and inflammatory responses in HK-2 cells, enhances cellular health, and may operate through the modulation of the ROS/NF-κB inflammasome pathway while also mitigating mitochondrial damage by inhibiting the Bax/caspase3 signalling pathway associated with mitochondria. This research offers an initial insight into the potential mechanisms by which LYC could aid in the clinical prevention and treatment of kidney stones, thereby opening new avenues

and concepts for addressing calcium oxalate kidney stones and the clinical utilization of LYC and analogous medications. Nonetheless, as the investigation primarily focuses on cellular models, it may not wholly replicate the mechanisms involved in the human body, indicating that the study has inherent limitations, warranting further exploration and validation.

ACKNOWLEDGEMENTS

Thanks for the support from the Special Project for the Promotion of Department Heads of Traditional Chinese Medicine Hospitals in Jiangsu Province.

Funding

This study was supported by the Special Project for the Promotion of Department Heads of Traditional Chinese Medicine Hospitals in Jiangsu Province(Y2021Z19).

Ethics approval and consent to participate

Not applicable, our study utilizes commercially available cell lines, and the Nanjing University of Chinese Medicine does not mandate ethics review for research conducted with such cell lines. So, there are no ethical issues or conflicts of interest.

Availability of data and materials

The datasets used and/or analyzed during the current study are available from the corresponding author on reasonable request.

Conflict of interests

All authors declare no conflict of interest.

Number ORCID of authors

- Liangwen Ye (LY): 0009-0003-9780-4688
- Yuhang Tang (YT): 0009-0009-6263-0570
- Zhijie Zhang (ZZ): 0009-0006-8535-0748
- Xiangyi Hou (XH): 0009-0004-5185-6965
- Wei Xu. (WX): 0009-0004-0948-5822
- Xianghui Suo (XS): 0009-0008-1688-0694
- Li Zhang (LZ): 0009-0002-2514-6690

Authors' Contributions

LY and YT designed the study; data acquisition, analysis, and interpretation were conducted by ZZ and XH; the manuscript underwent revision by LY, WX, and XS; LZ also played a role in the article's revision. Each author contributed to the paper and approved the final version submitted.

REFERENCES

1. **Tan S, Yuan D, Su H, Chen W, Zhu S, Yan B**, et al. Prevalence of urolithiasis in China: a systematic review and meta-analysis. BJU Int. 2024;133:34-43. *10.1111/bju.16179.*
2. **Qin B, Wang Q, Lu Y, Li C, Hu H, Zhang J**, et al. Losartan ameliorates calcium oxalate-induced elevation of stone-related proteins in renal tubular cells by inhibiting NADPH oxidase and oxidative stress. Oxid Med Cell Longev. 2018;2018:1271864. *10.1155/2018/1271864.*
3. **Kang J, Sun Y, Deng Y, Liu Q, Li D, Liu Y**, et al. Autophagy-endoplasmic reticulum stress inhibition mechanism of superoxide dismutase in the formation of calcium oxalate kidney stones. Biomed Pharmacother. 2020;121:109649. *10.1016/j.biopha.2019.109649.*
4. **Khan SR.** Reactive oxygen species as the molecular modulators of calcium oxalate kidney stone formation: evidence from clinical and experimental investigations. J Urol. 2013;189:803-11. *10.1016/j.juro.2012.05.078.*

5. **Liu CB, Wang R, Yi YF, Gao Z, Chen YZ**. Lycopene mitigates β-amyloid induced inflammatory response and inhibits NF-κB signaling at the choroid plexus in early stages of Alzheimer's disease rats. J Nutr Biochem. 2018;53:66-71. *10.1016/j.jnutbio.2017.10.014.*
6. **Caseiro M AA, Costa A, Creagh-Flynn J, Johnson M, Simões S**. Lycopene in human health. LWT. 2020;127. *10.1016/j.lwt.2020.109323.*
7. **Zhao Q, Yang F, Meng L, Chen D, Wang M, Lu X,** et al. Lycopene attenuates chronic prostatitis/chronic pelvic pain syndrome by inhibiting oxidative stress and inflammation via the interaction of NF-κB, MAPKs, and Nrf2 signaling pathways in rats. Andrology. 2020;8:747-755. *10.1111/andr.12747.*
8. **Sixing Y ZY**. Reconsiderations of several key issues in the treatment of urolithiasis. Chinese J of Urol. 2018;9. *10.3760/cma.j.issn.1000-6702.2018.09.002.*
9. **Thongboonkerd V**. Proteomics of crystal-cell interactions: a model for kidney stone research. Cells. 2019;8. *10.3390/cells8091076.*
10. **Liu Q, Liu Y, Guan X, Wu J, He Z, Kang J**, et al. Effect of M2 macrophages on injury and apoptosis of renal tubular epithelial cells induced by calcium oxalate crystals. Kidney Blood Press Res. 2019;44:777-791. *10.1159/000501558.*
11. **Mulay SR, Kulkarni OP, Rupanagudi KV, Migliorini A, Darisipudi MN, Vilaysane A,** et al. Calcium oxalate crystals induce renal inflammation by NLRP3-mediated IL-1β secretion. J Clin Invest. 2013;123:236-246. *10.1172/jci63679.*
12. **Zabłocka A, Janusz M**. [The two faces of reactive oxygen species]. Postepy Hig Med Dosw (Online). 2008;62:118-124.
13. **Joshi S, Khan SR**. Opportunities for future therapeutic interventions for hyperoxaluria: targeting oxidative stress. Expert Opin Ther Targets. 2019;23:379-391. *10.1080/14728222.2019.1599359.*
14. **Umekawa T, Tsuji H, Uemura H, Khan SR**. Superoxide from NADPH oxidase as second messenger for the expression of osteopontin and monocyte chemoattractant protein-1 in renal epithelial cells exposed to calcium oxalate crystals. BJU Int. 2009;104:115-120. *10.1111/j.1464-410X.2009.08374.x.*
15. **Patel M, Yarlagadda V, Adedoyin O, Saini V, Assimos DG, Holmes RP**, et al. Oxalate induces mitochondrial dysfunction and disrupts redox homeostasis in a human monocyte derived cell line. Redox Biol. 2018;15:207-215. *10.1016/j.redox.2017.12.003.*
16. **Zuo L, Tozawa K, Okada A, Yasui T, Taguchi K, Ito Y**, et al. A paracrine mechanism involving renal tubular cells, adipocytes and macrophages promotes kidney stone formation in a simulated metabolic syndrome environment. J Urol. 2014;191:1906-1912. *10.1016/j.juro.2014.01.013.*
17. **Boonla C, Hunapathed C, Bovornpadungkitti S, Poonpirome K, Tungsanga K, Sampatanukul P,** et al. Messenger RNA expression of monocyte chemoattractant protein-1 and interleukin-6 in stone-containing kidneys. BJU Int. 2008;101:1170-1177. *10.1111/j.1464-410 X.2008.07461.x.*
18. **Khan SR, Joshi S, Wang W, Peck AB**. Regulation of macromolecular modulators of urinary stone formation by reactive oxygen species: transcriptional study in an animal model of hyperoxaluria. Am J Physiol Renal Physiol. 2014;306:F1285-1295. *10.1152/ajprenal.00057.2014.*
19. **Lalier L, Vallette F, Manon S**. Bcl-2 family members and the mitochondrial import machineries: The roads to death. Biomolecules. 2022;12. *10.3390/biom12020162.*
20. **Hu L, Chen M, Chen X, Zhao C, Fang Z, Wang H**, et al. Chemotherapy-induced pyroptosis is mediated by BAK/BAX-caspase-3-GSDME pathway and inhibited by 2-bromopalmitate. Cell Death Dis. 2020;11:281. *10.1038/s41419-020-2476-2.*
21. **Khan SR**. Reactive oxygen species, inflammation and calcium oxalate nephrolithiasis. Transl Androl Urol. 2014;3:256-276. *10.3978/j.issn.2223-4683.2014.06.04.*

Invest Clin 66(2): 217 - 230, 2025 https://doi.org/10.54817/IC.v66n2a08

Impact of regional anesthesia vs general anesthesia on postoperative outcomes in elderly patients with hip fracture: a meta-analysis.

Feng Han[1], Yue Yang[1] and Xinxin Tian[2]

[1]Department of Anesthesiology, Hangzhou Geriatric Hospital, Hangzhou, China.
[2]Department of Infectious Diseases, Hangzhou Ninth People's Hospital, Hangzhou, China.

Keywords: hip fracture; anesthesia; elderly; meta-analysis.

Abstract. The objective of this study was to utilize meta-analysis to compare the impact of regional anesthesia (RA) versus general anesthesia (GA) on postoperative outcomes in elderly patients undergoing hip fracture surgery. Electronic databases (PubMed, Web of Science, Cochrane Library, and Embase) were searched for randomized controlled trials (RCTs) comparing the effects of RA and GA in elderly patients undergoing hip fracture surgery. The random or fixed-effects model was used to calculate pooled relative risks (RR) and mean differences (MD). Fourteen RCTs involving 5626 elderly patients undergoing hip fracture surgery were included. Meta-analysis indicated that RA was associated with a lower incidence of intraoperative blood loss (MD: -39.7 mL; 95% CI: -68.61, -10.84; p = 0.007), adverse events including intraoperative hypotension (RR: 1.09; 95% CI: 0.90, 1.32; p = 0.005) and postoperative cognitive dysfunction (RR: 0.56; 95% CI: 0.37, 0.86; p = 0.007) compared to GA. However, no statistically significant differences were found between RA and GA regarding surgical time, anesthesia time, intraoperative transfusion, hospital length, delirium, and mortality. RA can effectively reduce intraoperative blood loss and the risk of hypotension. Due to the current lack of evidence, no positive effects of RA on other postoperative outcomes were identified. A rigorously designed, high-quality study is warranted to determine the impact of anesthesia type on elderly hip fracture patients.

Corresponding author. Xinxin Tian. Department of Infectious Diseases, Hangzhou Ninth People's Hospital. No. 98 Yilong Road, Yipong Street, Qiantang District, Hangzhou, China. Tel: 86-18317898728.
Email: tianxinxintxxtxx@163.com

Impacto de la anestesia regional vs anestesia general en los resultados posoperatorios en pacientes ancianos con fractura de cadera: un meta-análisis.

Invest Clin 2025; 66 (2): 217 – 230

Palabras clave: fractura de cadera; anestesia; ancianos; meta-análisis.

Resumen. El objetivo de este estudio fue utilizar meta-análisis para comparar el impacto de la anestesia regional (AR) versus la anestesia general (AG) en los resultados posoperatorios en pacientes ancianos sometidos a cirugía de fractura de cadera. Se buscó en las bases de datos electrónicas (PubMed, Web of Science, Cochrane Library y Embase) ensayos controlados aleatorios (ECA) que compararan los efectos de AR vs AG en pacientes de edad avanzada sometidos a cirugía de fractura de cadera. Se utilizó el modelo de efectos aleatorios o fijos para calcular los riesgos relativos agrupados (RR) y las diferencias de medias (DM). Se incluyeron 14 ECA con 5.626 pacientes de edad avanzada sometidos a cirugía de fractura de cadera. El metanálisis indicó que la AR se asoció con una menor incidencia de pérdida de sangre intraoperativa (DM: -39,7 mL; IC 95%: -68,61, -10,84; p = 0,007), eventos adversos incluyendo hipotensión intraoperativa (RR: 1,09; IC del 95%: 0,90, 1,32; p = 0,005) y disfunción cognitiva posoperatoria (RR: 0,56; IC 95% : 0,37, 0,86; p = 0,007) comparado con GA. Sin embargo, no se encontraron diferencias estadísticamente significativas entre AR y AG en términos de tiempo quirúrgico, tiempo de anestesia, transfusión intraoperativa, duración hospital, delirio y mortalidad. La AR puede reducir eficazmente la pérdida de sangre intraoperatoria y el riesgo de hipotensión. Debido a la actual falta de pruebas, no se identificaron efectos positivos de la AR en otros resultados posoperatorios. Se justifica un estudio de alta calidad y rigurosamente diseñado para determinar el impacto del tipo de anestesia en pacientes ancianos con fractura de cadera.

Received: 21-10-2024 Accepted: 03-05-2025

INTRODUCTION

Hip fracture represents one of the significant challenges to healthcare in the 21st century. It is estimated that approximately 1.6 million people suffered from hip fractures globally in 2000, and this number is expected to rise to 4.5 million by 2050 due to the aging global population, imposing a substantial burden on both families and society [1-3]. Despite patients receiving optimal care, the postoperative survival of elderly patients remains poor [4].

Almost all hip fracture patients undergo surgical treatment, and the choice of anesthesia can influence postoperative recovery and long-term prognosis [5]. The application of regional anesthesia (RA) and general anesthesia (GA) in elderly patients with hip fractures has been debated. Approximately 60% of elderly patients receive GA, while 40% undergo spinal anesthesia (SA) or nerve blocks [6,7]. RA is favored by clinicians as an integral part of multimodal analgesia due to its ease of administration and reduced opioid consumption compared to GA [8]. Pre-

vious studies have shown that RA can reduce the incidence of postoperative cognitive dysfunction and the risk of death and major complications by limiting anesthesia and morphine use, compared to GA [9,10]. However, the complexity of RA, the high requirement for patient cooperation, and potential local complications have limited its application in certain situations. GA provides a more stable anesthetic effect and better surgical conditions but is associated with physiological suppression, postoperative cognitive dysfunction, and respiratory complications, raising concerns about its safety in elderly patients.

In recent years, with the continuous advancement of anesthetic techniques and drugs, comparative studies on the application of RA and GA in hip fracture surgery in the elderly have increased. However, existing results are inconsistent, with some studies supporting the superiority of RA [9,10], while others consider GA and RA to have equivalent efficacy [11]. This inconsistency may arise from differences in study design, patient population heterogeneity, and non-uniform postoperative assessment standards. This study aims to systematically evaluate and compare the efficacy and safety of RA and GA in hip fracture surgery in older patients through a meta-analys address. We will conduct a comprehensive analysis of existing randomized controlled trials to provide clinical physicians with a more scientific and objective basis for decision-making and improve the postoperative outcomes of elderly patients with hip fractures.

MATERIALS AND METHODS

In accordance with the PRISMA 2020 statement [12], a systematic search was conducted across four electronic databases: PubMed, Web of Science, Cochrane Library, and Embase. The search period was from the databases' inception to August 20, 2024. The search strategy included the following keywords: "Hip fracture," "General anesthesia," "Regional anesthesia," "Conduction Anesthesia," "Local Anesthesia," "Spinal anesthesia," OR "Epidural anesthesia." Additionally, targeted literature was identified by reviewing the reference lists of included studies.

Inclusion and exclusion criteria

Inclusion criteria: (1) Studies published in peer-reviewed journals in Chinese or English; (2) Study subjects were elderly patients aged ≥60 years (or with a majority aged ≥60 years) with hip fractures undergoing surgical treatment; (3) The experimental group received RA; (4) The control group received GA; (5) At least one of the following outcomes was reported: primary outcomes [surgical time, duration of anesthesia, blood loss, intraoperative transfusion (in units of packed red blood cells), and hospital length (from the day of admission to the day of discharge)], secondary outcomes [adverse events (intraoperative hypotension, postoperative cognitive dysfunction, intraoperative delirium, etc.)]; (6) Randomized controlled trials (RCT).

Exclusion criteria: (1) Non-population-based studies; (2) Conference papers, case reports, systematic reviews, and other study types; (3) Insufficient outcome information for data analysis; (4) Duplicate reporting of studies; (5) Studies where full-text articles could not be obtained.

Studies screening and data extraction

Two researchers independently conducted literature screening based on the inclusion and exclusion criteria. Initial screening was performed by reading the titles and abstracts of the literature, followed by a full-text review of potentially eligible studies. In cases of disagreement between the two researchers, a third researcher was consulted, and a consensus was reached through discussion. After the literature screening, two researchers independently extracted data according to a predefined data extraction form, which included information on publi-

cation details, demographic characteristics of the study subjects, intervention characteristics, study period, and outcome events.

Quality assessment

The quality of the literature was assessed using the Cochrane Collaboration's risk assessment tool[13], which evaluates aspects such as the method of randomization, allocation concealment, blinding, completeness of outcome data, selective reporting of study results, and other sources of bias.

STATISTICAL METHODS

Statistical analysis was performed using the Revman 5.3 software. Continuous data were expressed as mean differences (MD), and the effect size for categorical data was represented by the relative risk (RR), with the 95% confidence interval (CI) used to estimate the range of the effect size. Heterogeneity was assessed using the I^2 statistic and Q-test to determine the degree of heterogeneity. The values of I^2 <40%, I^2 = 40–60%, and I^2 > 60% indicated low, moderate, and high heterogeneity, respectively. If I^2 was <50% or $p>0.1$, a fixed-effect model was used for analysis; if I^2 was >50% or $p\leq0.1$, a random-effects model was used for analysis. If significant heterogeneity was present, sensitivity analysis was conducted to explore the sources of heterogeneity. Unless otherwise specified, the significance level was set at $p<0.05$.

RESULTS

Basic information of included studies

After searching the electronic databases, 3792 studies were identified and included in the literature review process, as shown in Fig. 1. After excluding 1731 duplicate studies and 1964 irrelevant studies, 97 studies were reviewed in full text to determine their eligibility for this study, and ultimately, 14 qualified studies were included [11, 14-26].

The publication years of the 14 RCTs spanned from 2003 to 2024, with four studies originating from China, two multi-country studies (USA and Canada), and the remaining studies from Israel (n=1), Iran (n=1), France (n=1), Greece (n=1), Korea (n=1), USA (n=1) Denmark (n=1) and the UK (n=1). The 14 studies involved 5626 elderly patients undergoing hip fracture surgery, of which 2768 patients received RA, and the remaining 2858 patients received GA. The average age of the study subjects ranged from 62.5 to 85 years, and in four studies, most of the patients were male (male≥50%). A summary of the basic information of the included studies is presented in Table 1.

Quality of included studies

We utilized the Cochrane Risk of Bias tool to assess the quality of the included studies, revealing a significant risk of bias in the implementation of blinding and a potential risk in allocation concealment, as shown in Supplementary Figs. 1-2. Overall, the quality of the included studies was acceptable.

Surgical time

Eight studies provided results on the impact of different anesthesia methods on surgical time for elderly patients with hip fractures, involving 1,231 patients who received RA and 1,245 patients who received GA. The heterogeneity assessment showed heterogeneity among the included studies (I^2=87%, $p<0.00001$), and the random-effects model was used to evaluate the impact of RA versus GA on surgical time. The meta-analysis results indicated no statistically significant difference in the impact of the two anesthesia methods on surgical time (MD: -3.10; 95%CI: -6.99, 0.79), as seen in Fig. 2.

Anesthesia time

Six studies provided results on the impact of different anesthesia methods on anesthesia time for elderly patients undergoing hip fracture surgery, involving 1,307 patients who received RA and 1,389 patients who received GA. The assessment of heterogeneity revealed

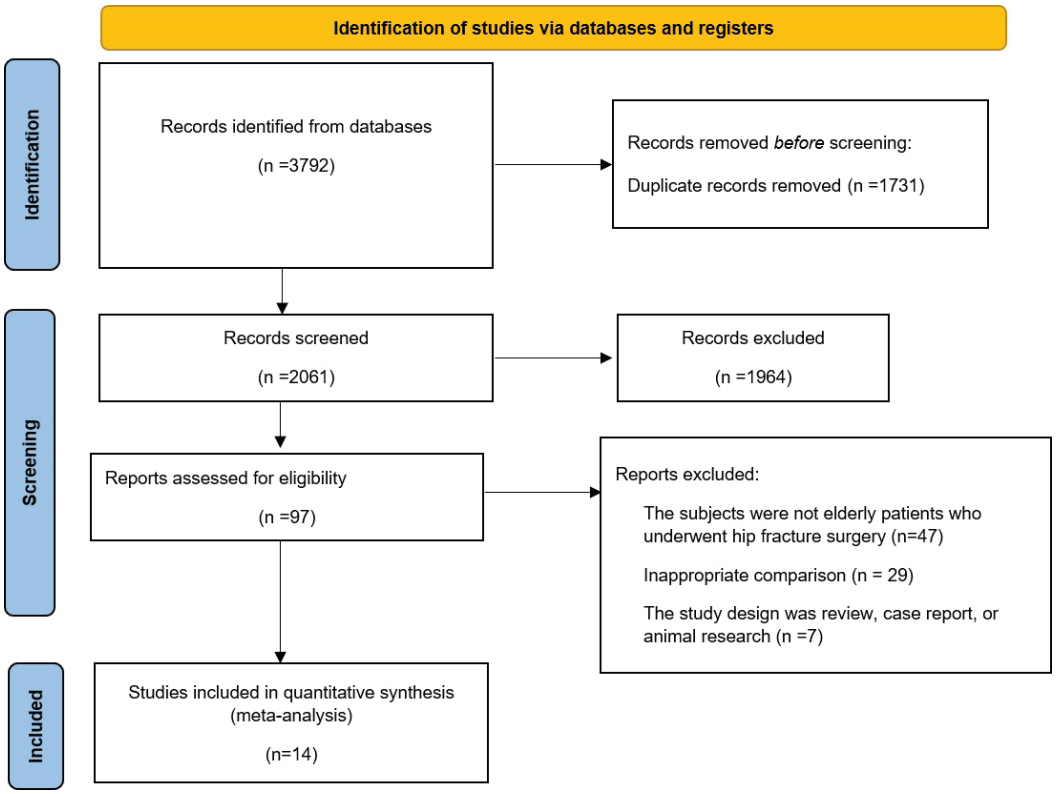

Fig. 1. Literature selection flowchart.

Table 1. Basic information of eligible studies.

Study	Location	Sample-RA	Sample-GA	Mean age	Male %	ASA
Rasmussen,2003	Denmark	211	217	70.8/71.1	84.36/88.02	I-IV
Hoppenstein,2005	Israel	30	30	81.5/83.5	NA	I-III
Parker,2015	UK	158	164	82.9/83.0	19.0/34.8	NA
Shi,2015	China	50	50	68.3	43	NA
Neuman,2016	USA	6	6	80.5/62.5	67/83	NA
Haghighi,2017	Iran	50	50	66.22/65.98	84/76	I-III
Meuret,2018	France	19	21	83/85	11/29	I-III
Tzimas,2018	Greece	37	33	77.11/75.09	47.14	I-III
Shin,2020	Korea	58	118	81.6/80.0	29.3/24.6	NA
Tang,2021	Chia	55	55	78.00/76.60	29.1/36.4	II-IV

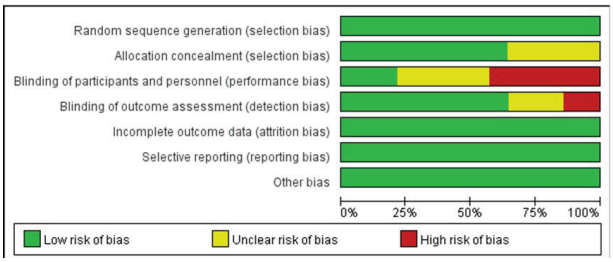

Supplementary Figure 1 Risk of bias graph.

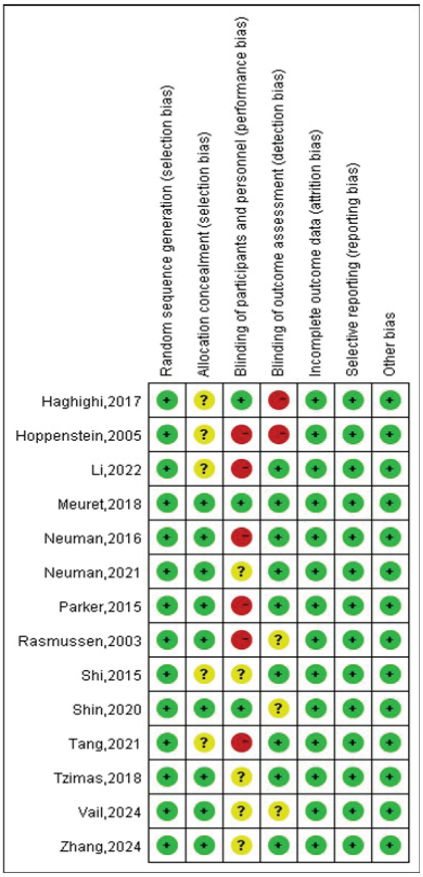

Supplementary Figure 2 Risk of bias summary.

heterogeneity among the included studies (I^2=69%, p=0.006), and the random-effects model was used to calculate the pooled effect size. The results indicated no statistically significant difference in the impact of RA versus GA on anesthesia time for elderly hip fracture surgery patients (MD: -0.87; 95%CI: -4.25, 2.50), as shown in Fig. 3.

Blood Loss

Five studies provided results on the impact of different anesthesia methods on intraoperative blood loss for elderly patients undergoing hip fracture surgery, involving 1,169 patients who received RA and 1,245 patients who received GA. The assessment of heterogeneity revealed heterogeneity among the included studies (I^2=97%, p<0.00001), and the random-effects model was used to calculate the pooled effect size. The results showed that, compared to GA, the use of RA in elderly patients during hip fracture surgery was associated with lower intraoperative blood loss (MD: -39.7 mL; 95%CI: -68.61, -10.84; p = 0.007), as depicted in Fig. 4.

Intraoperative transfusion

Five studies reported the impact of different anesthesia methods on intraoperative transfusion for elderly patients undergoing hip fracture surgery, involving 1,064 patients who received RA and 1,078 patients who received GA. The assessment of heterogeneity revealed heterogeneity among the included studies (I^2=85%, p<0.0001), and the random-effects

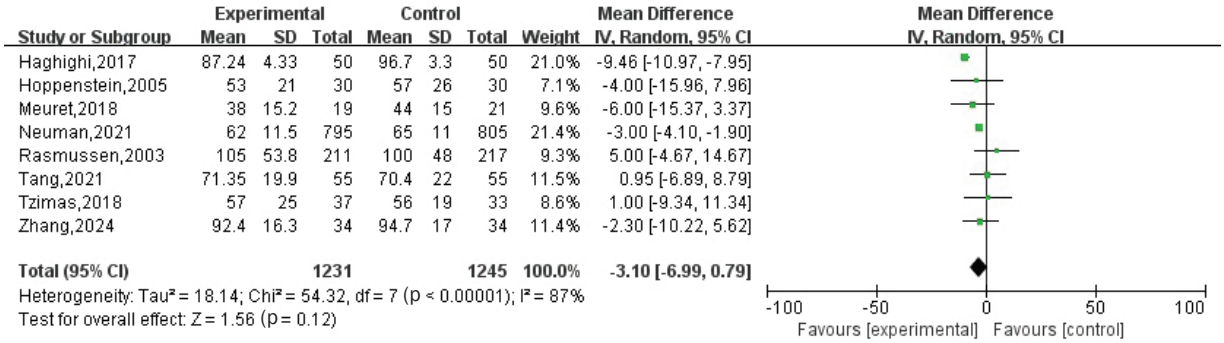

Fig. 2. Efficacy of RA and GA on surgery time in elderly patients for hip fracture surgery.

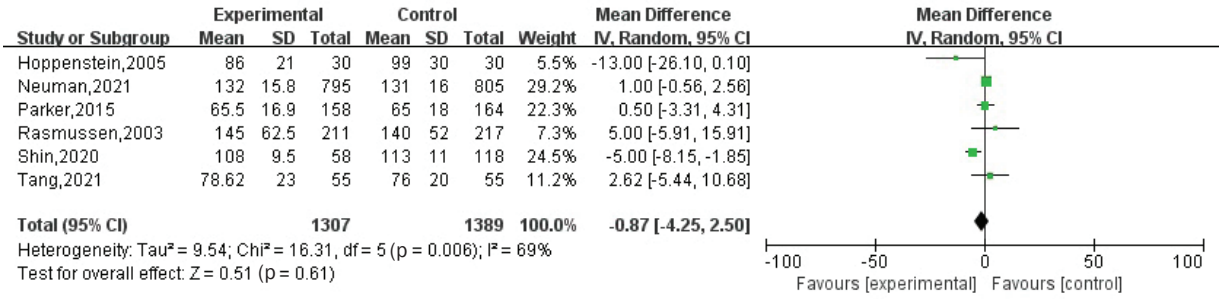

Fig. 3. Efficacy of RA and GA on anesthesia time in elderly patients for hip fracture surgery.

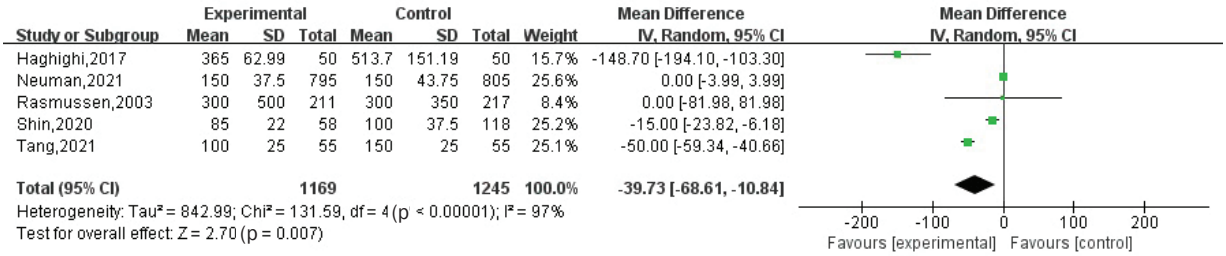

Fig. 4. Efficacy of RA and GA on blood loss (mL) in elderly patients for hip fracture surgery.

model was used to evaluate the impact of anesthesia methods. The meta-analysis results indicated no statistically significant difference in the impact of the two anesthesia methods on intraoperative transfusion for elderly hip fracture surgery patients (RR: 0.75; 95%CI: 0.41, 1.36), as illustrated in Fig. 5.

Hospital stay length

Five studies reported the impact of different anesthesia methods on postoperative hospital stay length for elderly patients who underwent hip fracture surgery, involving 932 patients who received RA and 1,004 patients who received GA. The assessment of heterogeneity revealed heterogeneity among the included studies (I^2=69%, p=0.01), and the random-effects model was used to calculate the pooled effect size. The results showed that RA did not have a significant positive effect on hospital stay length, and there was no statistically significant difference in the efficacy between the two anesthesia methods (MD: 0.05; 95%CI: -0.38, 0.49), as shown in Fig. 6.

Adverse events

Five studies reported the impact of different anesthesia methods on intraoperative hypotension for elderly patients undergoing hip fracture surgery, involving 737 patients who received RA and 745 patients who received GA. The meta-analysis based on the random-effects model showed that RA could significantly reduce the risk of intraoperative hypotension (RR: 0.58; 95%CI: 0.39, 0.85), as depicted in Fig. 7. Additionally, the analysis of two studies suggested that RA had an advantage in reducing the risk of postoperative cognitive dysfunction (RR: 0.56; 95%CI: 0.37, 0.86). However, a similar positive effect on cognitive function was not found in the risk of intraoperative delirium (RR: 1.09; 95%CI: 0.90, 1.32). For serious adverse events, the impact of RA versus GA on postoperative mortality was not statistically significant (RR: 1.01; 95%CI: 0.81, 1.26), as shown in Fig. 8.

Sensitivity analysis

We conducted a sensitivity analysis by excluding one study at a time to explore po-

tential bias risks and determine the stability of the results. After excluding one study [20], the heterogeneity among the included studies decreased from 87% to 0% for surgery time. The meta-analysis based on the fixed-effect model showed that RA was related to less surgery time for elderly patients with hip fractures by approximately (RR=-2.82; 95%CI: -3.88, -1.77, Fig. 9), but its clinical effect was limited. For intraoperative hypotension, after excluding one study24, the heterogeneity among the included studies decreased from 74% to 24%, and the evaluation results based on the combined effect model indicated that RA could still significantly reduce the risk of intraoperative hypotension (RR: 0.42; 95%CI: 0.37, 0.48), as shown in Fig. 10. Additionally, the sensitivity analysis for anesthesia time, blood loss, transfusion, and hospital length did not identify significant sources of heterogeneity, and there was no change in the direction of the results, indicating that the analysis results of this study are robust.

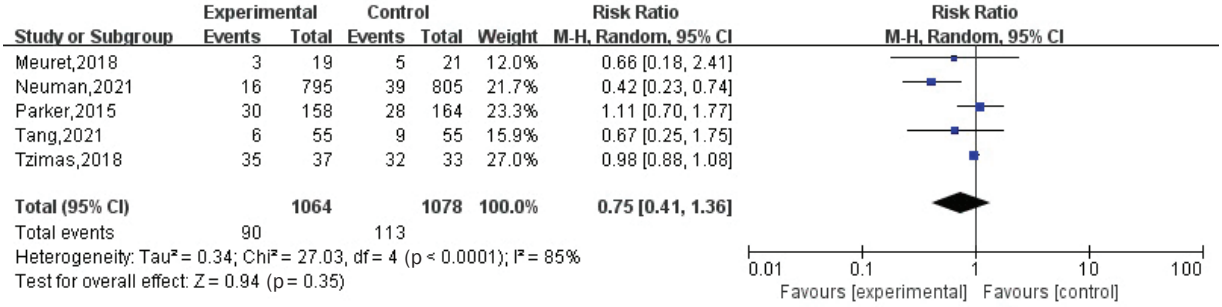

Fig. 5. Efficacy of RA and GA on blood transfusion in elderly patients for hip fracture surgery.

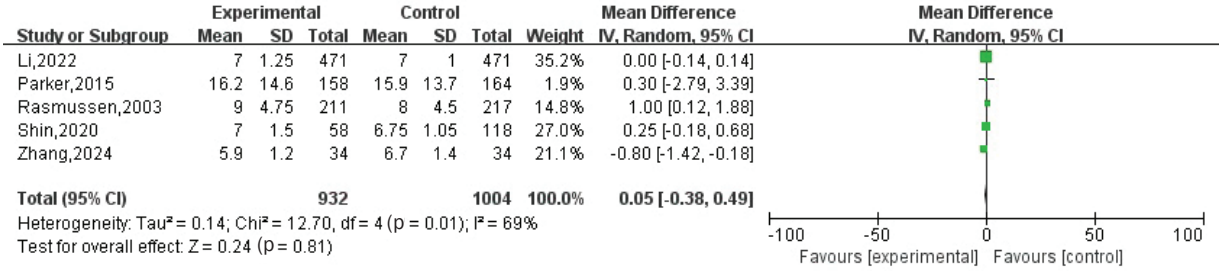

Fig. 6. Efficacy of RA and GA on hospital length of stay in elderly patients for hip fracture surgery.

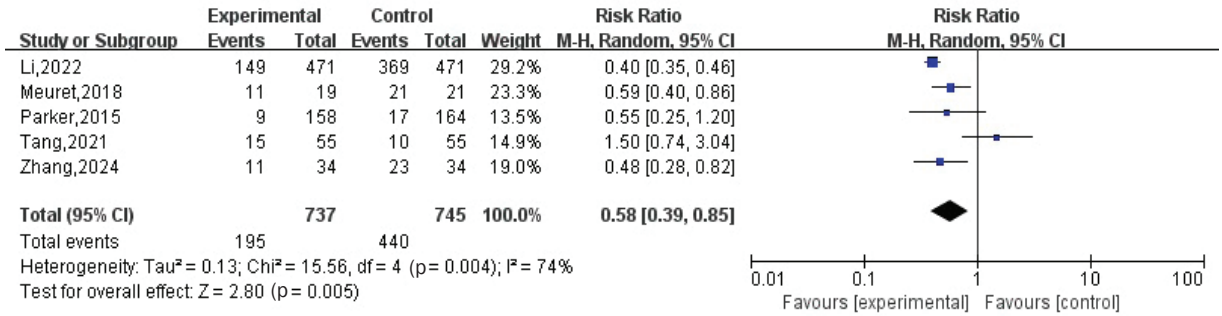

Fig. 7. Efficacy of RA and GA on intraoperative hypotension in elderly patients for hip fracture surgery.

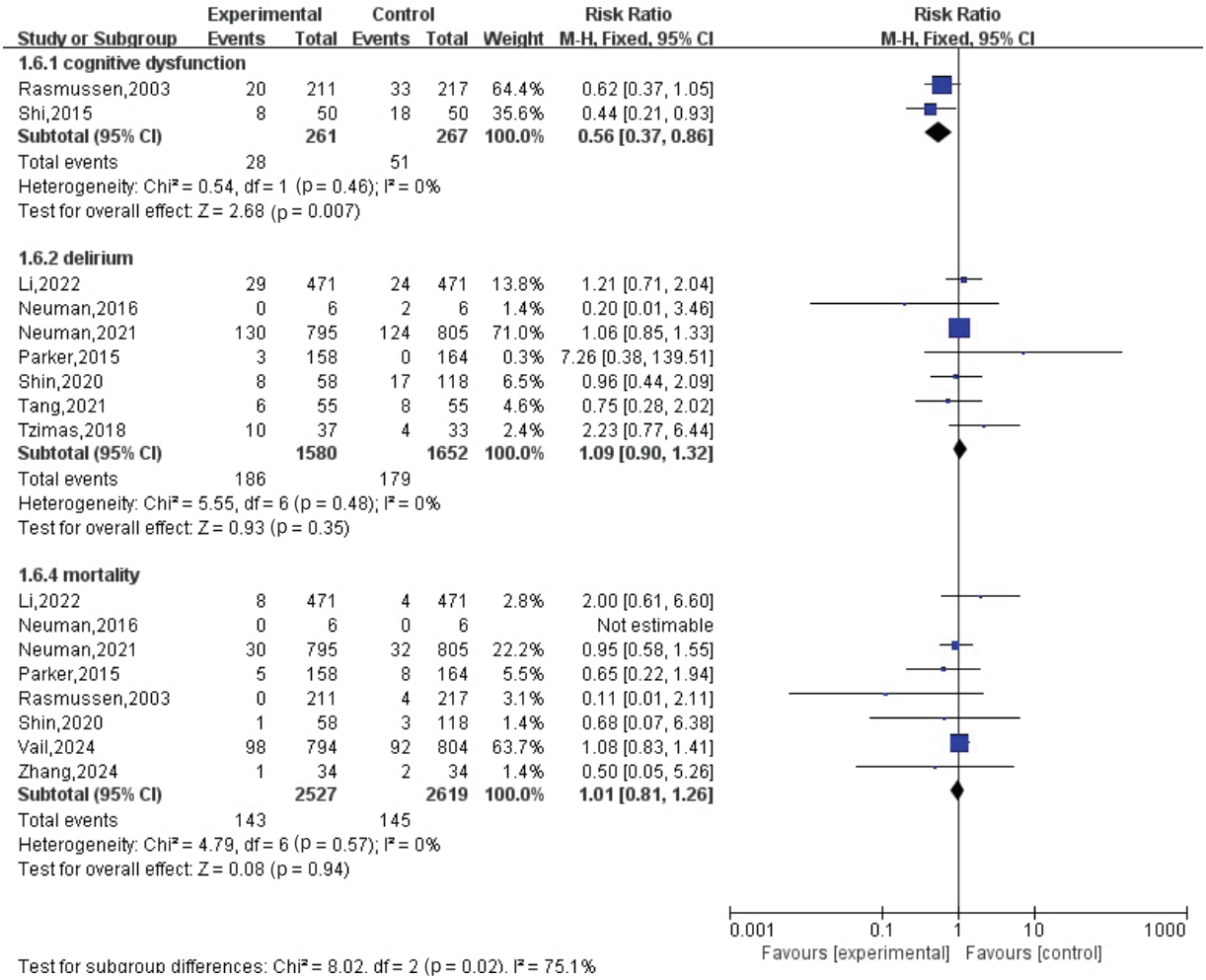

Fig. 8. Efficacy of RA and GA on cognitive dysfunction, delirium, and mortality in elderly patients for hip fracture surgery.

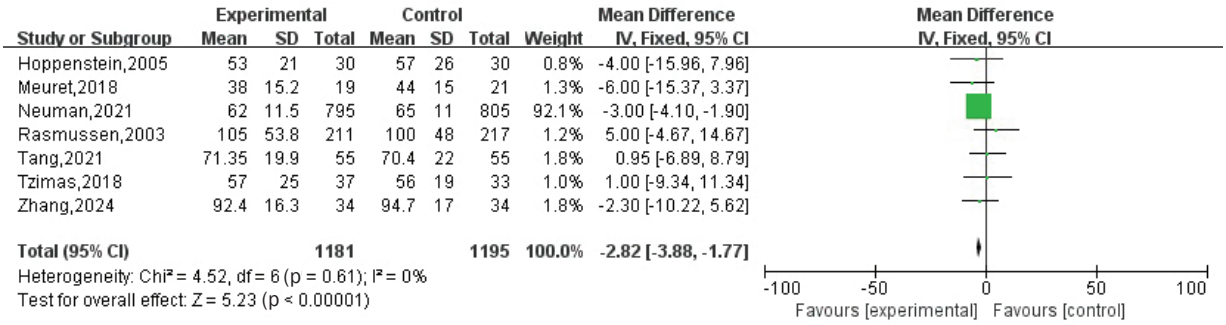

Fig. 9. Sensitivity analysis of RA and GA on surgery time in elderly patients for hip fracture surgery.

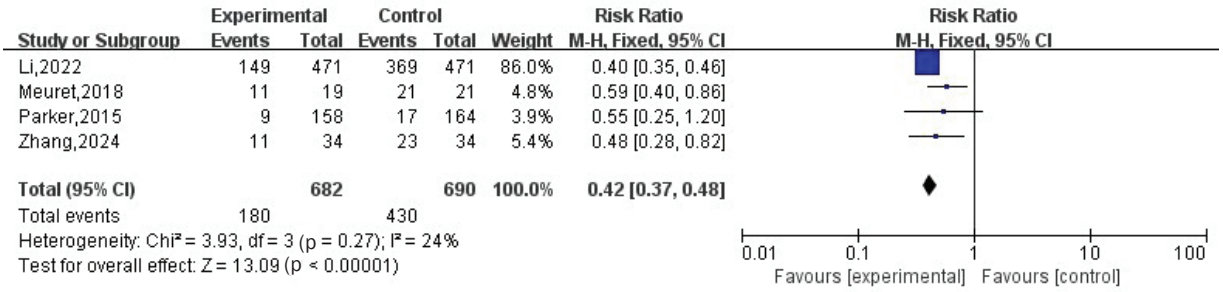

Fig 10. Sensitivity analysis of RA and GA on intraoperative hypotension in elderly patients for hip fracture surgery.

DISCUSSION

This study included research comparing the postoperative outcomes of RA and GA in elderly patients undergoing hip fracture surgery. Using meta-analysis, we evaluated the impact of RA versus GA on surgical time, anesthesia time, blood loss, intraoperative transfusion, hospital stay length, and adverse events. A total of 14 studies involving 5,626 elderly patients who underwent hip fracture surgery were included, of which 2,768 patients received RA, and the remaining 2,858 patients received GA during surgery. The meta-analysis results showed that RA had a significant positive effect on blood loss and intraoperative hypotension but did not find that this anesthesia method significantly improved other patient outcomes.

In our study, RA was significantly associated with a reduced risk of intraoperative hypotension, possibly related to its advantage in maintaining hemodynamic stability. Hypovolemia can decrease preload, subsequently causing a reduction in cardiac output and organ perfusion. Although GA is still widely used in hip fracture surgery, various RA techniques are becoming increasingly popular. The use of SA in hip fracture surgery has increased by 50% in the past decade[27]. SA can reduce the body's compensatory ability to change blood pressure, especially in patients with complex basic health status and physical weakness [28]. In addition, continuous spinal anesthesia (CSA), due to its low-dose medication characteristics, has been proven to be more effective in maintaining hemodynamic stability than single-shot spinal anesthesia [29,30].

Furthermore, lower doses of spinal anesthesia, through synergistic effects with opioids, can provide effective sensory blockage while minimizing systemic effects, including hemodynamic effects [31]. Multiple nerve blocks, as an alternative to spinal anesthesia, have been used to reduce the occurrence of hypotension, and some studies have reported positive effects [32,33]. Based on previous research evidence, choosing the appropriate anesthesia method is of great significance for improving the postoperative outcomes of elderly patients with hip fractures. Future research should explore the specific impact of different anesthesia methods on the postoperative recovery of elderly patients and how to optimize anesthesia strategies to improve surgical safety and patient satisfaction.

Delirium is an acute neuropsychiatric syndrome commonly seen in elderly patients undergoing hip fracture surgery and is associated with increased morbidity, mortality, and medical costs [34,35.] However, our study did not find a significant impact of RA and GA on the risk of postoperative delirium in patients. Although large-scale cohort studies targeting older people have shown that GA is associated with an increased risk of postoperative delirium [10], our study results are similar to previous meta-analysis results, which did not find that RA or GA affects the

incidence of postoperative delirium [36,37]. Delirium-related factors include age, cognitive impairment, frailty, comorbidities, surgery, and psychotropic medications, among others. Future research should further explore the efficacy differences of GA and RA in different population subgroups.

This study has the following limitations. First, eight of the 14 studies included had a sample size of less than 100 in each arm. Therefore, the results of the studies included with small sample sizes should be interpreted with caution. In addition, there is a particular risk of bias in implementing blinding and random concealment in the included studies, which may be the reason for the high heterogeneity in some of the study results. Furthermore, due to the purpose of the study, the original studies reported insufficiently on some postoperative outcomes, making it impossible for this study to conduct a quantitative evaluation.

CONCLUSION

In our study, compared with GA, RA can improve the incidence of intraoperative hypotension and reduce intraoperative blood loss in elderly patients undergoing hip fracture surgery. No significant improvement in other clinical indicators was found for RA. Due to the limitations of this study, the more comprehensive evaluation of evidence regarding RA and GA is still unclear, and more high-quality prospective studies are needed to systematically evaluate whether RA has significant clinical efficacy for elderly patients undergoing hip fracture surgery.

ACKNOWLEDGMENTS

Not applicable.

Funding

The study is funded by the Hangzhou Medical and Health Science and Technology Project (A20220667).

Ethical statement

An ethics statement is not applicable because this study is based exclusively on published literature.

Consent for publication

Not applicable.

Availability of data and materials

All data generated or analyzed during this study are included in this article.

Competing interest

The authors had no separate personal, financial, commercial, or academic conflicts of interest.

Number ORCID of author

- Feng Han: 0009-0007-6312-7526
- Yue Yang: 0009-0004-9317-8680
- Xinxin Tian: 0009-0001-9433-0064

Author contributions

HF conceived and designed the study. HF and TXX took part in the data collection and did the data analysis. All authors helped draft the manuscript. All authors helped to revise the manuscript. All authors read and approved the final manuscript.

REFERENCES

1. **Johnell O, Kanis JA**. An estimate of the worldwide prevalence and disability associated with osteoporotic fractures. Osteoporos Int. 2006;17(12):1726-1733.
2. **Cauley JA, Chalhoub D, Kassem AM, Fuleihan Gel-H.** Geographic and ethnic disparities in osteoporotic fractures. Nat Rev Endocrinol. 2014;10(6):338-351.

3. **Marsillo E, Pintore A, Asparago G, Oliva F, Maffulli N.** Cephalomedullary nailing for reverse oblique intertrochanteric fractures 31A3 (AO/OTA). Orthop Rev (Pavia). 2022 13;14(6):38560.
4. **Hawley S, Javaid MK, Prieto-Alhambra D, Lippett J, Sheard S, Arden NK, Cooper C, Judge A; REFReSH study group**. Clinical effectiveness of orthogeriatric and fracture liaison service models of care for hip fracture patients: population-based longitudinal study. Age Ageing. 2016;45(2):236-342.
5. **National hip fracture database (NHFD).** Annual report 2017. London: Royal College of Physicians; 2017.
6. **White SM, Moppett IK, Griffiths R.** Outcome by mode of anaesthesia for hip fracture surgery. An observational audit of 65 535 patients in a national dataset. Anaesthesia 2014;69(3):224-230.
7. **National Hip Fracture Database.** Annual report, The National Hip Fracture Database (nhfd.co.uk), 2020. Available from (Accessed April 21 2022).
8. **Zywiel MG, Prabhu A, Perruccio AV, Gandhi R.** The influence of anesthesia and pain management on cognitive dysfunction after joint arthroplasty: a systematic review. Clin Orthop Relat Res. 2014;472(5):1453-1466.
9. **Ahn EJ, Kim HJ, Kim KW, Choi HR, Kang H, Bang SR.** Comparison of general anaesthesia and regional anaesthesia in terms of mortality and complications in elderly patients with hip fracture: a nationwide population-based study. BMJ Open. 2019;9(9):e029245.
10. **Ravi B, Pincus D, Choi S, Jenkinson R, Wasserstein DN, Redelmeier DA.** Association of Duration of Surgery With Postoperative Delirium Among Patients Receiving Hip Fracture Repair. JAMA Netw Open. 2019;2(2):e190111.
11. **Li T, Li J, Yuan L, Wu J, Jiang C, Daniels J, et al.; RAGA Study Investigators.** Effect of regional vs general anesthesia on incidence of postoperative delirium in older patients undergoing hip fracture surgery: The RAGA Randomized Trial. JAMA. 2022;327(1):50-58.
12. **Page MJ, McKenzie JE, Bossuyt PM, Boutron I, Hoffmann TC, Mulrow CD, et al.** The PRISMA 2020 statement: an updated guideline for reporting systematic reviews. BMJ. 2021;372:n71.
13. **Higgins J, Altman DG.** Chapter 8: Assessing risk of biasin included studies. In Cochrane Handbook for Systematic Reviews of Interventions Version 5.0 (eds J. Higgins & S. Green), 2008. Available at:http://www.cochrane-handbook.org (last accessed July 20 2010).
14. **Rasmussen LS, Johnson T, Kuipers HM, Kristensen D, Siersma VD, Vila P, et al.; ISPOCD2(International Study of Postoperative Cognitive Dysfunction) Investigators.** Does anaesthesia cause postoperative cognitive dysfunction? A randomised study of regional versus general anaesthesia in 438 elderly patients. Acta Anaesthesiol Scand. 2003;47(3):260-266.
15. **Hoppenstein D, Zohar E, Ramaty E, Shabat S, Fredman B.** The effects of general vs spinal anesthesia on frontal cerebral oxygen saturation in geriatric patients undergoing emergency surgical fixation of the neck of femur. J Clin Anesth. 2005;17(6):431-438.
16. Vail EA, Feng R, Sieber F, Carson JL,et al ; REGAIN (Regional versus General Anesthesia for Promoting Independence after Hip Fracture) Investigators. Long-term Outcomes with Spinal versus General Anesthesia for Hip Fracture Surgery: A Randomized Trial. Anesthesiology. 2024;140(3):375-386.
17. **Parker MJ, Griffiths R.** General versus regional anaesthesia for hip fractures. A pilot randomised controlled trial of 322 patients. Injury. 2015;46(8):1562-1566.
18. **Shi HJ, Xue XH, Wang YL, Zhang WS, Wang ZS, Yu AL.** Effects of different anesthesia methods on cognitive dysfunction after hip replacement operation in elder patients. Int J Clin Exp Med. 2015;8(3):3883-3888.
19. **Neuman MD, Mehta S, Bannister ER, Hesketh PJ, Horan AD, Elkassabany NM.** Pilot randomized controlled trial of spinal versus general anesthesia for

hip fracture surgery. J Am Geriatr Soc. 2016;64(12):2604-2606.

20. **Haghighi M, Sedighinejad A, Nabi BN, Mardani-Kivi M, Tehran SG, Mirfazli SA, et al.** Is spinal anesthesia with low dose lidocaine better than sevoflorane anesthesia in patients undergoing hip fracture Surgery. Arch Bone Jt Surg. 2017;5(4):226-230.
21. **Meuret P, Bouvet L, Villet B, Hafez M, Allaouchiche B, Boselli E.** Hypobaric unilateral spinal anaesthesia versus general anaesthesia in rlderly patients undergoing hip fracture surgical repair: a prospective randomised Open Trial. Turk J Anaesthesiol Reanim. 2018;46(2):121-130.
22. **Tzimas P, Samara E, Petrou A, Korompilias A, Chalkias A, Papadopoulos G.** The influence of anesthetic techniques on postoperative cognitive function in elderly patients undergoing hip fracture surgery: General vs spinal anesthesia. Injury. 2018;49(12):2221-2226.
23. **Shin S, Kim SH, Park KK, Kim SJ, Bae JC, Choi YS.** Effects of anesthesia techniques on outcomes after hip fracture surgery in elderly patients: A prospective, randomized, controlled trial. J Clin Med. 2020;9(6):1605.
24. **Tang L, Fang P, Fang Y, Lu Y, Xu G, Liu X.** Comparison of effects between combined lumbar-sacral plexus block plus general anesthesia and unilateral spinal anesthesia in elderly patients undergoing hip fracture surgery: A pilot randomized controlled trial. Evid based complement alternat med. 2021;2021:6685497.
25. **Neuman MD, Feng R, Carson JL, Gaskins LJ, Dillane D, Sessler DI, et al.; REGAIN Investigators.** Spinal anesthesia or general anesthesia for hip surgery in older adults. N Engl J Med. 2021;385(22):2025-2035.
26. **Zhang A, Gao H, Lu Y, Jiang L, Xu C.** Fascia iliaca block combined with low-dose spinal anesthesia for hip fracture surgery in the elderly: effects on severe hypotension and analgesia. A randomized controlled trial. Pain Physician. 2024;27(5):E579-E587.
27. **Maxwell BG, Spitz W, Porter J.** Association of increasing use of spinal anesthesia in hip fracture repair with treating an aging patient population. JAMA Surg. 2020;155(2):167-168.
28. **Boddaert J, Raux M, Khiami F, Riou B.** Perioperative management of elderly patients with hip fracture. Anesthesiology. 2014;121(6):1336-1341.
29. **Biboulet P, Jourdan A, Van Haevre V, Morau D, Bernard N, Bringuier S, et al.** Hemodynamic profile of target-controlled spinal anesthesia compared with 2 target-controlled general anesthesia techniques in elderly patients with cardiac comorbidities. Reg Anesth Pain Med. 2012;37(4):433-440.
30. **Futier E, Lefrant JY, Guinot PG, Godet T, Lorne E, Cuvillon P, et al.; INPRESS Study Group.** Effect of individualized vs standard blood pressure management strategies on postoperative organ dysfunction among high-risk patients undergoing major surgery: A eandomized clinical trial. JAMA. 2017;318(14):1346-1357.
31. **Messina A, La Via L, Milani A, Savi M, Calabrò L, Sanfilippo F, et al.** Spinal anesthesia and hypotensive events in hip fracture surgical repair in elderly patients: a meta-analysis. J Anesth Analg Crit Care. 2022;2(1):19.
32. **de Visme V, Picart F, Le Jouan R, Legrand A, Savry C, Morin V.** Combined lumbar and sacral plexus block compared with plain bupivacaine spinal anesthesia for hip fractures in the elderly. Reg Anesth Pain Med. 2000;25(2):158-162.
33. **Johnston DF, Stafford M, McKinney M, Deyermond R, Dane K.** Peripheral nerve blocks with sedation using propofol and alfentanil target-controlled infusion for hip fracture surgery: a review of 6 years in use. J Clin Anesth. 2016;29:33-39.
34. **Yang Y, Zhao X, Dong T, Yang Z, Zhang Q, Zhang Y.** Risk factors for postoperative delirium following hip fracture repair in elderly patients: a systematic review and meta-analysis. Aging Clin Exp Res. 2017;29(2):115-126.
35. **Inouye SK, Bogardus ST Jr, Charpentier PA, Leo-Summers L, Acampora D, Holford TR, et al.** A multicomponent intervention

to prevent delirium in hospitalized older patients. N Engl J Med. 1999;340(9):669-676.

36. **Patel V, Champaneria R, Dretzke J, Yeung J.** Effect of regional versus general anaesthesia on postoperative delirium in elderly patients undergoing surgery for hip fracture: a systematic review. BMJ Open. 2018;8(12):e020757.

37. **Guay J, Parker MJ, Gajendragadkar PR, Kopp S.** Anaesthesia for hip fracture surgery in adults. Cochrane Database Syst Rev. 2016;2(2):CD000521.

Investigación Clínica
Vol. 66 Nº 2 / June 2025
Bilingual - Abstracts in Spanish and English

Contents

Investigación Clínica
Vol. 66 Nº 2 /Junio 2025
Bilingüe - Resúmenes en Español e Inglés

Contenido